Report 2334

DAVID TAYLOR MODEL BASIN
WASHINGTON, D.C.

DEPARTMENT OF THE NAVY

HYDROMECHANICS

O

AERODYNAMICS

O

STRUCTURAL MECHANICS

O

APPLIED MATHEMATICS

O

ACOUSTICS AND VIBRATION

PERFORMANCE ESTIMATES OF CAPTURED AIR BUBBLE VEHICLES WITH WATER JET PROPULSION

by

Robert M. Williams

AERODYNAMICS LABORATORY
RESEARCH AND DEVELOPMENT REPORT

February 1967 Report 2334

125

PERFORMANCE ESTIMATES OF CAPTURED AIR BUBBLE VEHICLES WITH WATER JET PROPULSION

by

Robert M. Williams

The distribution of this document is unlimited.

February 1967

Report 2334
Aero Report 1119

ACKNOWLEDGMENT

The author is deeply indebted to Dr. Harvey R. Chaplin for his guidance and assistance in all phases of this report.

SYMBOLS

A_j jet area at exit, square feet

A_p pump cross-sectional area, square feet

b beam of bubble, feet

C_{D_e} coefficient of external aerodynamic drag $\left(\frac{1}{5(\ell/b)}\right)$

C_f turbulent skin friction coefficient $\left[0.482\left(\log_{10}R_\ell\right)^{-2.618} + 0.0004\right]$

C_L coefficient of external aerodynamic lift

C_1 correction factor for first-order estimate of wetted area associated with "additional sidewall depth" (ℓ_s/ℓ)

C_2 constant which regulates pump operation $\left(H_p/Q^2\text{, for constant efficiency}\right)$, sec^2/ft^5

C_6 equivalent wetted depth, feet (defined by $\left(\frac{\text{total wetted sidewall area}}{\text{average wetted sidewall length}}\right)$, where the numerator is the total immersed area of the sidewall when on the bubble, at zero speed and with no waves)

d_p diameter of pump cross section, feet

D drag, pounds

D_c discharge coefficient $\left(Q/S_g V_c\right)$

D_w wavemaking drag

D_e aerodynamic drag

D_r ram drag

$D_{s,a}$ additional sidewall drag

$D_{s,b}$ sidewall drag due to bubble

D_t trunk drag

g acceleration due to gravity, 32.2 ft/sec/sec

H average wave height, feet

H_D	head loss in ducts and nozzles, feet
H_{dyn}	dynamic head at pump entrance $\left(\frac{Q^2}{2gA_p^{\,2}}\right)$, feet
H_p	pump head rise, feet
H_{spi}	static pump head at inlet, feet
H_V	vapor head, feet
h	daylight gap (for ACV), feet
h_a	additional sidewall depth, feet $\left(0.5\ H + C_6\right)$
K_D	duct and nozzle loss coefficient
K_{D_D}	duct and nozzle design-speed loss coefficient
K_{D_s}	duct and nozzle static loss coefficient
K_L	total internal head loss coefficient
K_{L_D}	design internal head loss coefficient
k	velocity ratio $\left(\frac{V_j - V}{V} = \frac{\Delta V}{V}\right)$
k_{opt}	optimum velocity ratio for maximum efficiency
L	lift, pounds
ℓ	length of bubble, feet
$\frac{\ell}{b}$	length/beam ratio (bubble)
ℓ_s	wetted sidewall length, feet
n	number of wetted sides
q_a	dynamic pressure of air ($q_a \approx 0.0012\ q_w$), lb/ft^2
q_w	dynamic pressure of water $\left(2.85\ V_k^{\,2}\right)$, lb/ft^2
P_o	pressure of the central pressure distribution in the sequence of images, lb/ft^2
P_R	power required, lb-ft/sec

Q	volume flow rate, ft^3/sec
R_ℓ	Reynolds number $\left(1.30\ V_k \ell \times 10^5\right)$
S	bubble area, ft^2
S_g	air gap area (ACV), ft^2
T	thrust (= drag), pounds
V	forward velocity, ft/sec
V_D	design forward velocity, ft/sec
V_j	exit velocity, ft/sec
V_k	forward velocity, knots
$V_k/\sqrt{\ell}$	speed/length parameter
W	weight, pounds
w	specific weight (W/S), lb/ft^2
$\frac{w}{\sqrt{S}}$	specific cushion loading, lb/ft^3
$\frac{w}{\ell}$	pressure/length parameter, lb/ft^3 (pressure of bubble region (w) ÷ length of bubble (ℓ))
η_e	pump efficiency
η_p	propulsive efficiency
ρ_a	density of air, $slugs/ft^3$
ρ_w	density of water, $slugs/ft^3$
σ	cavitation index

TABLE OF CONTENTS

LIST OF TABLES

LIST OF ILLUSTRATIONS

TABLE OF CONTENTS (Concluded)

SUMMARY

Performance predictions of Captured Air Bubble (CAB) vehicles utilizing water jet propulsion are presented. The analysis was made for various combinations of gross weight, specific loading, length-to-beam ratio, and wave height. In addition, the effect of varying the ducting loss coefficient has also been investigated.

It was found that the total drag "hump" of low length-to-beam ratios (ℓ/b) was eliminated at higher ℓ/b values. This effect is due to the complex behavior of the wavemaking drag component. It was further found that for a particular length-to-beam ratio (ℓ/b), a value of specific cushion loading existed which optimized the performance (as measured by the ratio of weight to horsepower required). The lighter specific cushion loadings offered definite performance advantages at the lower length-to-beam ratios.

INTRODUCTION

Current interest in CAB vehicles has been based almost exclusively on estimates of their high-speed performance. As the theory upon which these estimates are based is updated by additional research, it is necessary from time to time to modify the original performance predictions. This report employs the most recent theory available (References 1, 2, and 3), programmed for an IBM 7090/SC-4020 computer-plotter combination. It is felt that the results presented here represent the most complete and reliable predictions available at this time.

ANALYSIS

The computer model calculates CAB performance by determining drag and power requirements at specified increments of the speed/length parameter, $V_k/\sqrt{\ell}$.

The important program inputs are: vehicle gross weight, length-to-beam ratio (ℓ/b), specific cushion loading parameter, $w/\sqrt{S}$, sidewall factors C_1 and C_6 , configuration aerodynamic lift coefficient C_L , water

jet pump efficiency η_e , and duct and nozzle loss coefficient K_D . Pertinent combinations of these design parameters have been plotted and analyzed in this report. The tabulated variation is given in Table 1.

An exact formulation of the wave drag theory of Reference 2 has been incorporated into the program. However, the values on the sub-hump side are faired to a slope of 2.0 (on log-log paper), as shown in Figure 1; and secondary humps have been neglected. This fairing is essentially arbitrary, although it does agree reasonably well with the small amount of experimental data available. Experiments are presently being undertaken to ascertain the validity of this drag theory and that of Reference 1 for CAB vehicles of various length-to-beam ratios, with emphasis on the values of wavemaking drag in the sub-hump region.

The advantages of water jet propulsion in CAB applications are numerous; e.g., higher propulsive efficiencies are more readily obtainable at high speeds than is the case with conventional propellers. Since inlets and exhausts are located at or below the water line, there is relatively little potential energy loss or water weight penalty incurred (as in a hydrofoil application). Noise propagation will be less than with conventional propulsors. Debris and shallow water problems are minimized, since the entire unit may be given a low-profile configuration, particularly if multiple pump arrays are used. A variable-area intake and exit will permit large flow rates at low speeds, thus providing sufficient thrust for rapid acceleration.

Pump efficiencies of 90 percent are considered feasible for water jets. With this assumption, the propulsive efficiency $\left(\eta_p\right)$ becomes dependent on the duct loss coefficient $\left(K_D\right)$ and velocity ratio $k = \left(\frac{V_j - V}{V}\right)$. The value of k may be optimized to give maximum η_p at a given design condition of wave height and velocity. The value of K_D is a function of the flow-through velocity and the particular ducting system utilized to channel the water to and from the pumps.

BASIC CAB PERFORMANCE EQUATIONS

The following equations are given as a concise summary of the theory developed in References 1 and 2.

(a) Wavemaking Drag (Figure 1)

$$\frac{D_w}{W} = \left[\left(\frac{w}{\ell}\right)^2 \left(1 - 0.0012\ C_L \frac{q_w}{w}\right)^2 \frac{\ell^3}{\rho_w g W}\right]\left(\frac{\rho_w g D}{P_o^{\,2}\ell}\right)$$

where $\frac{\rho_w g D}{P_o^{\,2}\ell}$ is computed for a channel of infinite depth and width equal to ten times the bubble length by the following formula:

$$\frac{\rho_w g D}{P_o^{\,2}\ell} = 4\gamma\left\{\left(\frac{\beta}{\gamma}\sin\Omega\right)^2 + \frac{1}{4N\pi^2} + \frac{1}{\pi^2}\sum_{n=1}^{N}\frac{1}{n^2}\left[1 + \frac{1}{\sqrt{1+\left(\frac{2\pi n}{\gamma\,\Omega}\right)^2}}\right]\cdot\right.$$

$$\left.\sin^2\left(n\pi\frac{\beta}{\gamma}\right) \cdot \sin^2\left[\Omega\sqrt{\frac{1}{2} + \frac{1}{2}\sqrt{1+\left(\frac{2\pi n}{\gamma\,\Omega}\right)^2}}\right]\right\}$$

In the above equation, the following definitions apply:

$$\beta = \frac{\text{bubble width}}{\ell} = \frac{1}{\ell/b}$$

$$\gamma = \frac{\text{width of channel}}{\ell} = 10$$

$$\Omega = \frac{g\ell}{2V^2}$$

The summation of the above equation is transmitted when

$$\frac{1}{n}\left[1 + \frac{1}{\sqrt{1+\left(\frac{2\pi n}{\gamma\,\Omega}\right)^2}}\right] \le 0.001$$

The values of $\frac{\rho_w g D}{P_o^2 \ell}$ versus $\frac{V}{\sqrt{g}\sqrt{S}}$ on the pre-hump side are then altered to a slope of 2 on log-log paper.

(b) Additional Sidewall Drag:

$$\frac{D_{s,a}}{W} = n\left(\frac{\ell}{b}\right) C_1 C_f \left(\frac{h_a}{\ell}\right) \frac{q_w}{w}$$

(c) Sidewall Drag Due to Bubble:

$$\frac{D_{s,b}}{W} = \left(\frac{\ell}{b}\right) C_1 C_f \left(\frac{q_w}{w}\right)\left[\frac{D_w}{W} - \frac{h}{\ell}\right]^2 \frac{1}{\frac{D_w}{W}} \quad , \quad \frac{V_k}{\sqrt{\ell}} \geq K$$

or

$$\frac{D_{s,b}}{W} = \left(\frac{\ell}{b}\right) C_1 C_f \left(\frac{q_w}{w}\right)\left[\left(\frac{D_w}{W}\right)_{max} - \frac{h}{\ell}\right]^2 \left(\frac{1}{\left(\frac{D_w}{W}\right)_{max}}\right) \quad , \quad \frac{V_k}{\sqrt{\ell}} < K$$

where K is the value of $V_k/\sqrt{\ell}$ taken at the wave drag "hump" $\left(\frac{D_w}{W}\right)_{max}$ for a specified ℓ/b.

(d) Aerodynamic Drag:

$$\frac{D_e}{W} = C_{D_e} \frac{q_a}{w}$$

(e) Trunk Drag:

$$\frac{D_t}{W} = 0.00792 \left(\frac{H - 2h}{\ell}\right)^{1.2} \frac{q_w}{w} \cdot \left(\frac{b}{b + \ell}\right)$$

(f) Ram Drag:

$$\frac{D_r}{W} = 2\, D_c \left(1 - C_L \frac{q_a}{w}\right)^{\frac{1}{2}} \left(\frac{q_a}{w}\right)^{\frac{1}{2}} \left(\frac{S_g}{S}\right)$$

(g) Total Drag:

$$\frac{D}{W} = \frac{D_w}{W} + \frac{D_{s,a}}{W} + \frac{D_{s,b}}{W} + \frac{D_e}{W} + \frac{D_t}{W} + \frac{D_r}{W}$$

(h) Propulsive Power-to-Weight Ratio:

$$\frac{HP_p}{W} = \left(\frac{D}{W}\right) \frac{V_k}{326\, \eta_p}$$

(i) Cushion Power-to-Weight Ratio:

$$\frac{HP_c}{W} = 0.14 \left(\frac{D}{W}\right) \frac{V_k}{326}$$

(j) Weight-to-Horsepower Ratio:

$$\frac{W}{HP} = \left[\frac{HP_p}{W} + \frac{HP_c}{W}\right]^{-1}$$

(k) Specific Power:

$$\frac{P_R}{WV} = \frac{326}{V_k\ (W/HP)}$$

BASIC WATER JET EQUATIONS

As previously noted, the water jet model used in the analysis was a variable-geometry configuration for which the theory discussed in Reference 3 is appropriate. A parabolic variation of K_D with V/V_D was assumed for the duct system with the design value of K_D remaining constant at values of $V/V_D > 1.0$ (Figure 2).

The pumps were assumed to be capable of continuous operation at 90 percent efficiency η_e, while conforming to a pump head/flow rate relationship of $H_p = C_2 Q^2$. The constant C_2 is defined at a specified design speed and wave height and remains constant at all off-design conditions. The procedure for determining C_2 and other design constants is as follows:

An optimum value of the velocity ratio, $k = \frac{V_j - V}{V} = \frac{\Delta V}{V}$, is determined by computing the optimum total internal loss coefficient at design conditions:

(a)

$$K_{L_D} = \left[1 - \frac{1}{\left(1 + k_{opt}\right)^2}\right] \cdot \frac{1 - \eta_e}{\eta_e} + \frac{K_{D_D}}{\eta_e}$$

where the value $k_{opt} = \sqrt{\frac{K_L}{\left(1 + K_L\right)}}$ is determined by an iterative process. The following computations of design values are then made:

(b) Flow Rate at Design Speed:

$$Q_D = D_D / \left(k_{opt} V_D \rho_w\right)$$

(c) Exit Velocity:

$$V_{j_D} = V_D \left(k_{opt} + 1\right)$$

(d) Thrust:

$$T_D = D_D = \rho_w Q_D \left(V_{j_D} - V_D\right)$$

(e) Pump Head:

$$H_{p_D} = \frac{\left(1 + K_{D_D}\right) V_{j_D}{}^2 - V_D{}^2}{2g}$$

(f) Total Exit Area:

$$A_{j_D} = \frac{Q_D}{V_j} = Q_D \sqrt{\frac{1 + K_{D_D}}{2g\ H_{p_D} + V_D^2}}$$

(g) Pump Constant ($H_p = C_2\ Q^2$)

$$C_2 = \frac{H_{p_D}}{Q^2} = \frac{1 + K_{D_D}}{2g\ A_{j_D}^2} - \frac{V_D^2}{2g\ Q_D^2}$$

(h) The Efficiency is given by:

$$\eta_{p_D} = \frac{2\ K_D}{\left(1 + k_{opt}\right)^2 \left(1 + K_{L_D}\right) - 1} = 1 - k_{opt}$$

(i) The Shaft Horsepower is given by:

$$SHP = \frac{D_D\ V_D}{550\ \eta_p}$$

and the pump diameter is determined by the empirical relation:

$$d_p = \sqrt{\frac{SHP}{1000}}$$

After the design values have been determined, the program determines the off-design performance by computing for each increment of velocity the following variables:

(j) Duct Loss Coefficient (Figure 2):

$$K_D = \left(K_{D_s} - K_{D_D}\right)\left(\frac{V}{V_D} - 1\right)^2 + K_{D_D}$$

(k) Volume Flow Rate (by iterative method)·

$$D = T = \rho_w\ Q\left(\sqrt{\frac{2g\ C_2\ Q^2 + V^2}{1 + K_D}} - V\right)$$

(ℓ) Velocity Ratio:

$$k = \frac{D}{\rho_w \, Q \, V}$$

(m) Pump Head:

$$H_p = C_2 \, Q^2$$

(n) Exit Velocity:

$$V_j = (k + 1) \, V$$

(o) Nozzle Exit Area:

$$A_j = Q \sqrt{\frac{1 + K_D}{2g \, C_2 \, Q^2 + V^2}}$$

(p) Total Loss Coefficient:

$$K_L = \left[1 - \frac{1}{(1 + k)^2}\right] \frac{1 - \eta_e}{\eta_e} + \frac{K_D}{\eta_e}$$

(q) Propulsive Efficiency:

$$\eta_p = \frac{2k}{(1 + k)^2 \, (1 + K_L) - 1}$$

(r) A suitable indication of the onset of cavitation may be the ratio of the pump inlet static head to the pump head rise:

$$\sigma = \frac{H_{spi}}{H_p} = \frac{H_{atm} - H_v - H_D + H_{dyn} - \dfrac{Q^2}{2g \, A_p^{\,2}}}{H_p}$$

or

$$\sigma = \frac{32.51 - \dfrac{K_D \, V_j^{\,2}}{2g} + \dfrac{V^2}{2g} - \dfrac{Q^2}{2g \, A_p^{\,2}}}{C_2 \, Q^2}$$

The minimum noncavitating values of σ for specified operating conditions and duct-pump combinations have not been ascertained fully.

DISCUSSION

Table 1 shows the variation of the main design parameters evaluated by the program. Four gross weights and three length-to-beam ratios were selected as inputs. The values of ℓ/b were 2.0, 7.0, and 3.74 (which represents the geometric mean between 2.0 and 7). The selection of design speeds and wave heights was arbitrary; however, the propulsive efficiency was insensitive to relatively large variations of these two parameters so that little benefit was realized by optimization.

Both the weight-to-horsepower ratios (W/HP) and the specific power P_R/WV have been presented as performance figures of merit. From the standpoint of conventional power, the parameter P_R/WV affords a satisfactory prediction of the range-speed-payload capabilities of the vehicle. However, when nuclear power is considered, the principal consideration becomes the allowable weight per horsepower of the propulsion machinery, which must be a reasonable fraction of the total vehicle weight per horsepower. In the graphs of W/HP versus V_k , W/HP may be considered as an "equivalent" L/D ratio when plotted for a single velocity.

A study of the graphical data revealed several interesting trends in W/HP as a function of the primary design parameters (weight, length-to-beam ratio, and specific cushion loading, $w/\sqrt{S}$). In general, a combination of these parameters exists that will maximize W/HP for a given operating mode of velocity and sea state. However, due to the complexities and interactions involved in this type of analysis, it is difficult to make any simple statements on formulations with regard to optimizing performance. Rather, the procedure used here will be to illustrate graphically the optimizing trends attributed to variations of the design parameters and to indicate limiting factors in these trends.

Figure 3 is a summary plot computed from six different ℓ/b designs of a 20,000-ton vessel operating in ten-foot waves. It should be noted that the data for this particular vessel were computed using conventional

water propellers and not water jets. A value of $w/\sqrt{S} = 1.1$ was selected, based on structural considerations. Figure 4 shows the influence of varying the specific loading $w/\sqrt{S}$. For a speed of 50 knots at $w/\sqrt{S} = 0.5$, the ℓ/b for best W/HP is approximately 5 and, at $w/\sqrt{S} = 2.1$, the optimum ℓ/b value from a W/HP standpoint is 9.0. It may be noted that the peak value of the $w/\sqrt{S} = 1.1$ curve corresponds with the value of W/HP at 50 knots shown in Figure 3.

Referring again to Figure 3, it is evident that at the higher speeds the lower ℓ/b provides better performance, and the drag hump is present only at the lower ℓ/b. These phenomena are attributable directly to the nature of the wavemaking drag, as shown in Figure 1. The total drag curve (D/W) at high ℓ/b increases rapidly with velocity. As the percentage contribution of wavemaking drag is sharply reduced with increasing ℓ/b, the sidewall hydrodynamic drag begins to dominate, because of the greatly increased bubble length. The low ℓ/b advantage of super-hump operation is therefore eliminated and sub-hump operation now becomes attractive. At ℓ/b values above 7.0, the sideboard drag exceeds 80 percent of the total drag. The tradeoff beyond this point is straightforward. An increase of ℓ/b produces a decrease of the wave drag component and a corresponding increase of sidewall drag so that no net drag reduction is possible. Another drag tradeoff is evident in Figure 4. As $w/\sqrt{S}$ increases, at any given ℓ/b, the wavemaking drag increases $\left(D_w/W \text{ and } D_{s,b}/W\right)$ and the sidewall hydrodynamic drag $D_{s,a}/W$ is reduced. The intersection of these drag curves represents a minimum value of total drag and an optimum of $w/\sqrt{S}$. This relationship is evident in Figure 4 at an ℓ/b of 9.0 where $w/\sqrt{S} = 0.5$ represents a pre-minimum value; but, at a value of 1.1, the D/W ratio is optimized. The effect of weight variation is illustrated in Figure 5.

The primary intent of this paper has been to indicate tradeoffs in performance obtainable by varying the primary design parameters. However, much additional information may be derived by studying and cross-plotting the data. In particular, the variation of the cavitation index σ with ℓ/b,

weight, $w/\sqrt{S}$, wave height, and K_D is presented. Before additional refinements are added to the CAB design, the seriousness of the cavitation problem should be ascertained and modifications of K_D, pump geometry, etc. should be determined.

Multiple graphs (Figure 6 through Figure 17) have been prepared for all the data. By interpolation of these graphs, the CAB performance can be estimated. If precise information on a specific design is desired, however, a detailed computer analysis would be required.

Aerodynamics Laboratory
David Taylor Model Basin
Washington, D. C. 70007
January 1967

REFERENCES

1. Newman, J. N. and F. A. B. Poole. Wave Resistance of a Moving Pressure Distribution in a Canal. Wash., Mar 1962. 7 p. incl. illus. (David Taylor Model Basin. Rpt. 1619) (Reprint from Schiffstechnik v.9, Jan 1962)

2. Chaplin, Harvey R. and Allen G. Ford. Some Design Principles of Ground Effect Machines. Section D: Drag. Wash., Jun 1966. 26 p. incl. illus. (David Taylor Model Basin. Rpt. 2121D. Aero Rpt. 1100D) (DDC AD 636 277)

3. Levy, Joseph. The Design of Water-Jet Propulsion Systems for Hydrofoil Craft. <u>Marine Technology</u> (N. Y.), v.2, Jan 1965, p. 15-41

Table 1

Variation of CAB Input Parameters

W in tons	ℓ/b	$w/\sqrt{3}$	K_{D_s}	K_{D_D}	V_k Design	H Design (ft)	C_L	C_{D_e}	C_1	C_6	ℓ	C_2	A_p (ft^2)	Figure
100	2.00	1.1	0.08	0.04	83.19	1.00	0.200	0.100	1.133	0.763	83.203	1.042×10^{-3}	2.123	6a
		1.7			83.10						71.965	1.174×10^{-3}	1.992	6b
		1.1	0.16	0.08	83.14						83.203	2.108×10^{-3}	2.333	6c
		1.7			83.10						71.965	2.377×10^{-3}	2.190	6d
100	3.74	1.1	0.08	0.04	82.87	4.00	0.200	0.053	1.133	0.763	113.8	7.572×10^{-4}	2.460	7a
		1.7			83.78						98.41	8.021×10^{-4}	2.470	7b
		1.1	0.16	0.08	82.87						113.8	1.533×10^{-3}	2.705	7c
		1.7			83.78						98.41	1.623×10^{-3}	2.715	7d
100	7.00	1.1	0.08	0.04	42.14	4.00	0.200	0.029	1.133	0.763	155.7	1.268×10^{-4}	0.7910	8a
		1.7			41.16						134.6	1.225×10^{-4}	0.7494	8b
		1.1	0.16	0.08	42.19						155.7	2.566×10^{-4}	0.8694	8c
		1.7			41.16						134.6	2.479×10^{-4}	0.8237	8d
1000	2.00	1.1	0.08	0.04	126.6	4.00	0.200	0.100	1.133	1.644	179.3	4.016×10^{-5}	38.12	9a
		1.7			126.2						155.0	4.675×10^{-5}	34.96	9b
		1.1	0.16	0.08	126.6						179.3	8.130×10^{-5}	41.90	9c
		1.7			126.2						155.0	9.462×10^{-5}	38.43	9d
1000	3.74	1.1	0.08	0.04	124.3	4.00	0.200	0.053	1.133	1.644	245.1	5.659×10^{-5}	30.36	10a
		1.7			125.4						212.0	5.817×10^{-5}	33.83	10b
		1.1	0.16	0.08	124.3						245.1	1.145×10^{-4}	33.37	10c
		1.7			125.4						212.0	1.177×10^{-4}	30.78	10d
1000	7.00	1.1	0.08	0.04	64.95	10.00	0.200	0.029	1.133	1.644	335.4	8.986×10^{-6}	10.78	11a
		1.7			66.16						290.1	8.300×10^{-6}	11.96	11b
		1.1	0.16	0.08	64.95						335.4	1.819×10^{-6}	11.95	11c
		1.7			66.16						290.1	1.680×10^{-5}	13.15	11d

Table 1 (Concluded)

W in tons	ℓ/b	w/S	K_{D_s}	K_{D_D}	V_k Design	H Design (ft)	C_L	C_{D_e}	C_1	C_6	ℓ	C_2	A_p (ft^2)	Figure
10,000	2.00	1.1	0.08	0.04	166.0	7.00	0.200	0.100	1.133	3.541	386.2	2.079×10^{-6}	377.1	12a
		1.7			166.7						334.0	2.282×10^{-6}	364.8	12b
		1.1	0.16	0.08	166.0						386.2	4.208×10^{-6}	414.5	12c
		1.7			166.7						334.0	[illegible]	401.0	12d
10,000	3.74	1.1	0.08	0.04	166.9	7.00	0.200	0.053	1.133	3.541	528.1	[illegible] $\times 10^{-6}$	436.4	13a
		1.7			166.1						456.8	1.599×10^{-6}	430.8	13b
		1.1	0.16	0.08	166.9						528.1	3.251×10^{-6}	479.7	13c
		1.7			166.1						456.8	3.236×10^{-6}	473.5	13d
10,000	7.00	1.1	0.08	0.04	90.80	10.00	0.200	0.029	1.133	3.541	722.5	7.064×10^{-6}	106.0	14a
		1.7			92.89						624.9	6.003×10^{-8}	123.0	14b
		1.1	0.16	0.08	90.80						722.5	1.430×10^{-7}	116.5	14c
		1.7			92.89						624.9	1.215×10^{-7}	135.3	14d
100,000	2.00	1.1	0.08	0.04	165.6	7.00	0.200	0.100	1.133	7.628	832.0	4.863×10^{-8}	2452	15a
		1.7			167.6						719.6	3.959×10^{-8}	2817	15b
		1.1	0.16	0.08	165.6						832.0	9.843×10^{-6}	2695	15c
		1.7			167.6						719.6	8.013×10^{-8}	3097	15d
100,000	3.74	1.1	0.08	0.04	165.2	7.00	0.200	0.053	1.133	7.628	1137.8	4.899×10^{-8}	2424	16a
		1.7			164.2						984.1	3.426×10^{-8}	2848	16b
		1.1	0.16	0.08	165.2						1137.8	9.915×10^{-6}	2665	16c
		1.7			164.2						984.1	6.934×10^{-8}	3131	16d
100,000	7.00	1.1	0.08	0.04	126.6	10.00	0.200	0.029	1.133	7.628	1556.6	5.970×10^{-8}	988.2	17a
		1.7			123.9						1346.3	4.470×10^{-8}	1071	17b
		1.1	0.16	0.08	126.6						1556.6	1.208×10^{-8}	1086	17c
		1.7			123.9						1346.3	9.049×10^{-8}	1178	17d

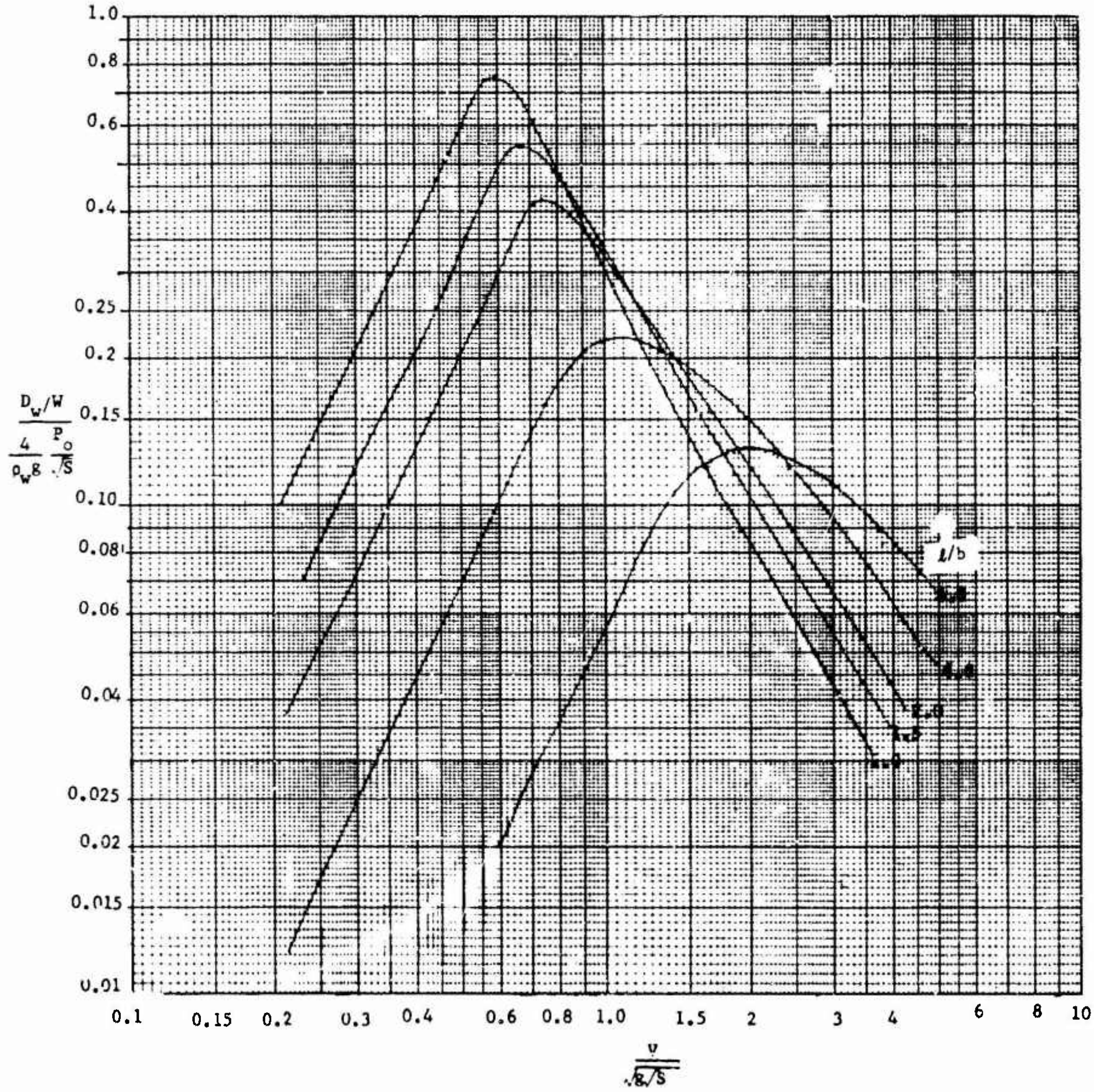

Figure 1 - Wavemaking Drag of Rectangular Planform

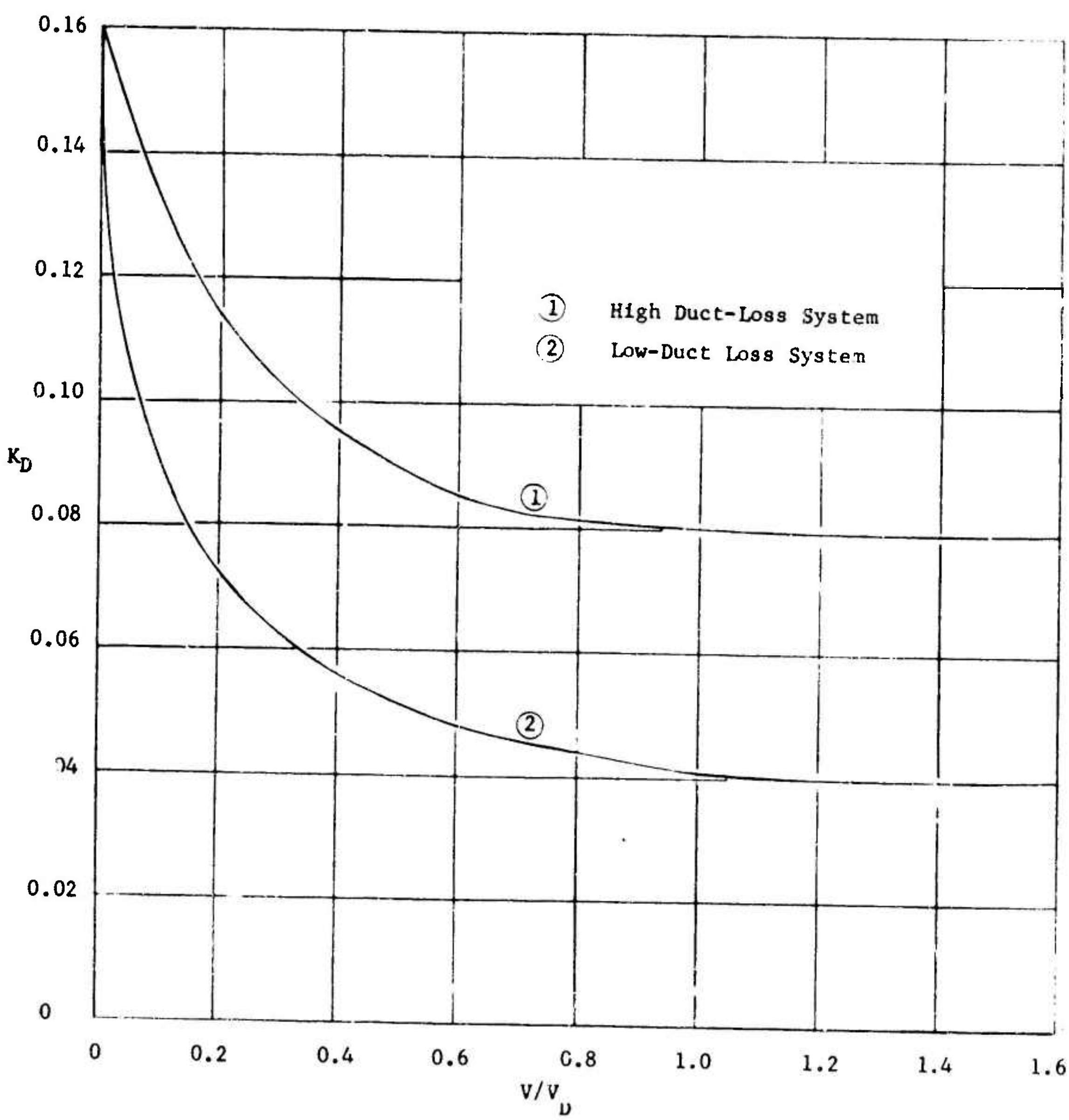

Figure 2 - Assumed Parabolic Variations of Duct Loss Coefficient, K_D

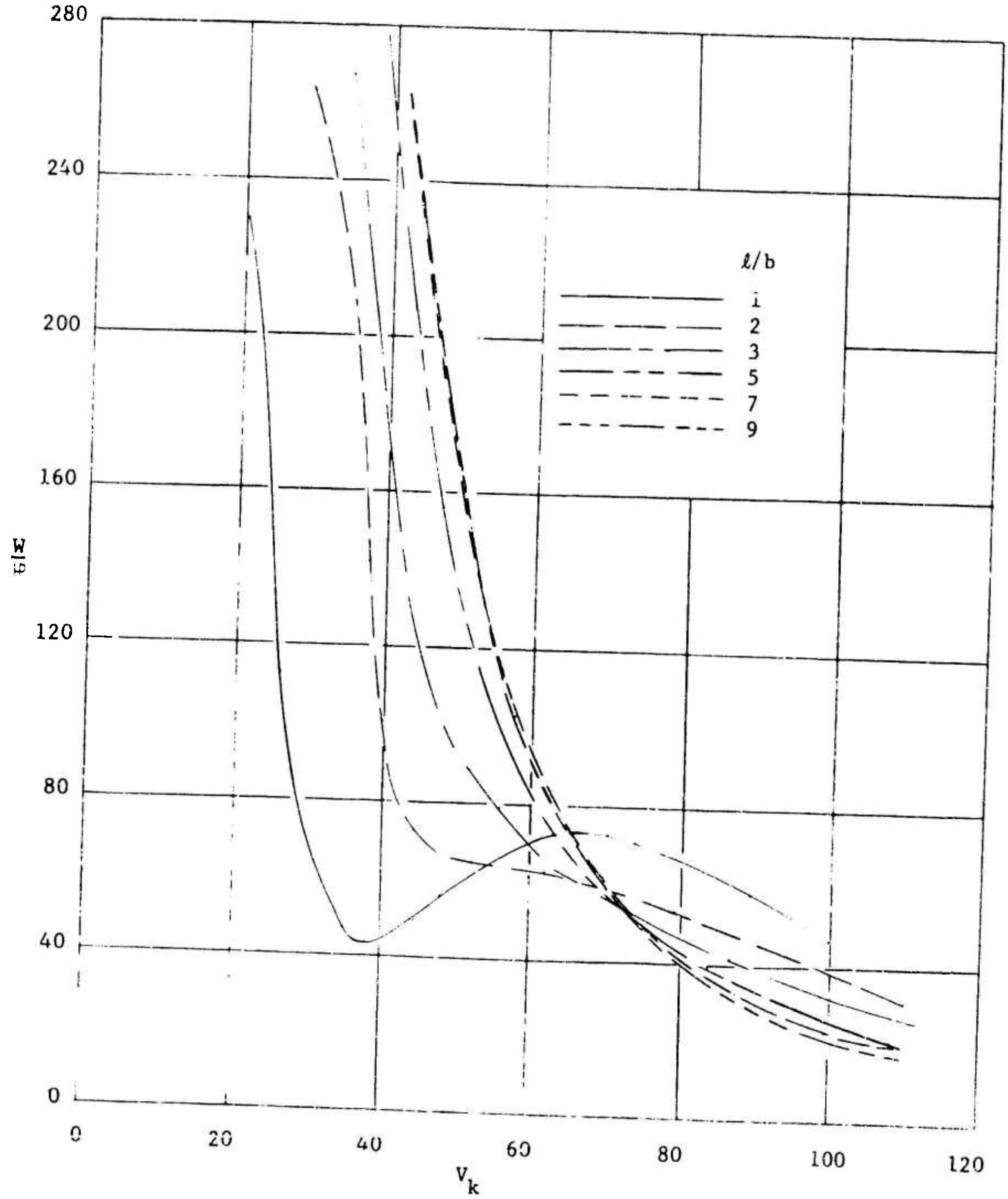

Figure 3 - Effect of Length-to-Beam Ratio on CAB Performance
W = 20,000 Tons; H = 10 Feet; $w/\sqrt{S}$ = 1.1 lb/ft^3

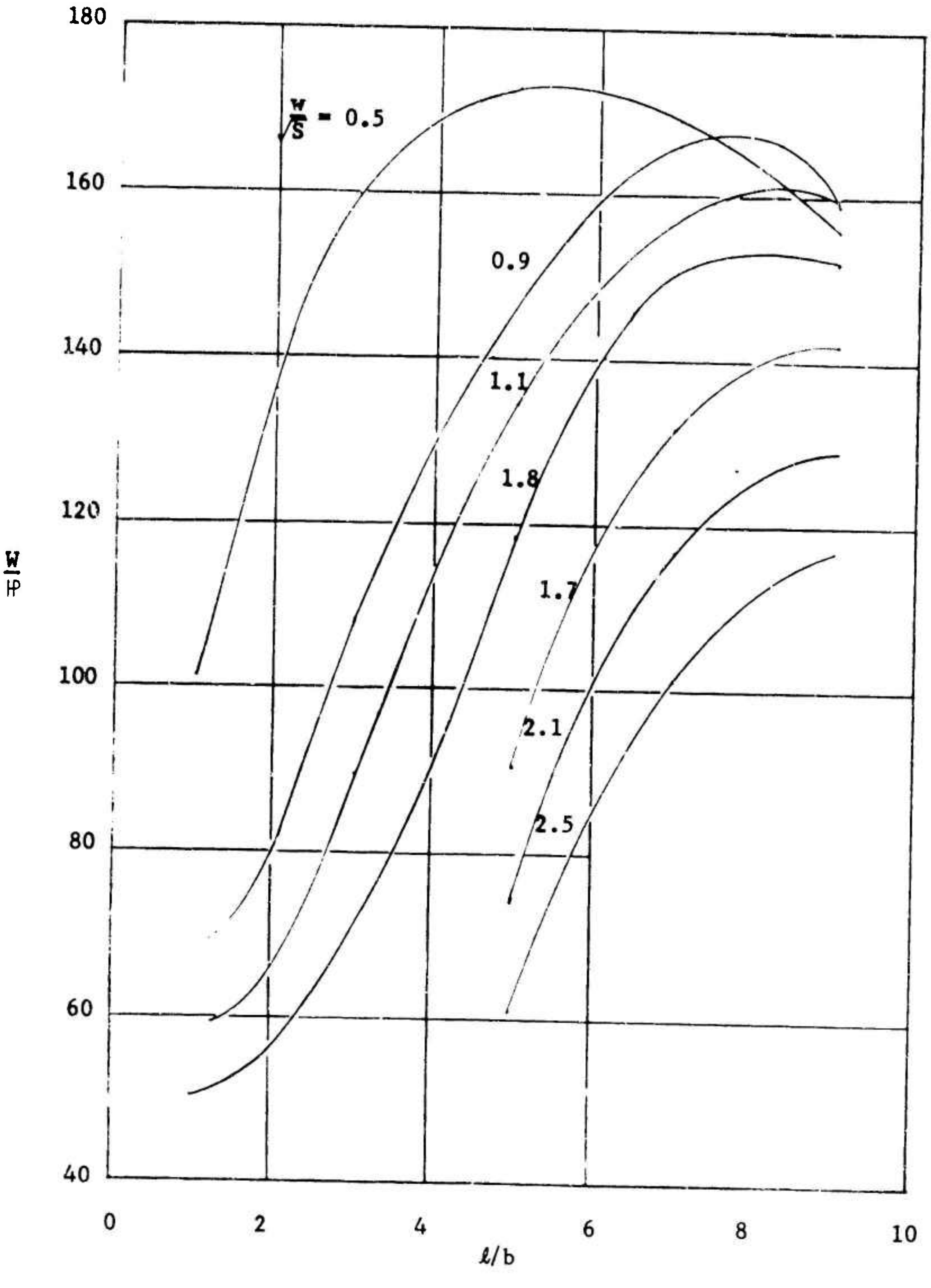

Figure 4 - Effect of Specific Cushion Loading on CAB Performance
$W = 20{,}000$ Tons; $V_k = 50$ Knots; $H = 10$ Feet

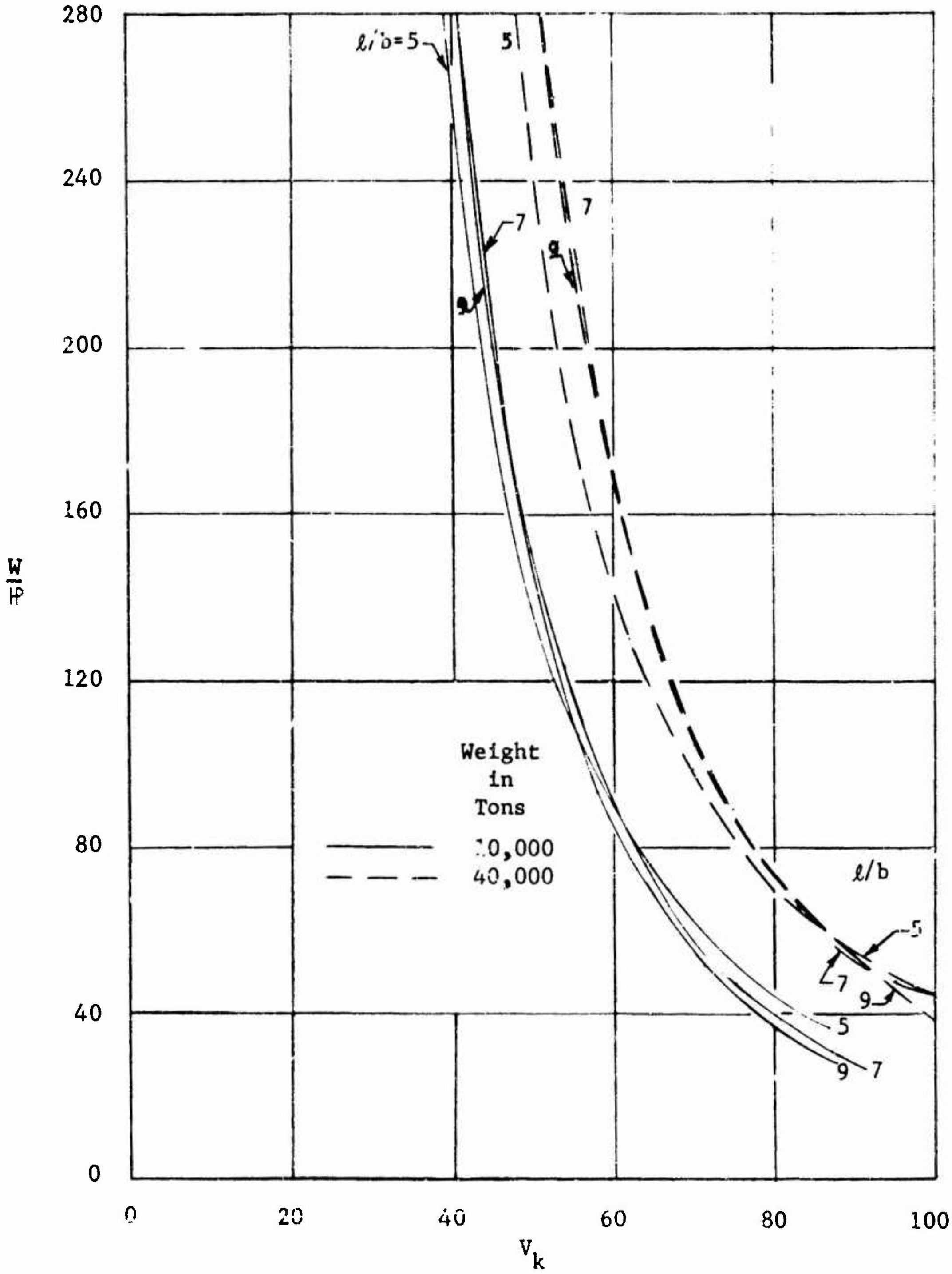

Figure 5 - Effect of Weight Variation on CAB Performance
H = 10 Feet; $w/\sqrt{S}$ = 1.1 lb/ft^3

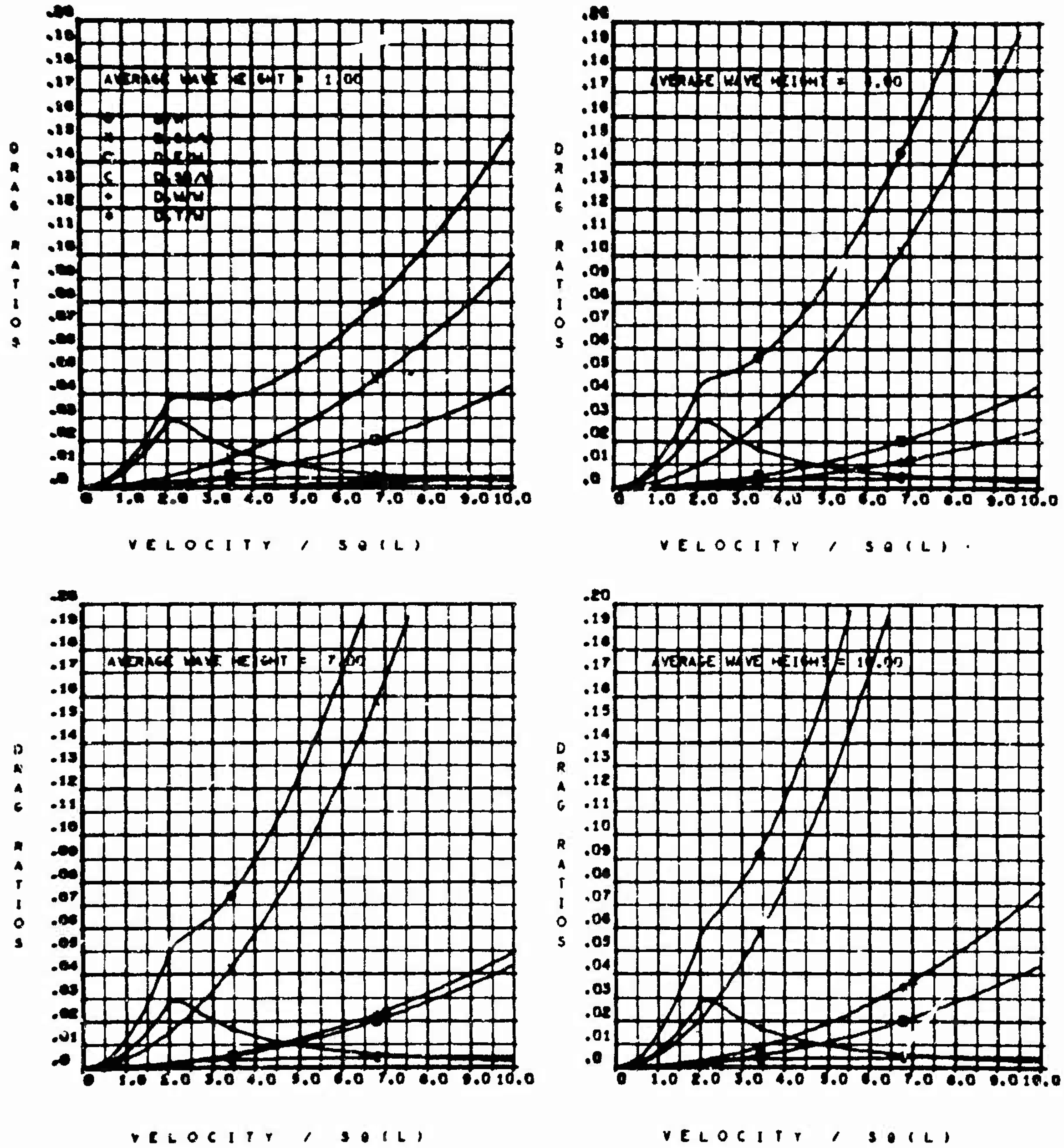

DRAG RATIOS VERSUS VELOCITY / SQ(L)

Figure 6 - General Performance Parameters of 100 Ton CAB

With $\ell/b = 2.0$

(a) $K_{D_D} = 0.04$, $K_{D_s} = 0.08$, $w/\sqrt{S} = 1.1$

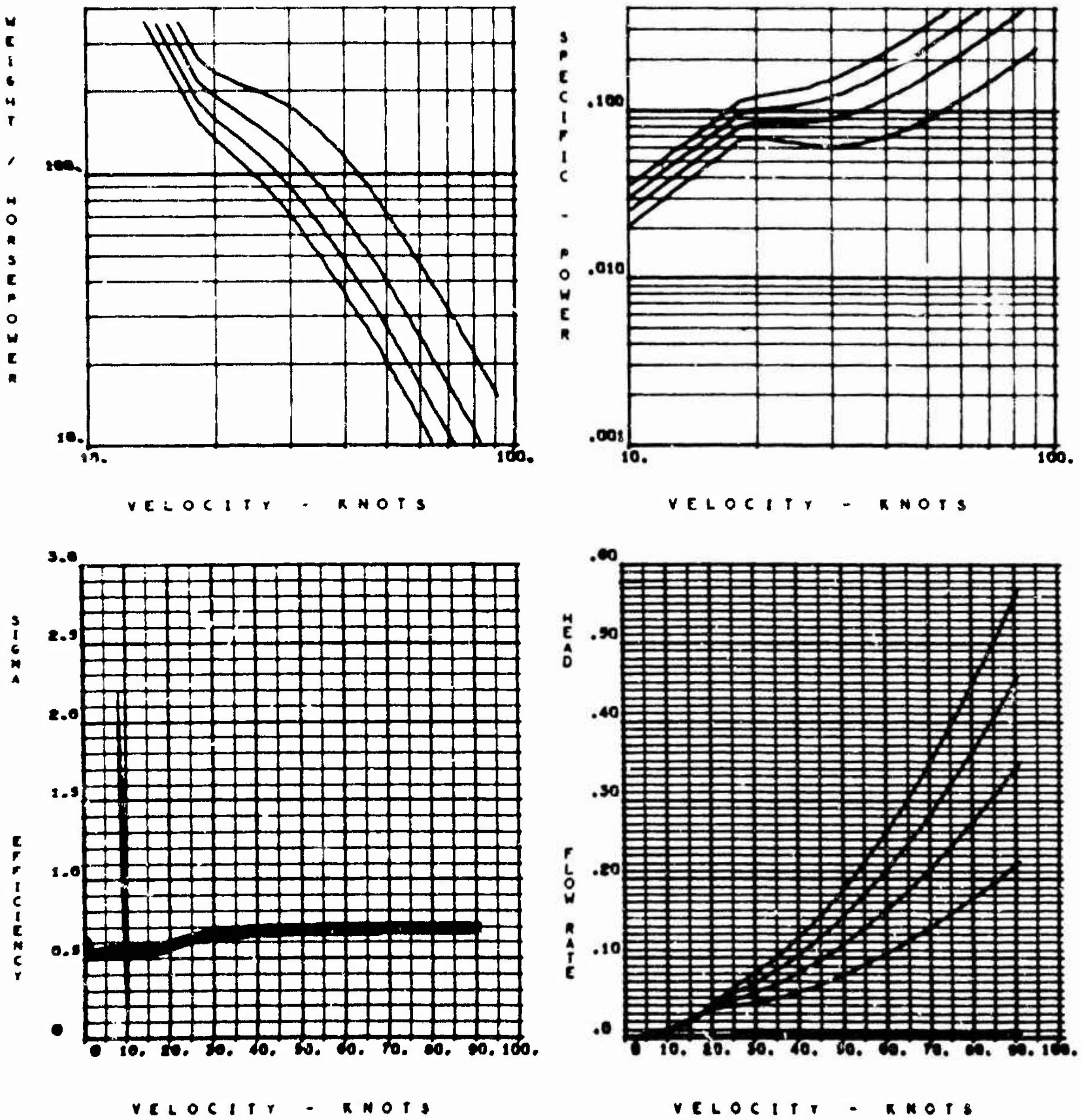

Figure 6 (Continued)

(a) Concluded

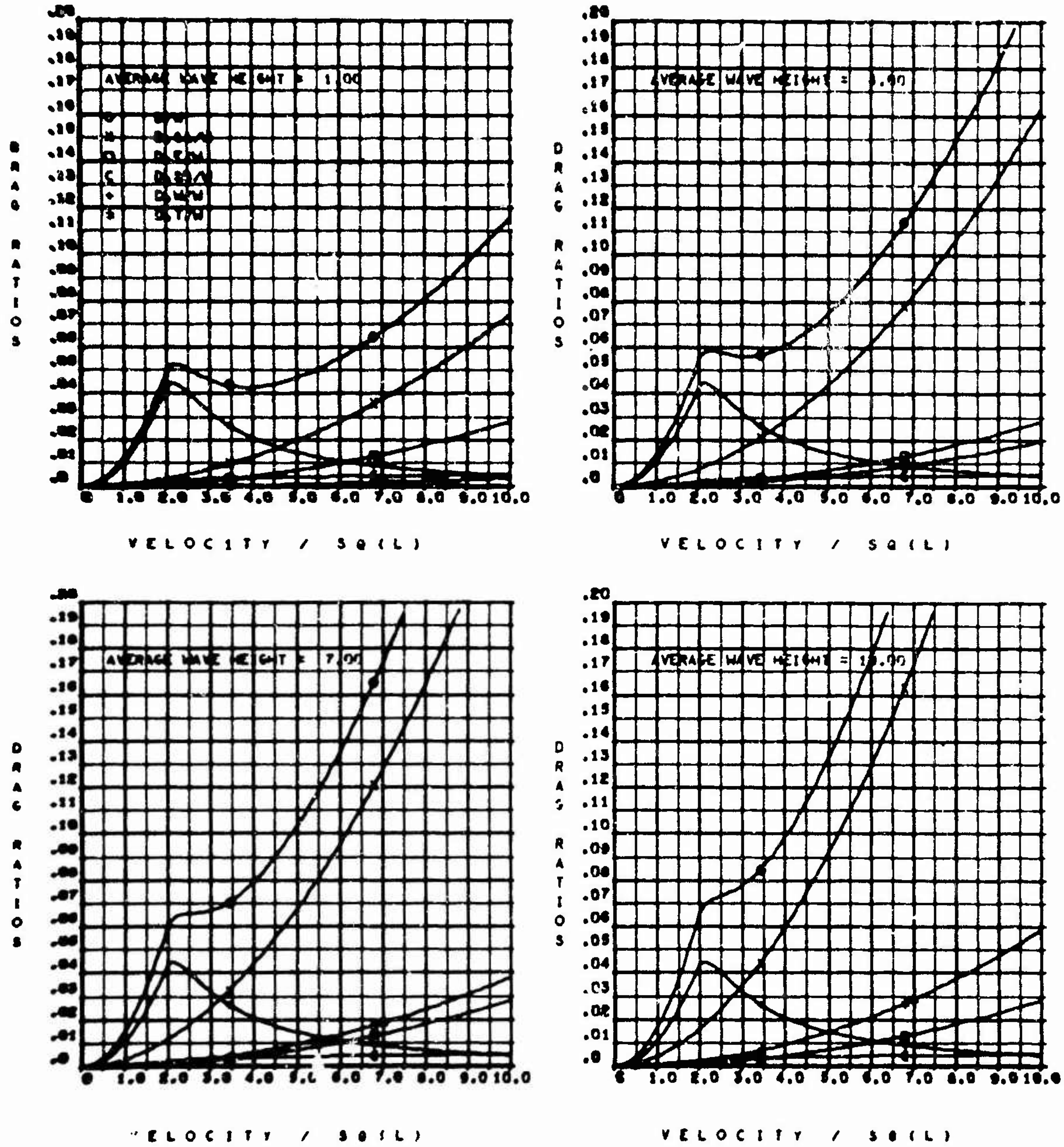

DRAG RATIOS VERSUS VELOCITY / SQ(L)

Figure 6 (Continued)

(b) $K_{D_D} = 0.04$, $K_{D_s} = 0.08$, $w/\sqrt{S} = 1.7$

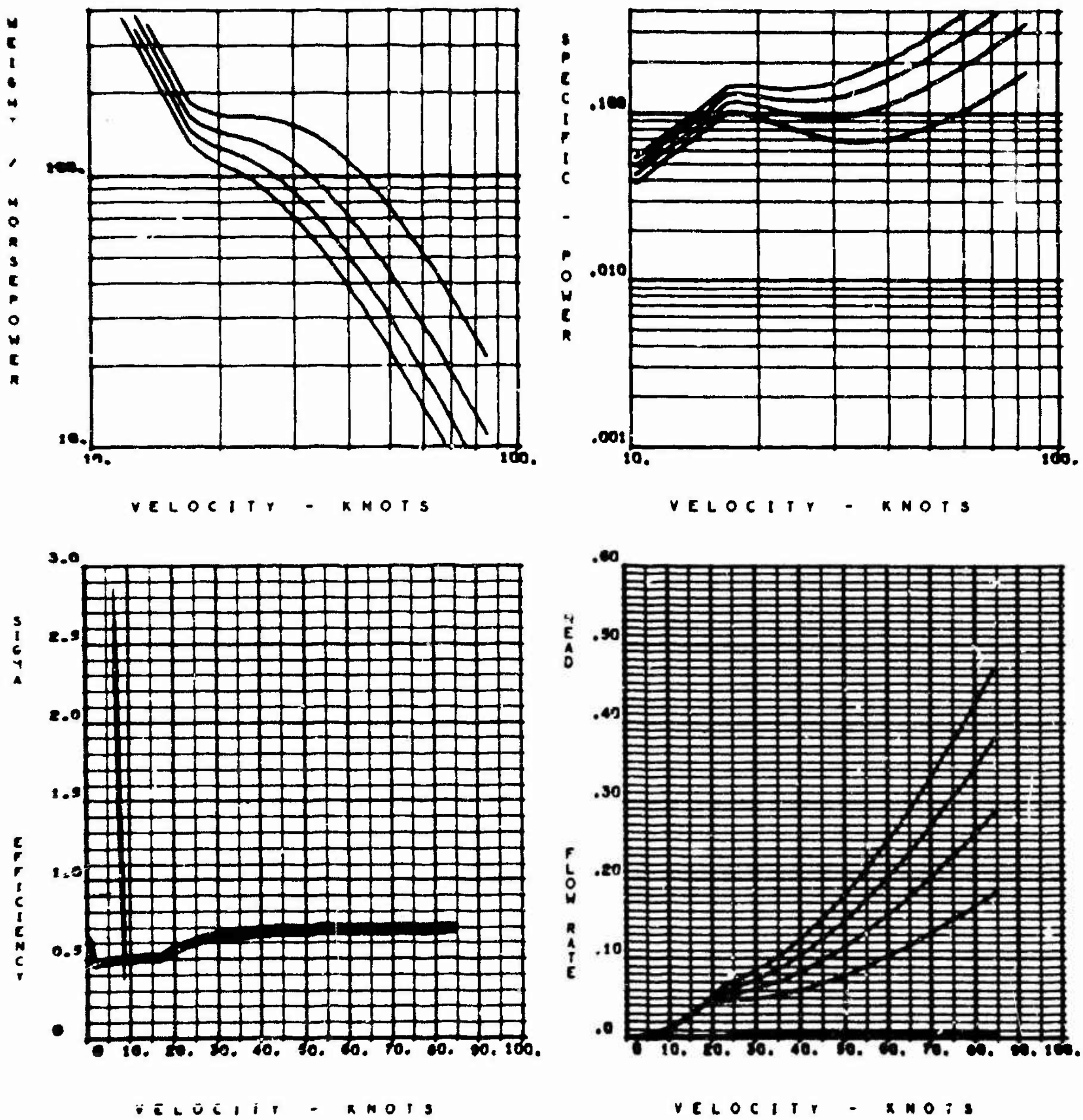

Figure 6 (Continued)

(b) Concluded

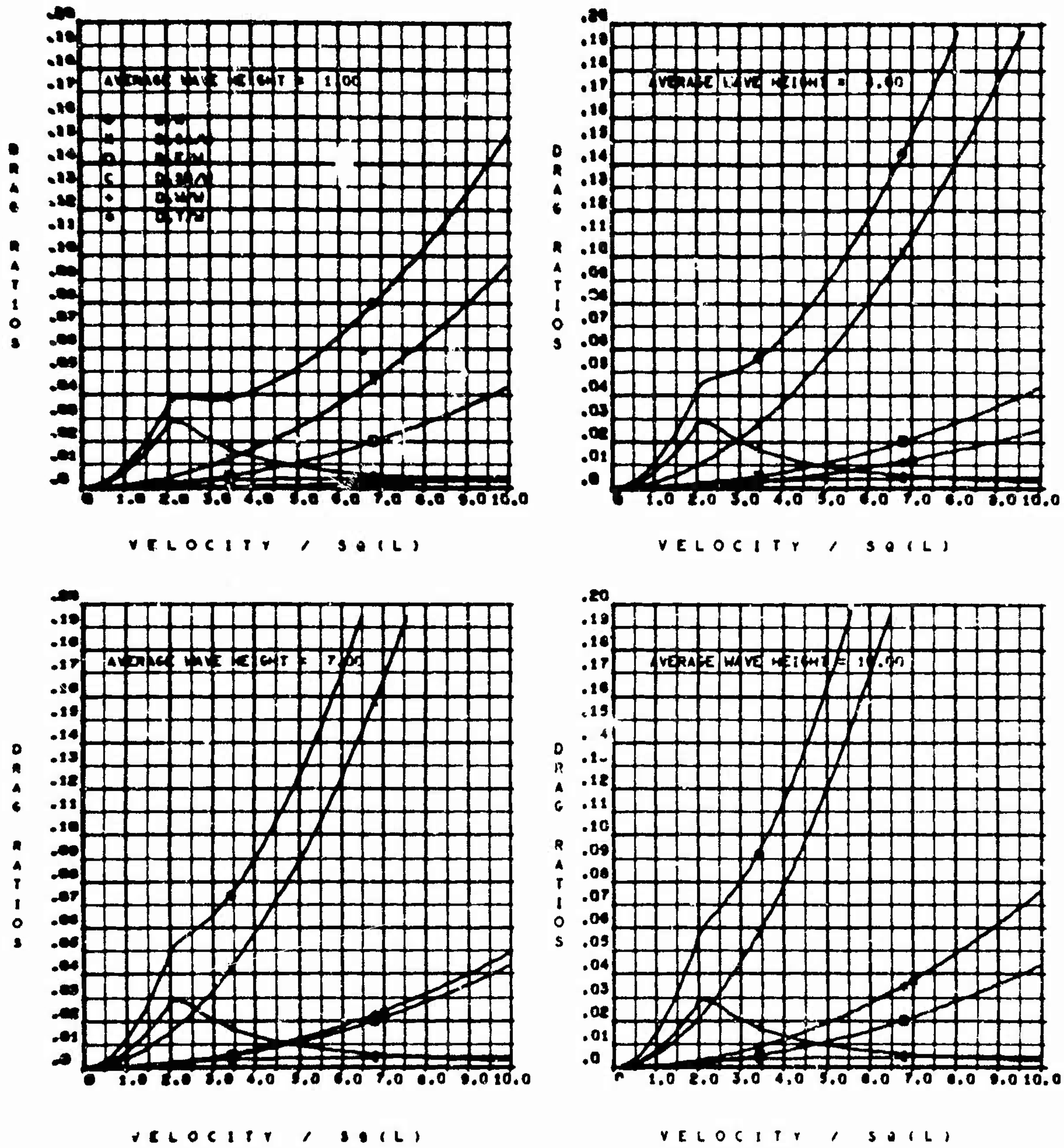

DRAG RATIOS VERSUS VELOCITY / SQ(L)

Figure 6 (Continued)

(c) $K_{D_D} = 0.08$, $K_{D_s} = 0.16$, $w/\sqrt{S} = 1.1$

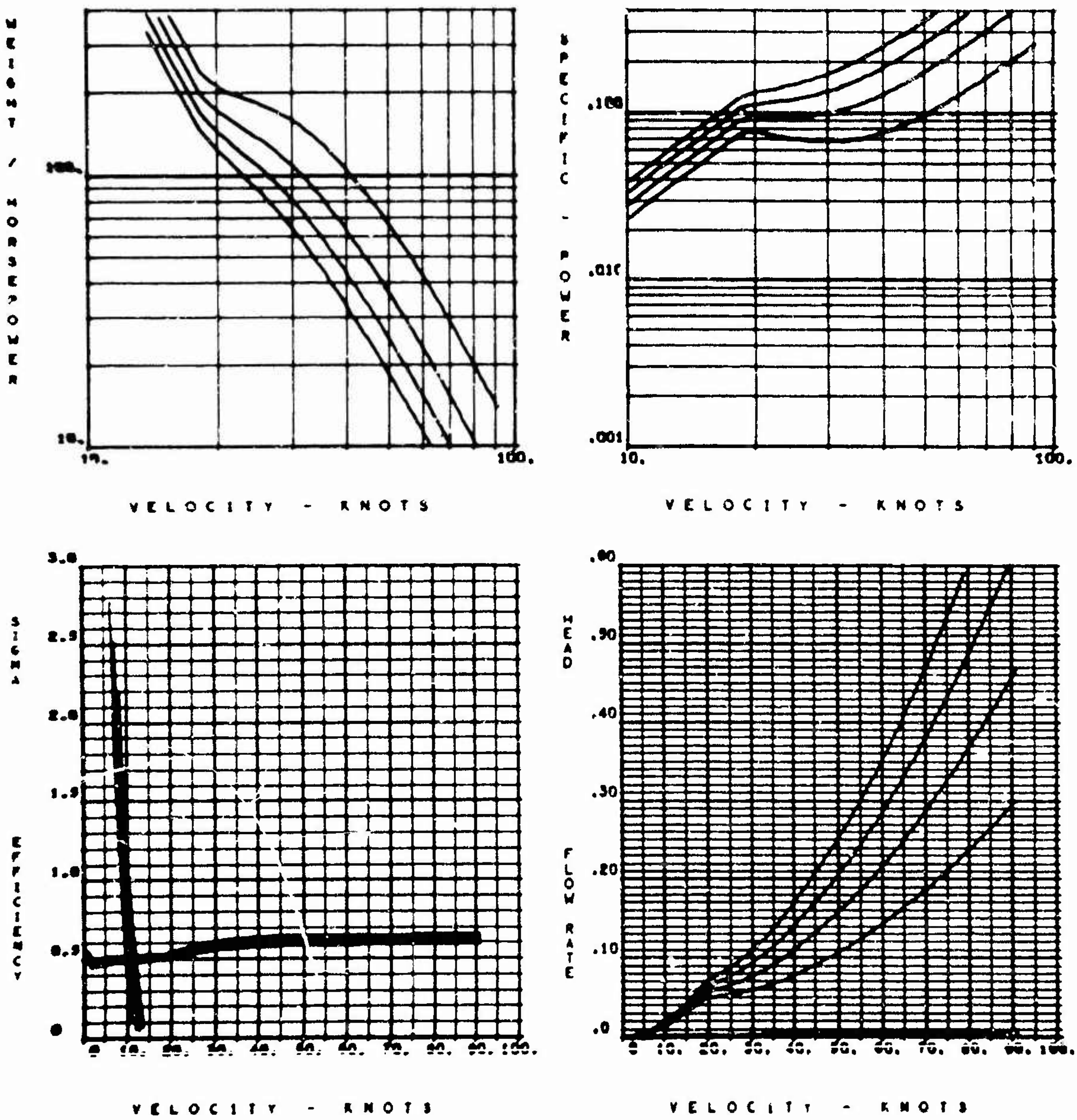

Figure 6 (Continued)
(c) Concluded

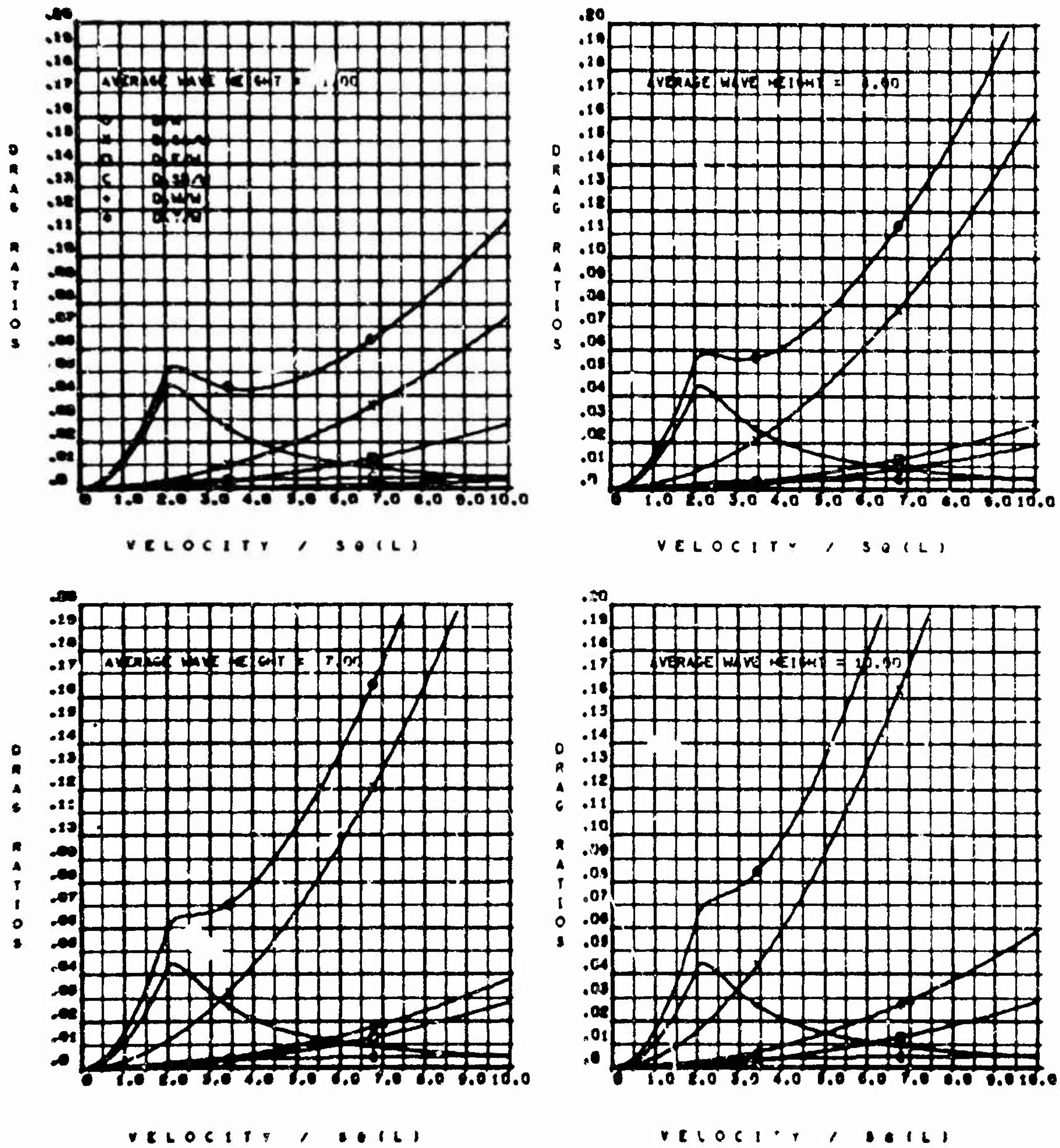

DRAG RATIOS VERSUS VELOCITY / SQ(L)

Figure 6 (Continued)

(d) $K_{D_D} = 0.08$, $K_{D_s} = 0.16$, $w/\sqrt{S} = 1.7$

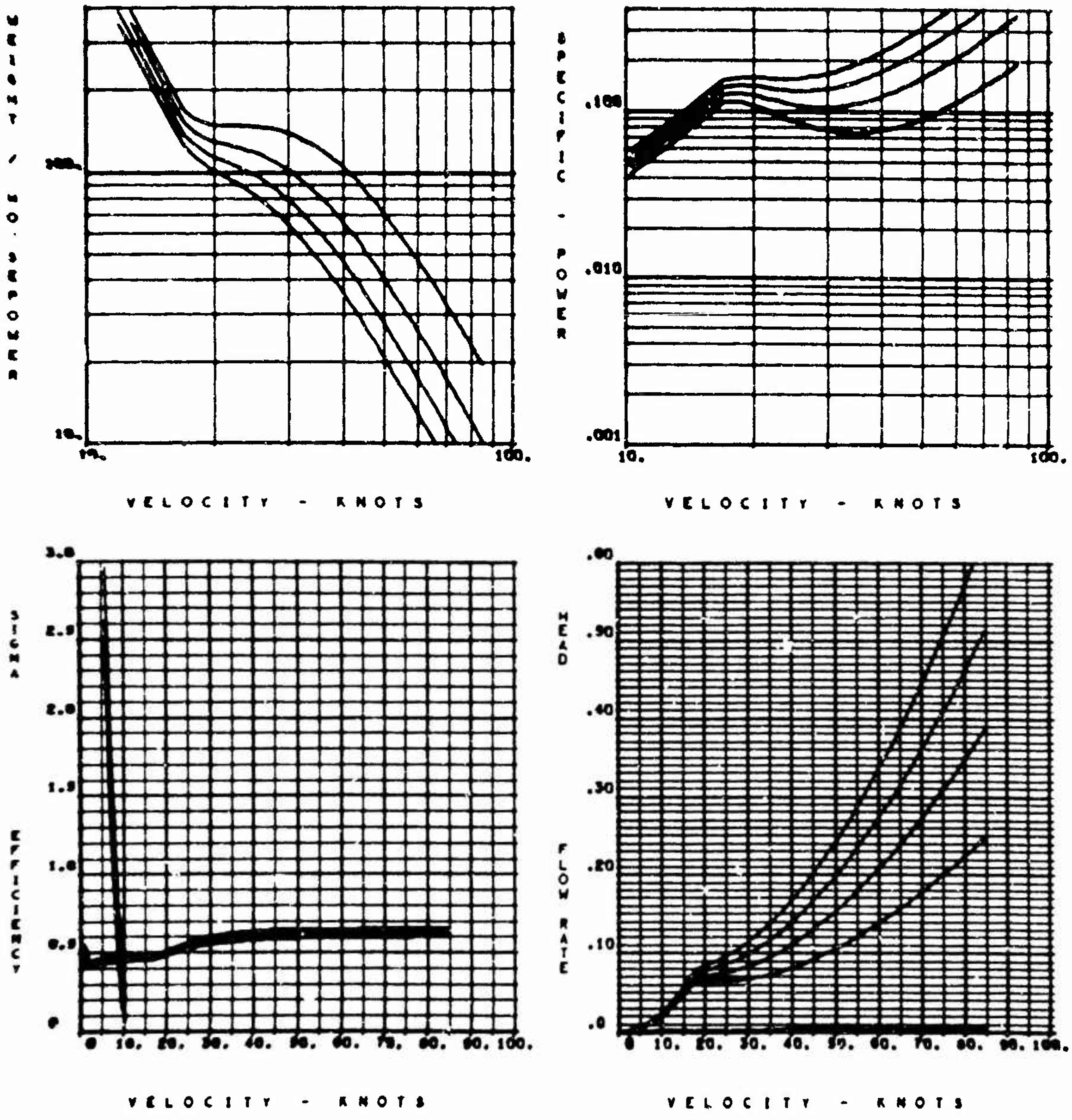

Figure 6 (Concluded)

(d) Concluded

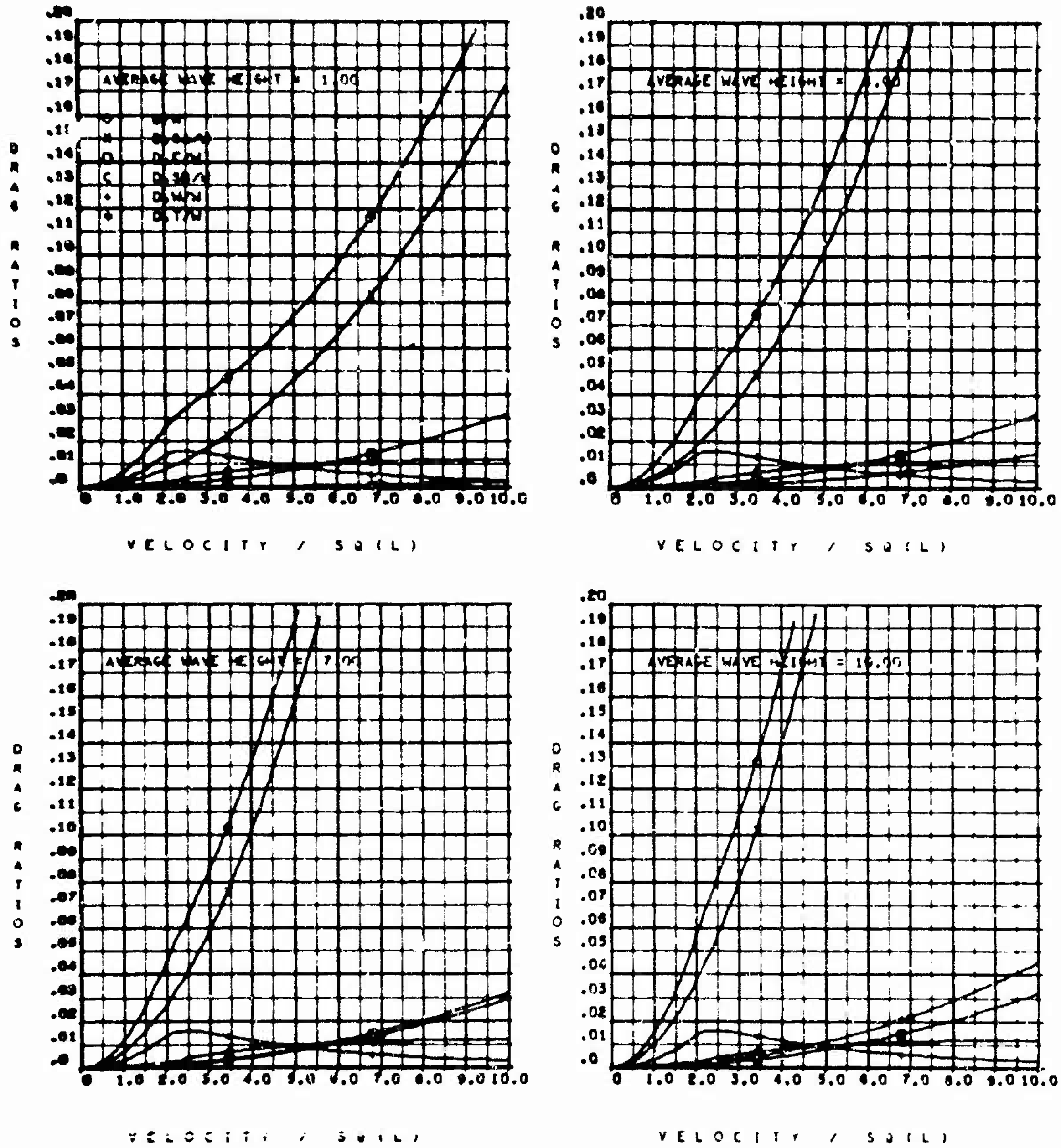

DRAG RATIOS VERSUS VELOCITY / SQ(L)

Figure 7 - General Performance Parameters of 100 Ton CAB

With $\ell/b = 3.74$

(a) $K_{D_D} = 0.04$, $K_{D_S} = 0.08$, $w/S = 1.1$

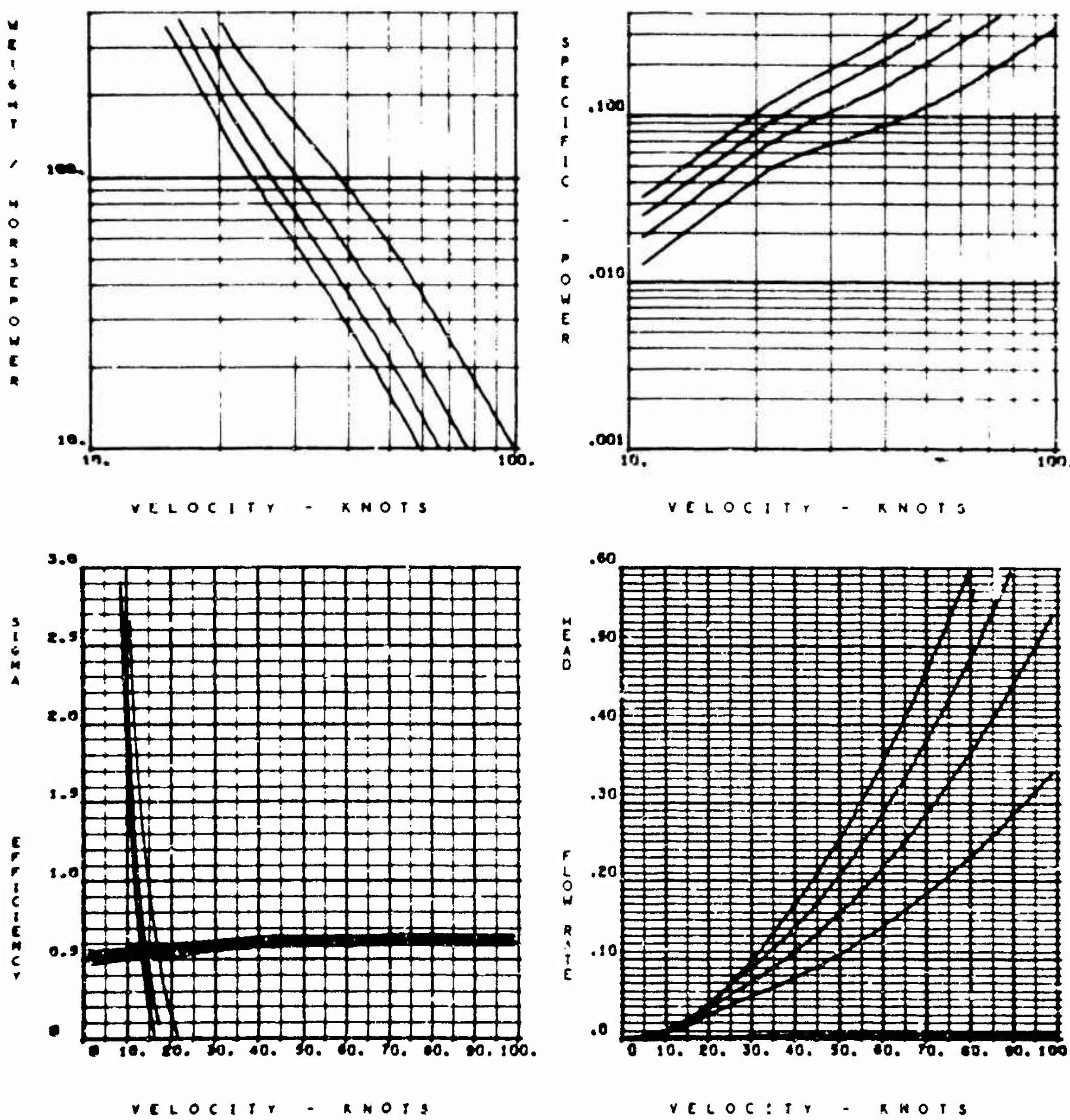

Figure 7 (Continued)

(a) Concluded

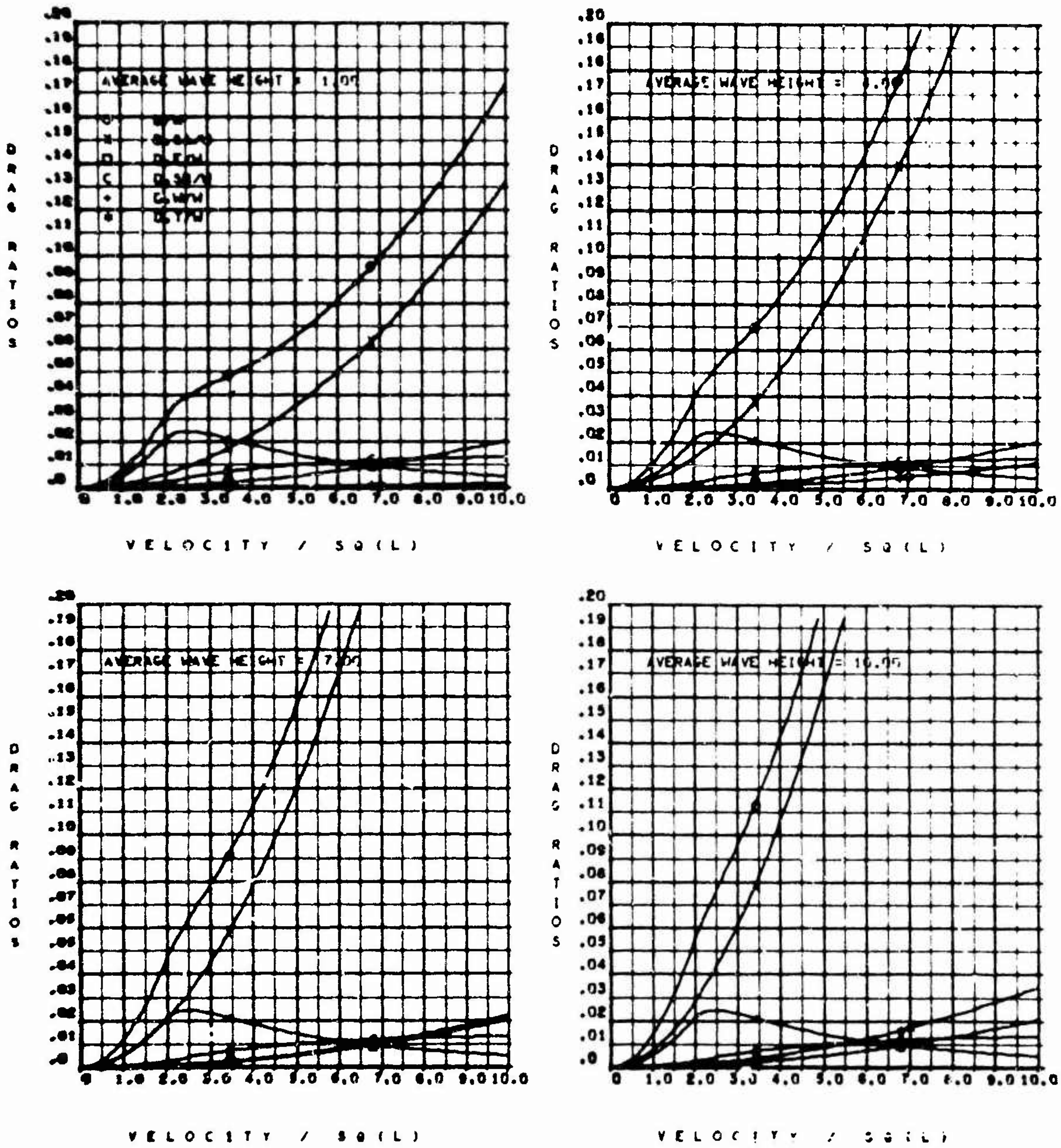

DRAG RATIOS VERSUS VELOCITY / SQ(L)

Figure 7 (Continued)

(b) $K_{D_D} = 0.04$, $K_{D_s} = 0.08$, $w/\Delta S = 1.7$

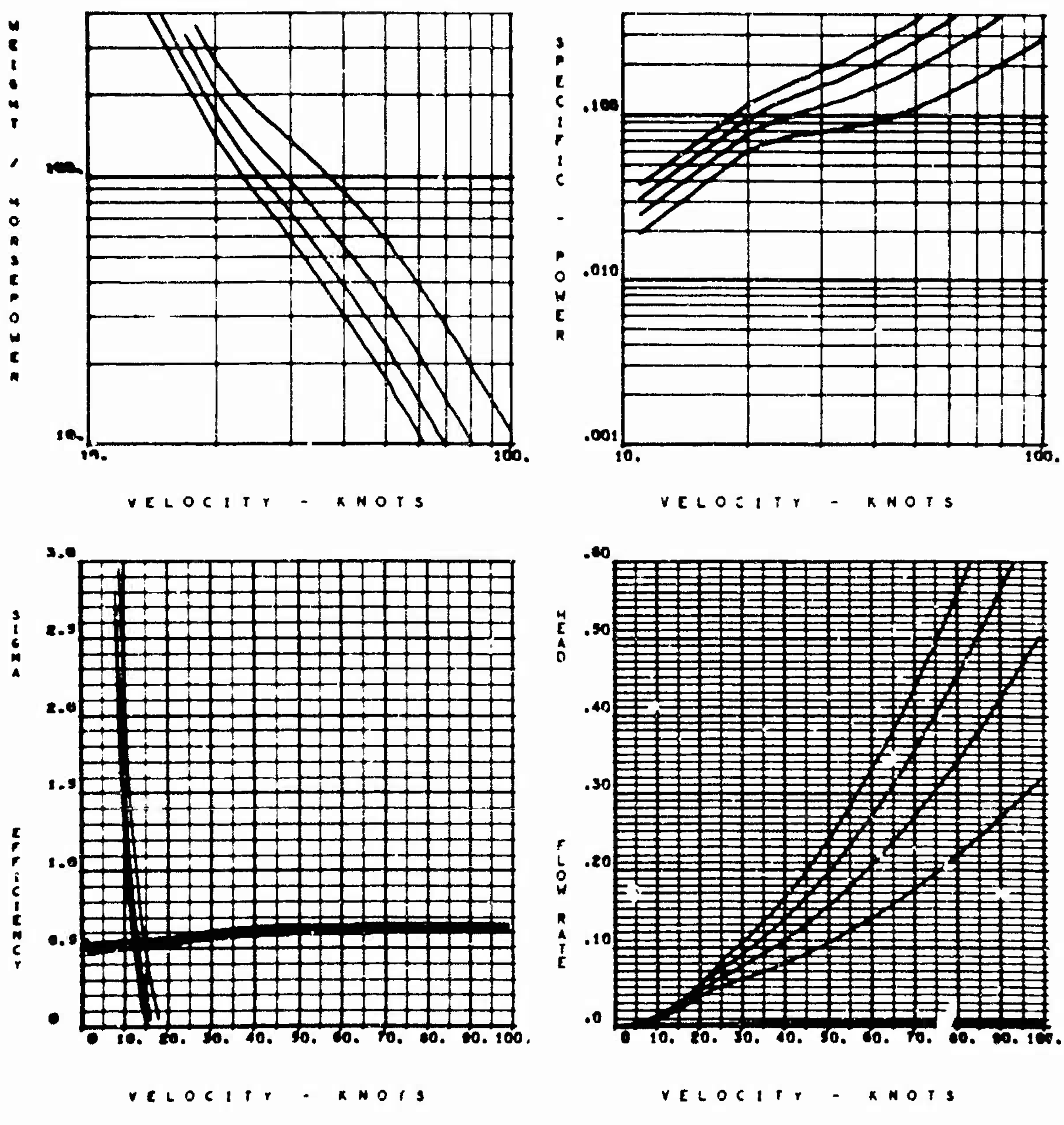

Figure 7 (Continued)

(b) Concluded

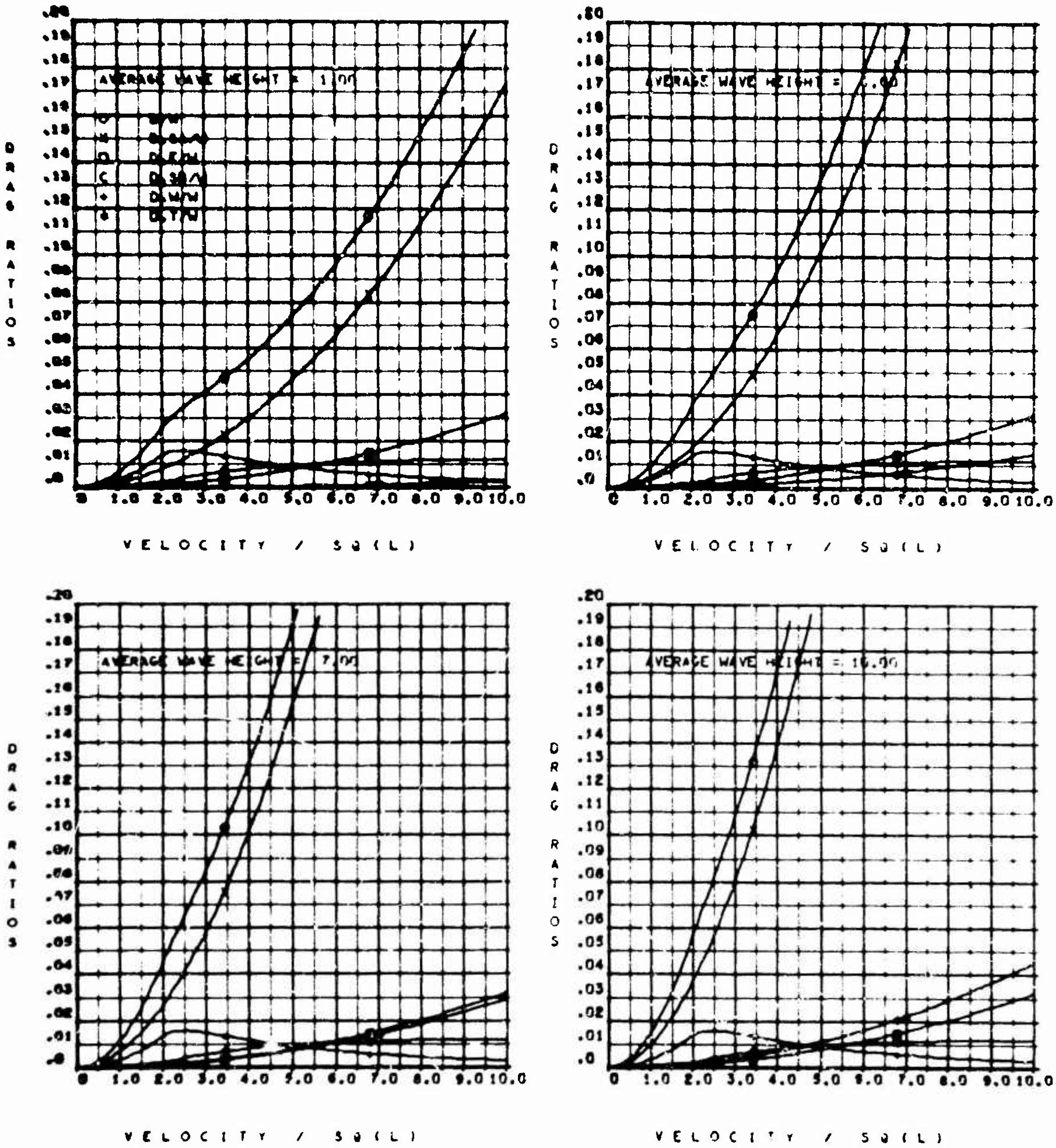

DRAG RATIOS VERSUS VELOCITY / SQ(L)

Figure 7 (Continued)

(c) $K_{D_D} = 0.08$, $K_{D_s} = 0.16$, $w/S = 1.1$

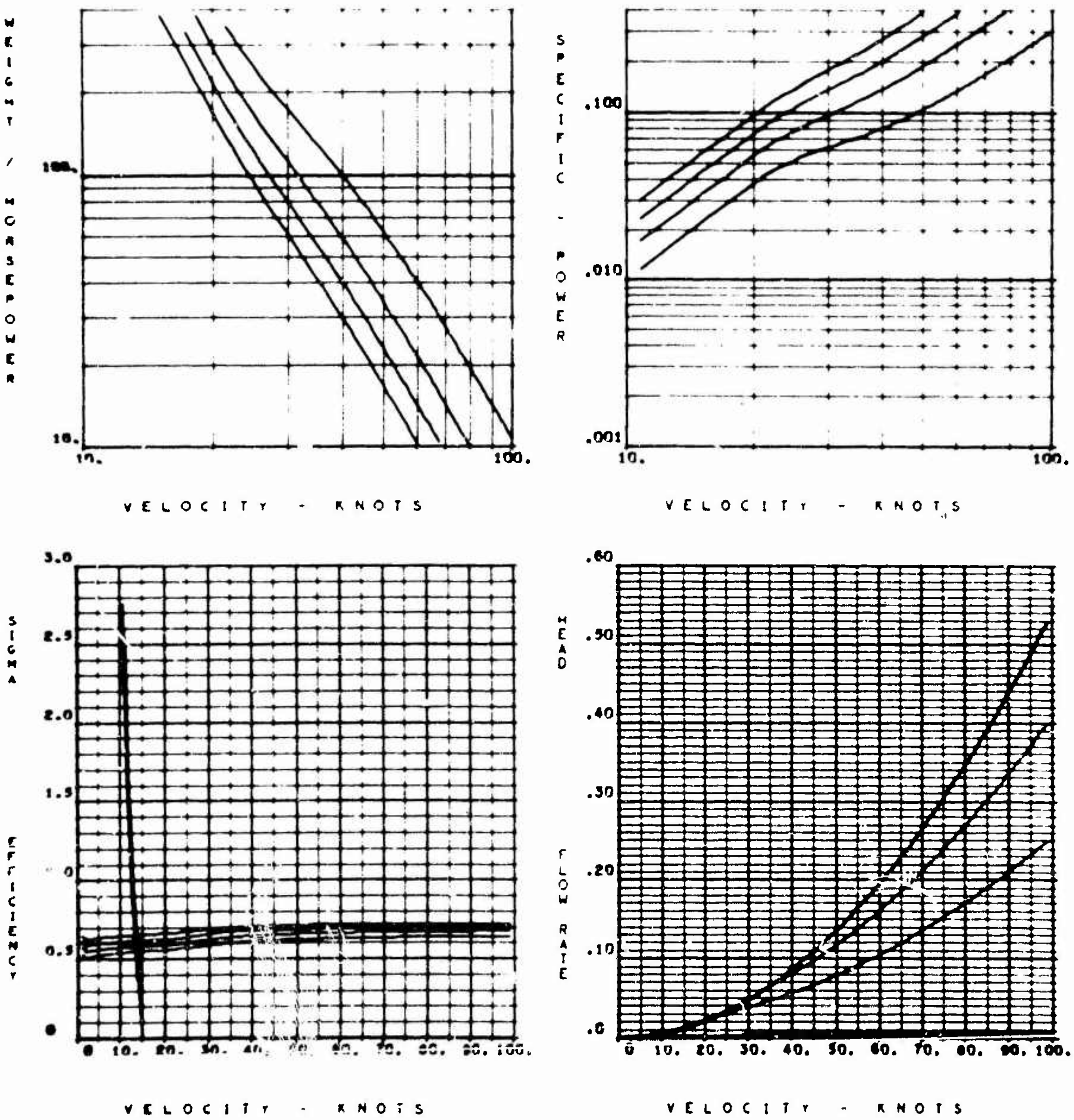

Figure 7 (Continued)

(c) Concluded

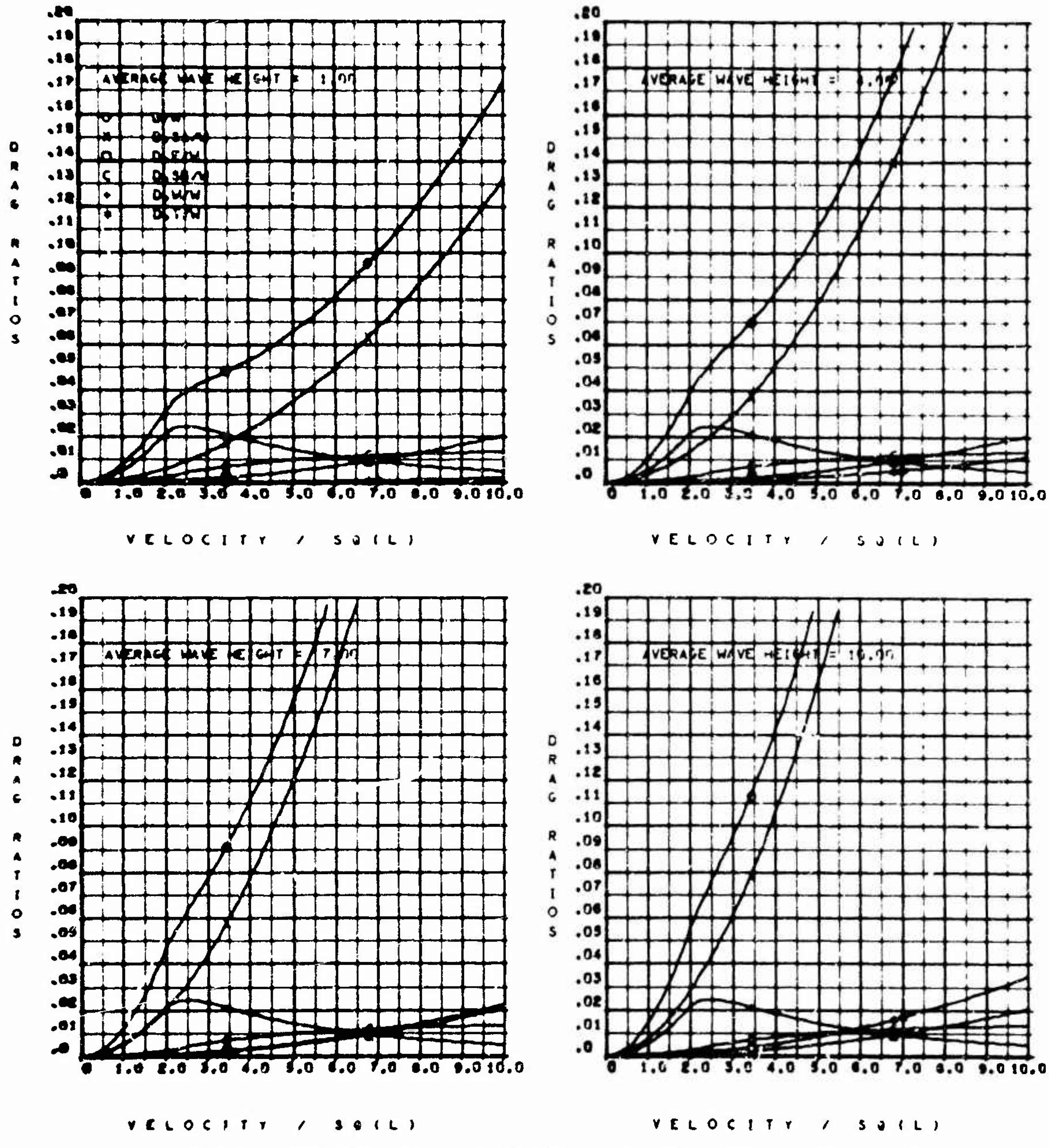

DRAG RATIOS VERSUS VELOCITY / SQ(L)

Figure 7 (Continued)

(d) $K_{D_D} = 0.08$, $K_{D_S} = 0.16$, $w/\sqrt{S} - 1.7$

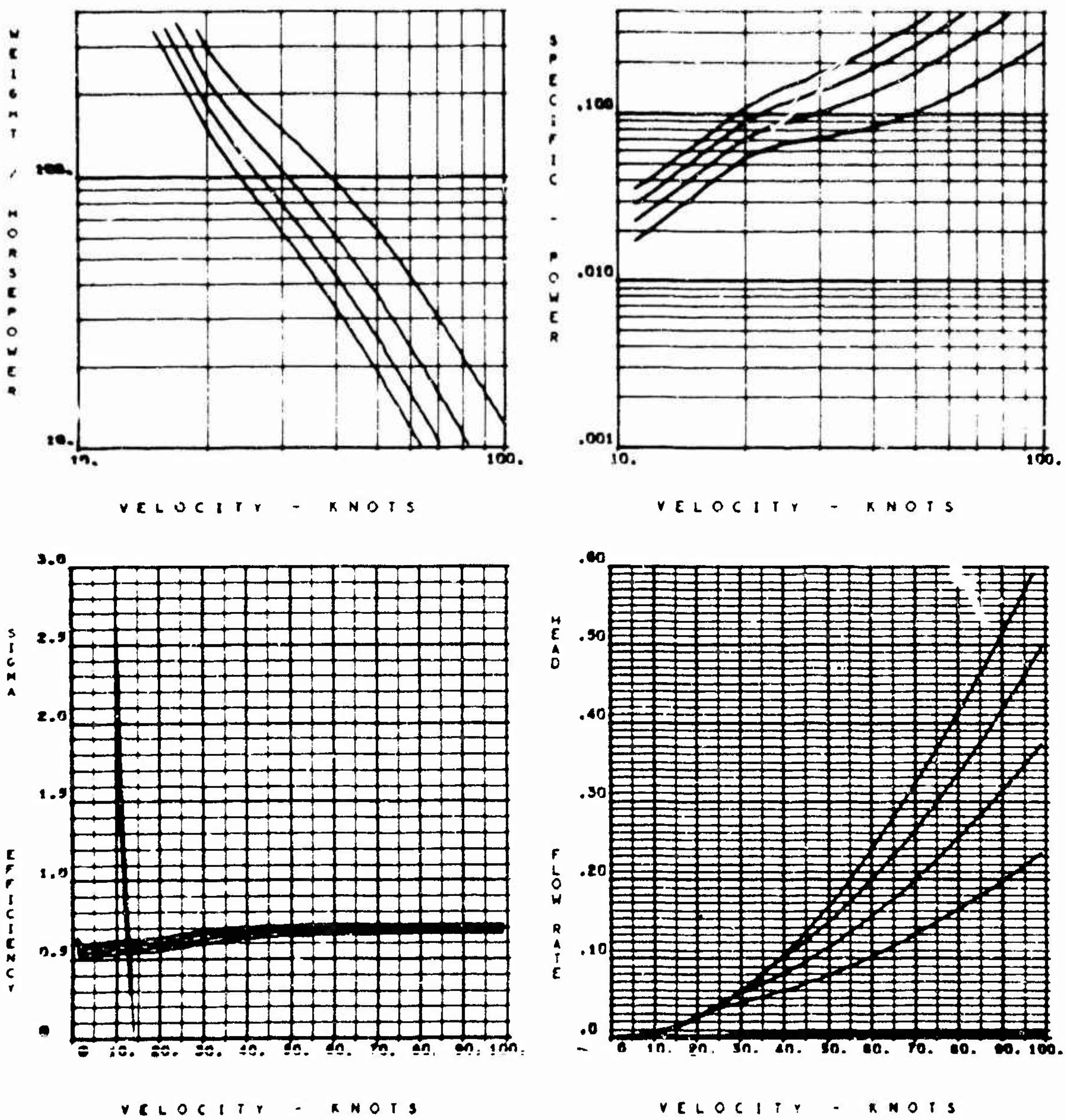

Figure 7 (Concluded)

(d) Concluded

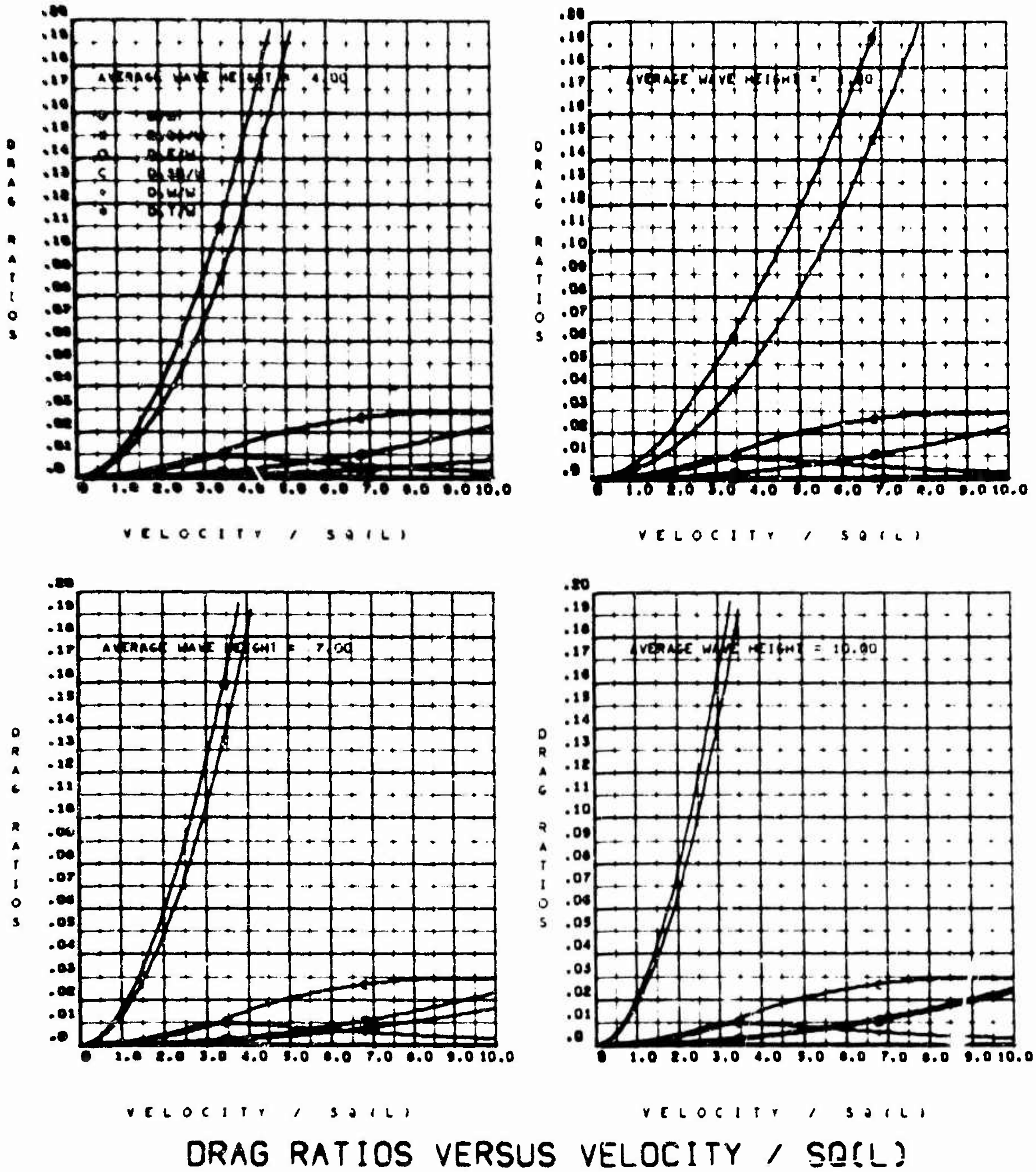

Figure 8 - General Performance Parameters of 100 Ton CAB
With $\ell/b = 7.0$

(a) $K_{D_D} = 0.04$, $K_{D_s} = 0.08$, $w/\sqrt{S} = 1.1$

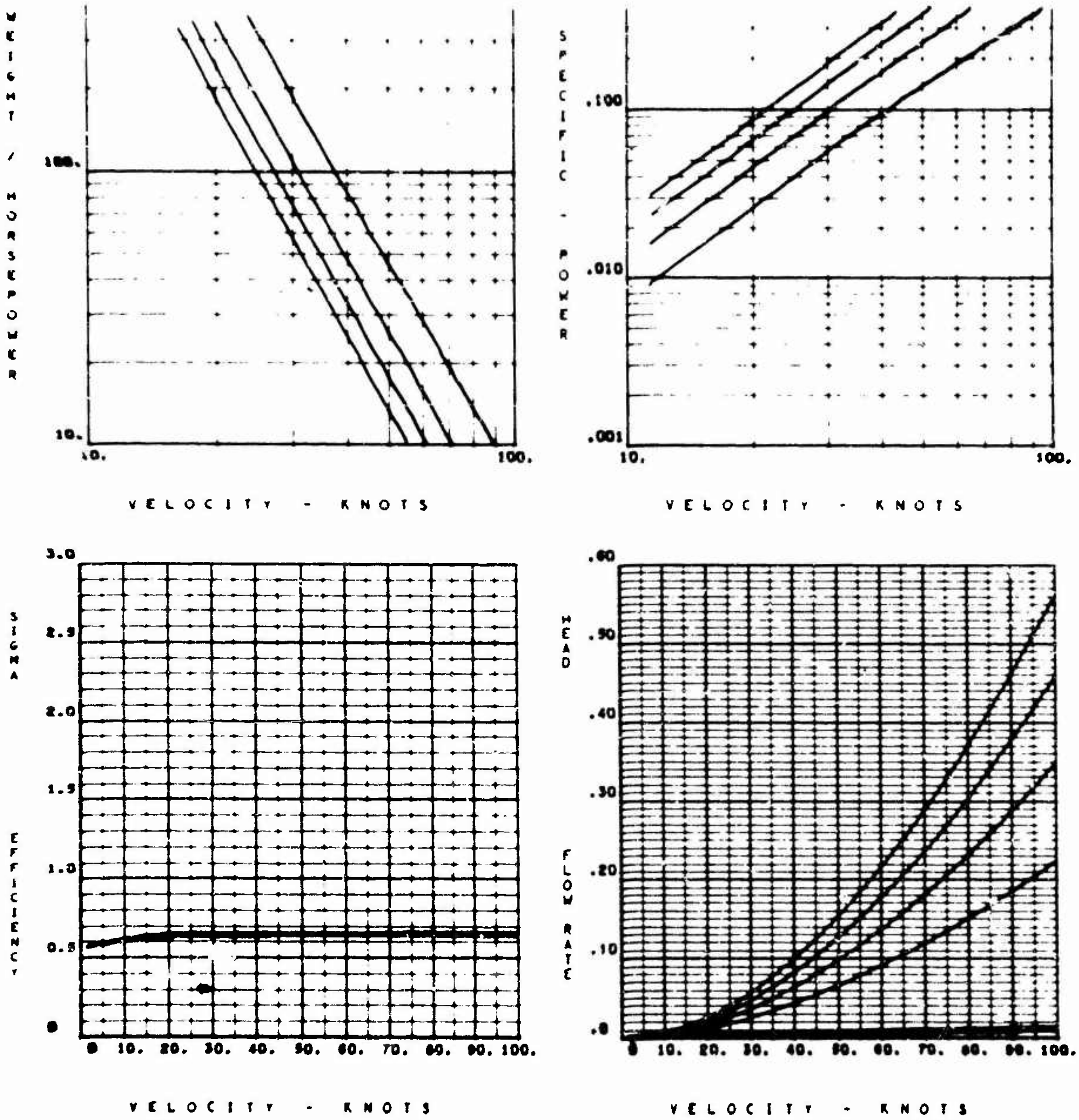

Figure 8 (Continued)

(a) Concluded

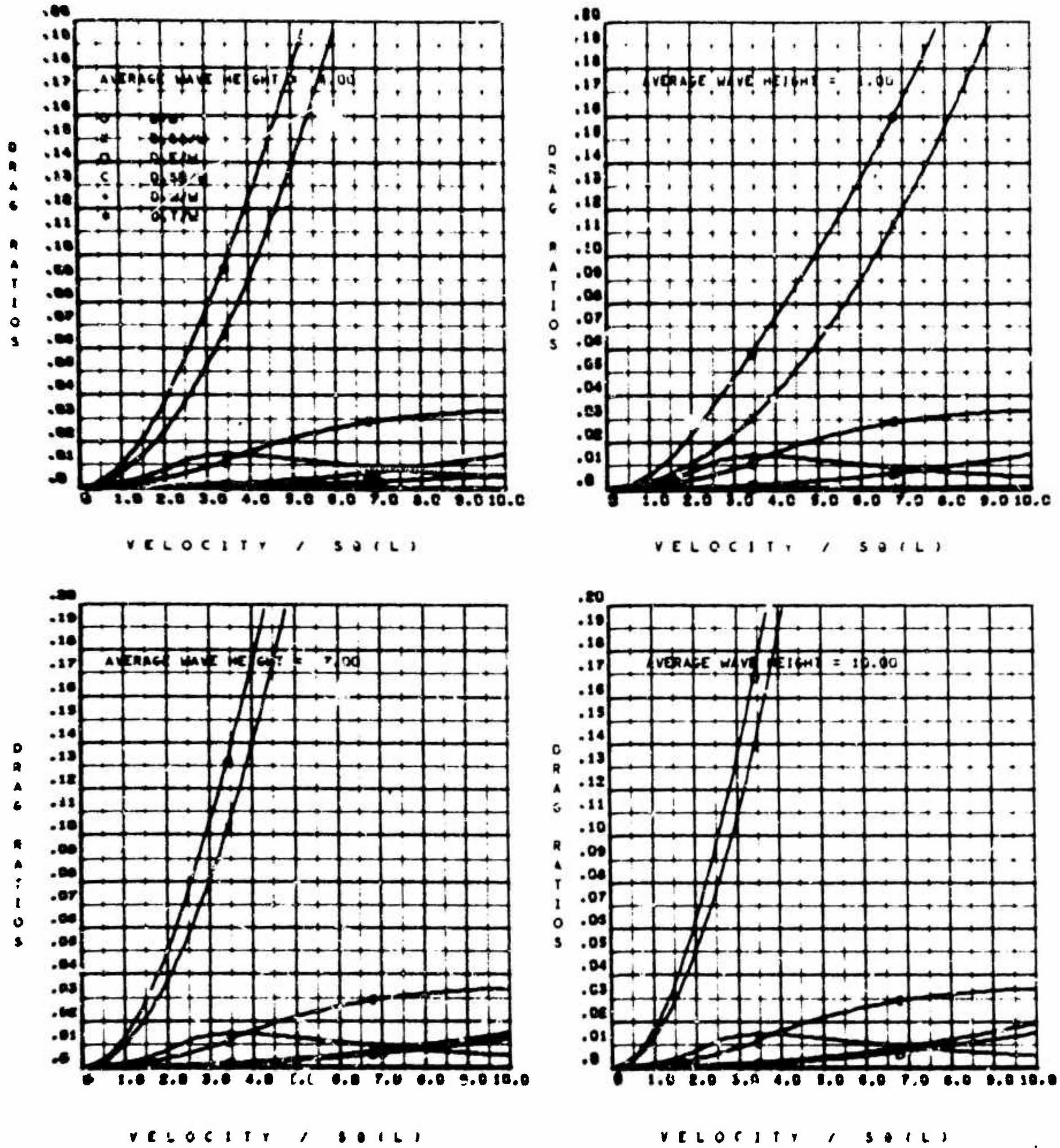

DRAG RATIOS VERSUS VELOCITY / SQ(L)

Figure 8 (Contin: .d)

(b) $K_{D_D} = 0.04$, $K_{D_s} = 0.08$, $w/\sqrt{S} = 1.7$

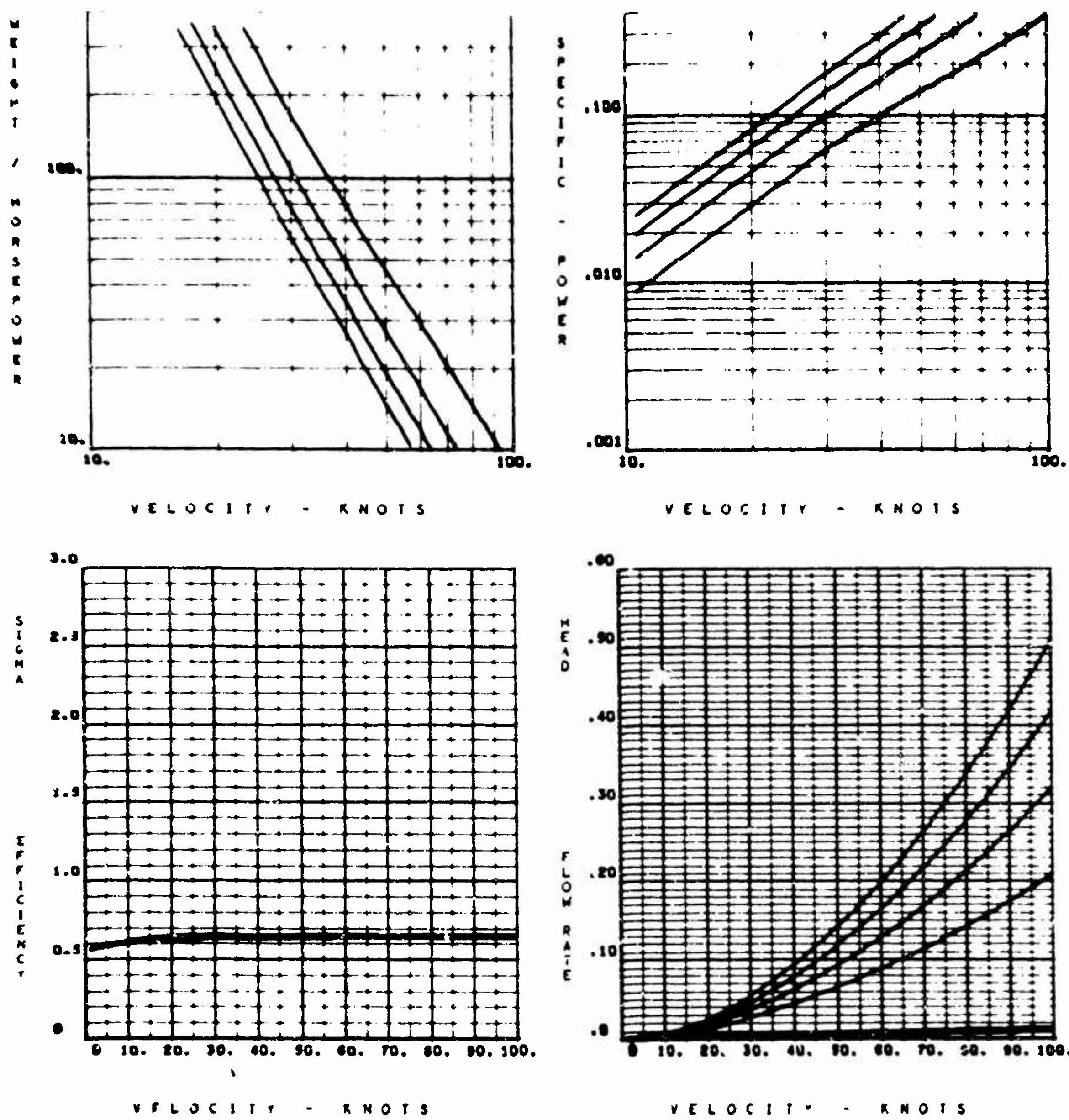

Figure 8 (Continued)

(b) Concluded

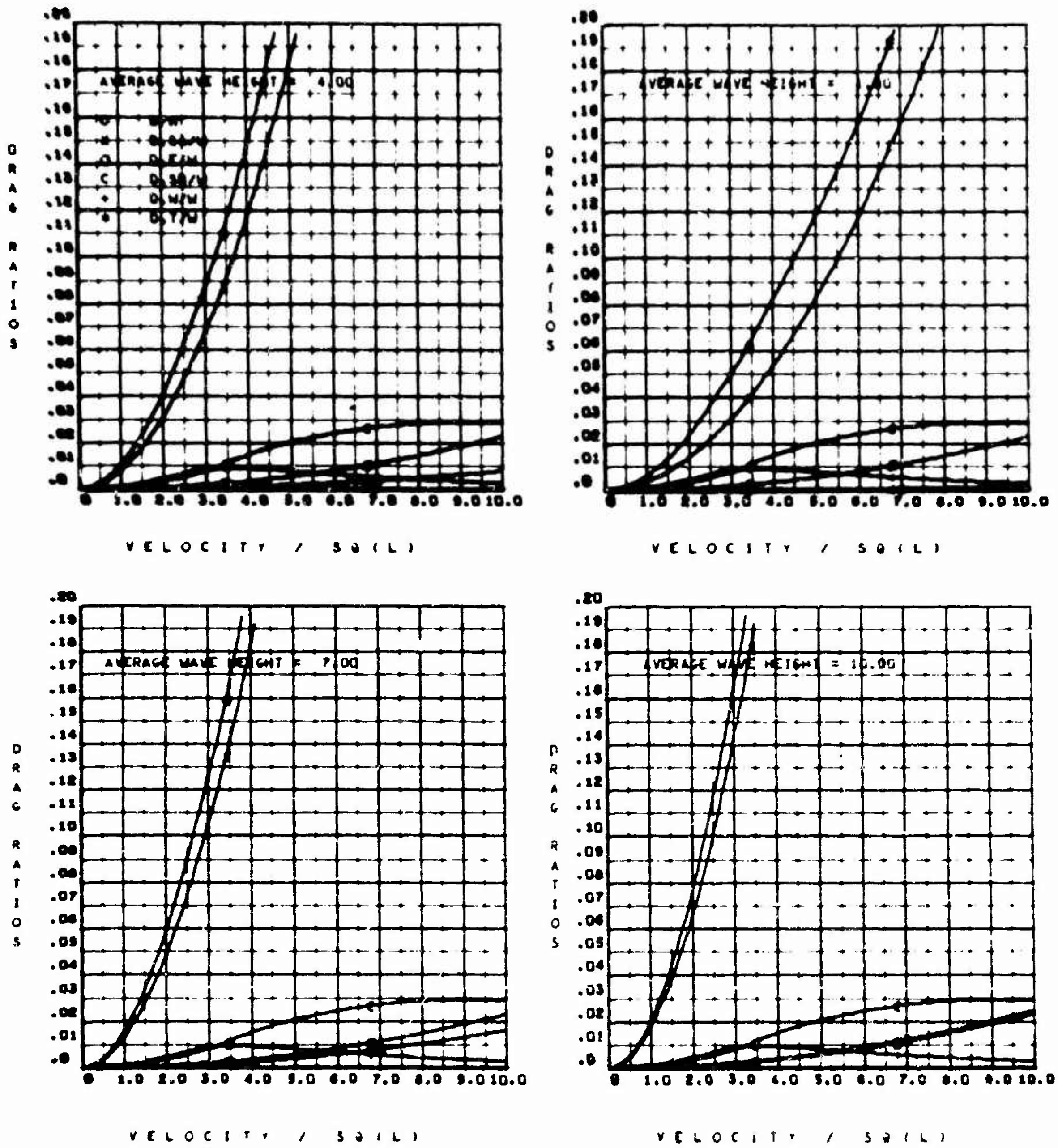

DRAG RATIOS VERSUS VELOCITY / SQ(L)

Figure 8 (Continued)

(c) $K_{D_D}=0.08$, $K_{D_S} = 0.16$, $w/S = 1.1$

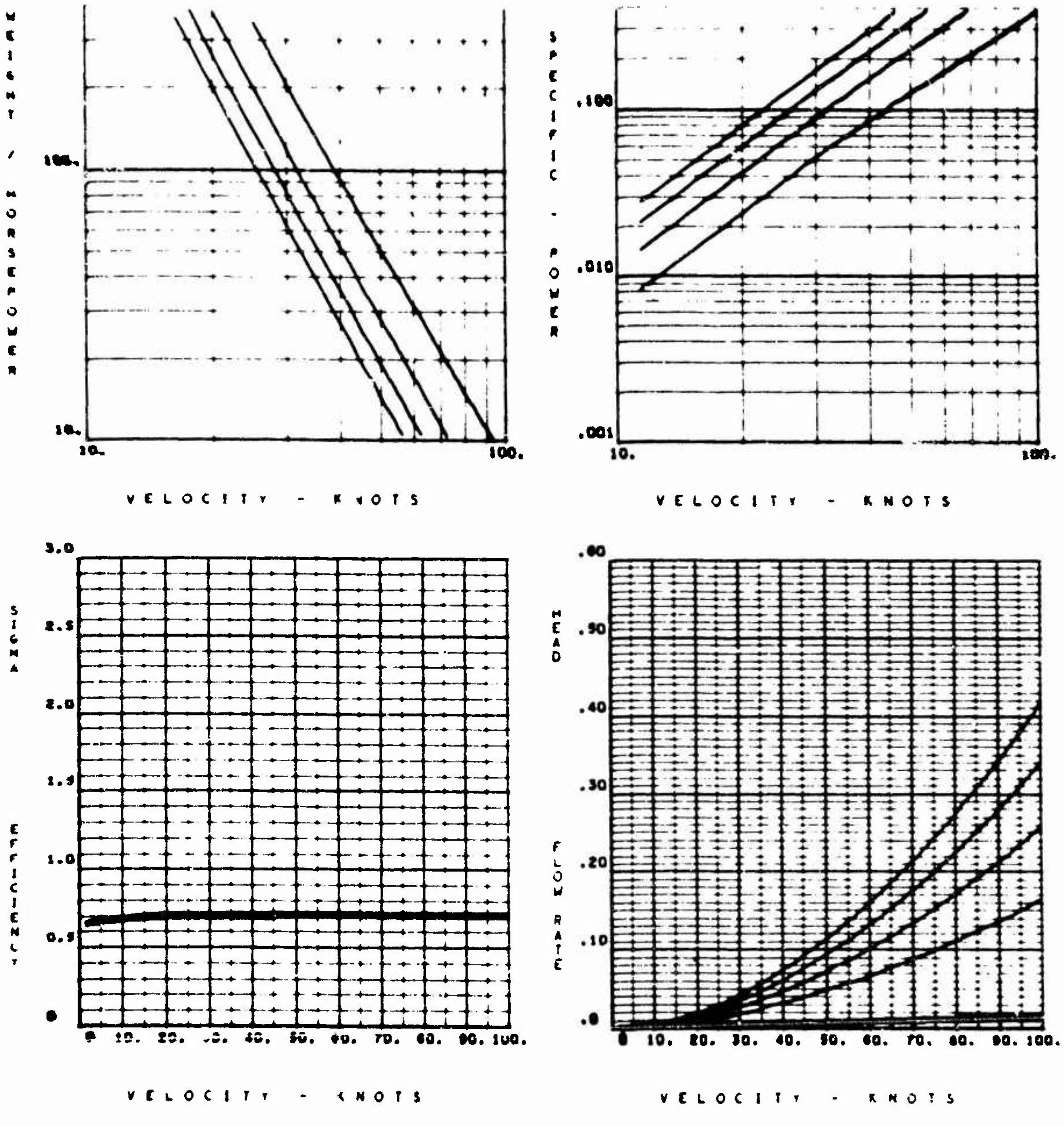

Figure 8 (Continued)
(c) Concluded

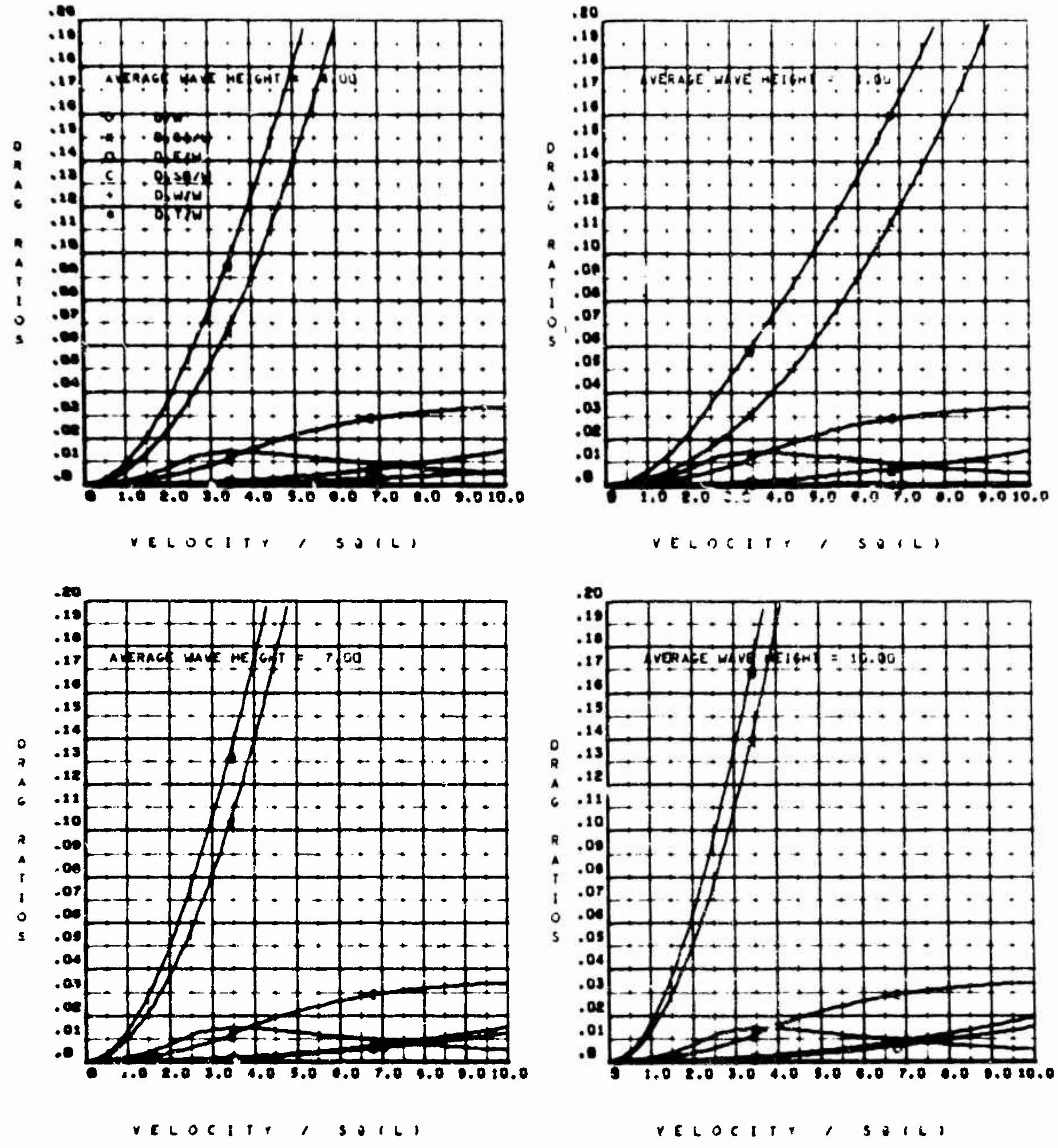

DRAG RATIOS VERSUS VELOCITY / SQ(L)

Figure 8 (Continued)

(d) $K_{D_D} = 0.08$, $K_{D_s} = 0.16$, $w/\sqrt{S} = 1.7$

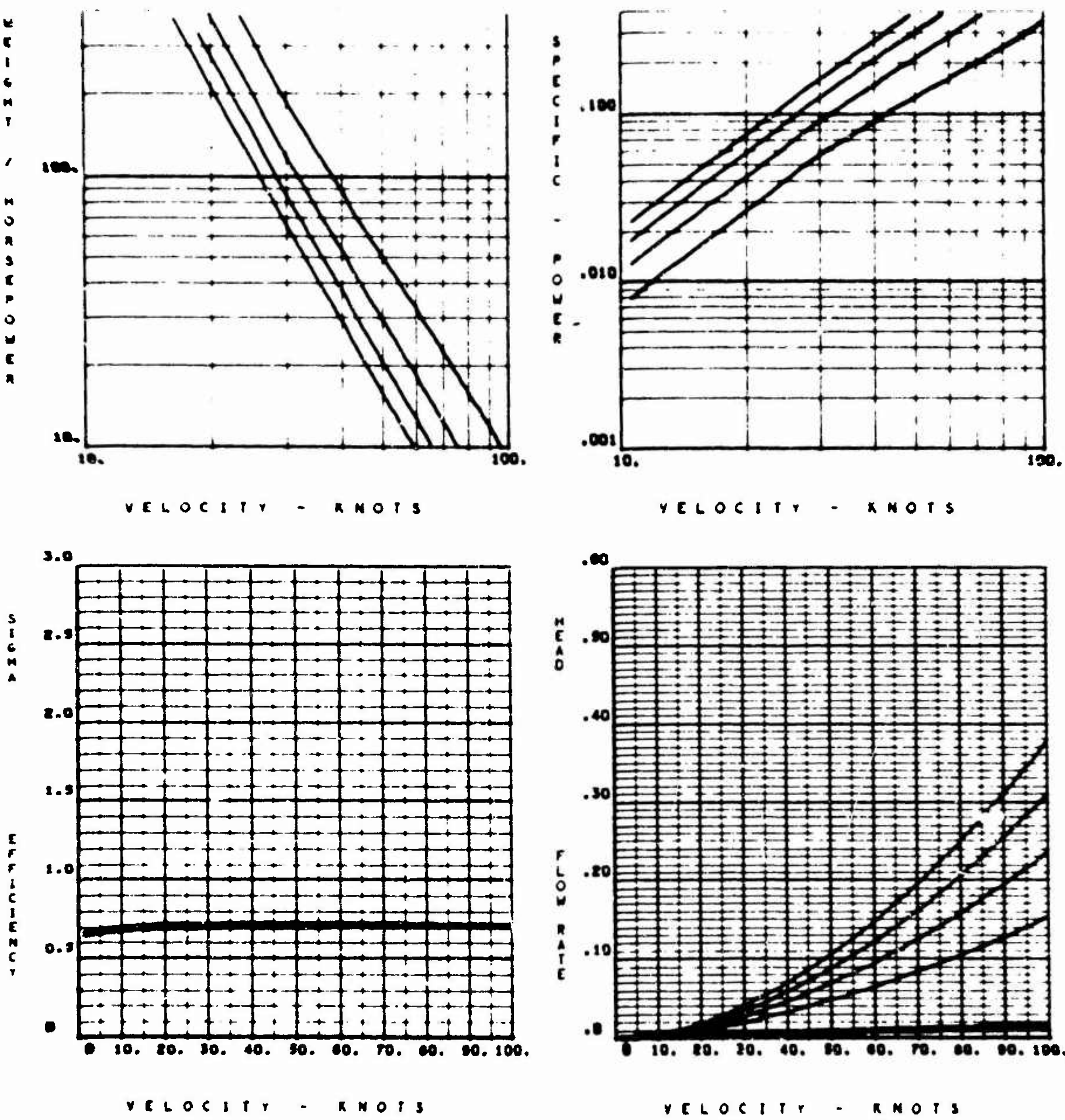

Figure 8 (Concluded)

(d) Concluded

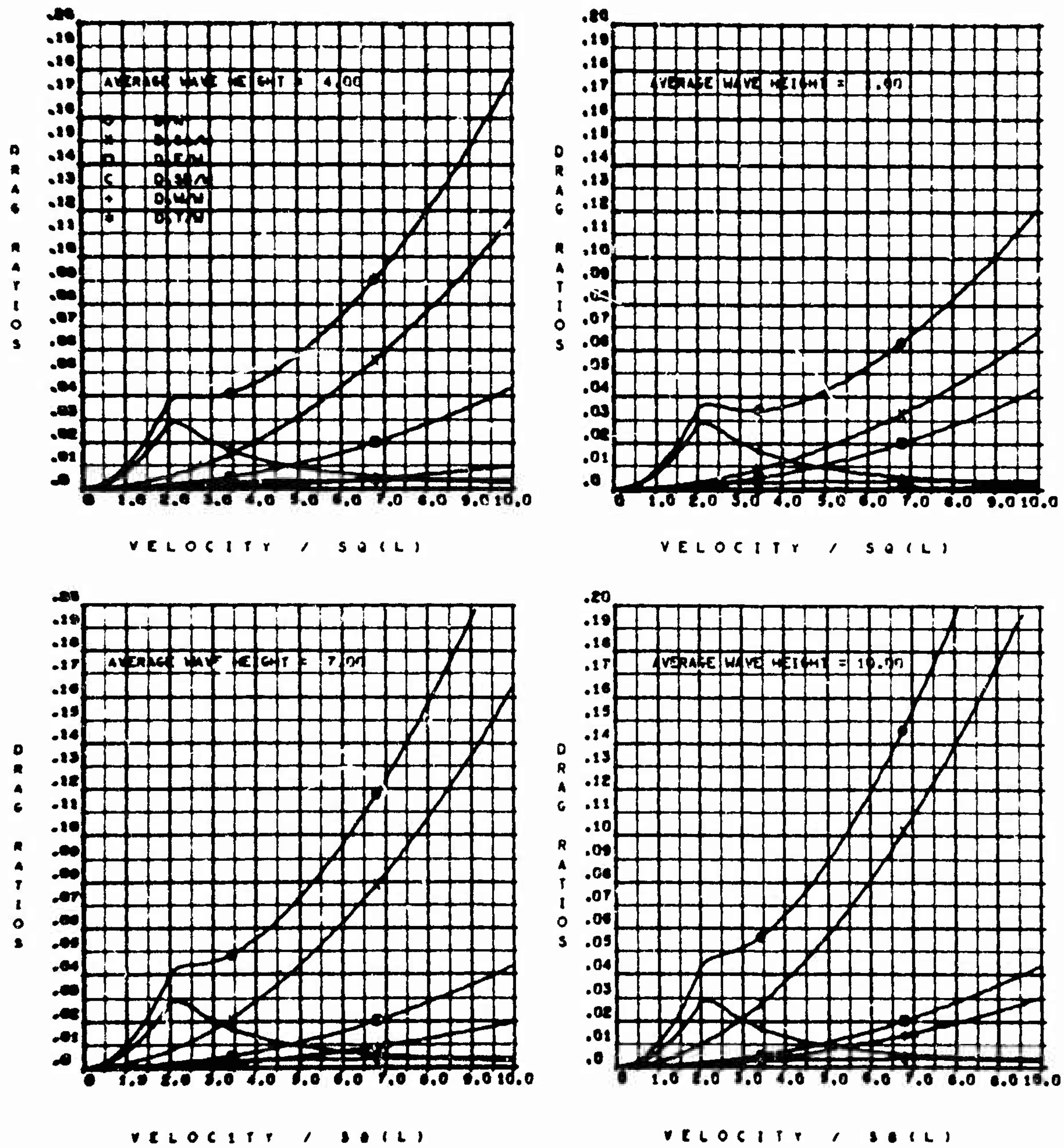

DRAG RATIOS VERSUS VELOCITY / SQ(L)

Figure 9 - General Performance Parameters of 1000 Ton CAB

With $\ell/b = 2.0$

(a) $K_{D_D} = 0.04$, $K_{D_S} = 0.08$, $w/\sqrt{S} = 1.1$

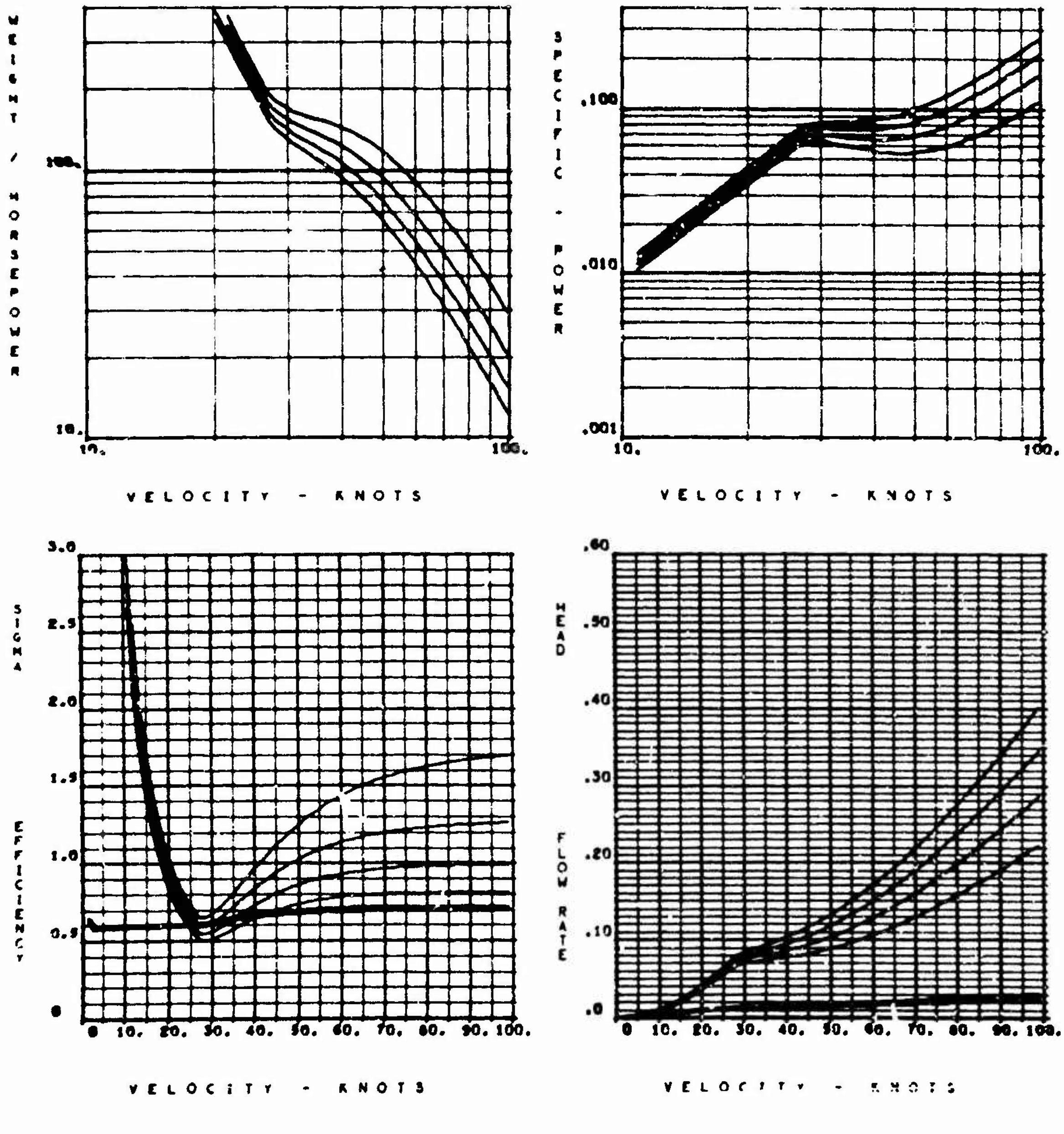

Figure 9 (Continued)

(a) Concluded

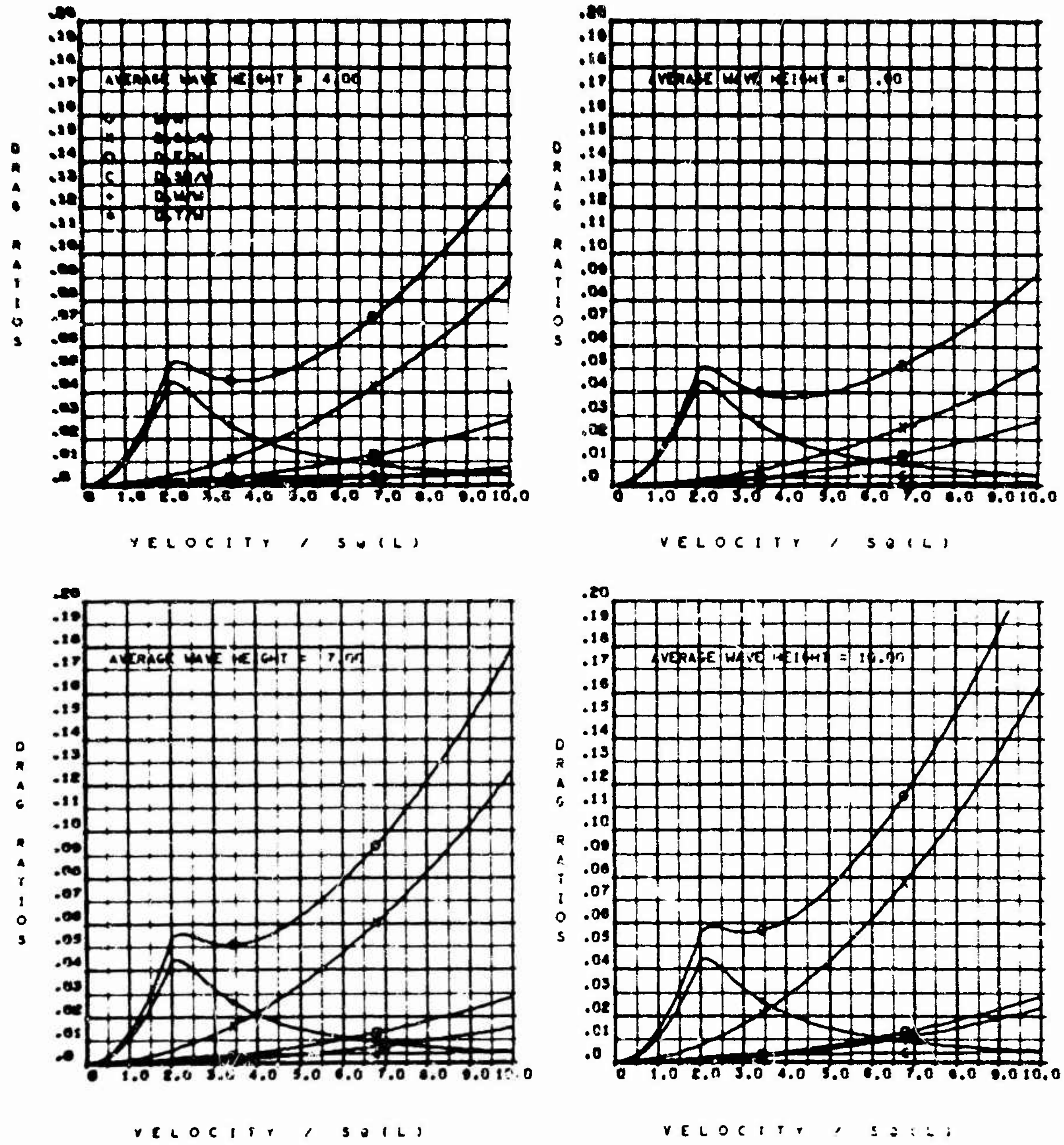

DRAG RATIOS VERSUS VELOCITY / SQ(L)

Figure 9 (Continued)

(b) $K_{D_D} = 0.04$, $K_{D_S} = 0.08$, $w/\sqrt{S} = 1.7$

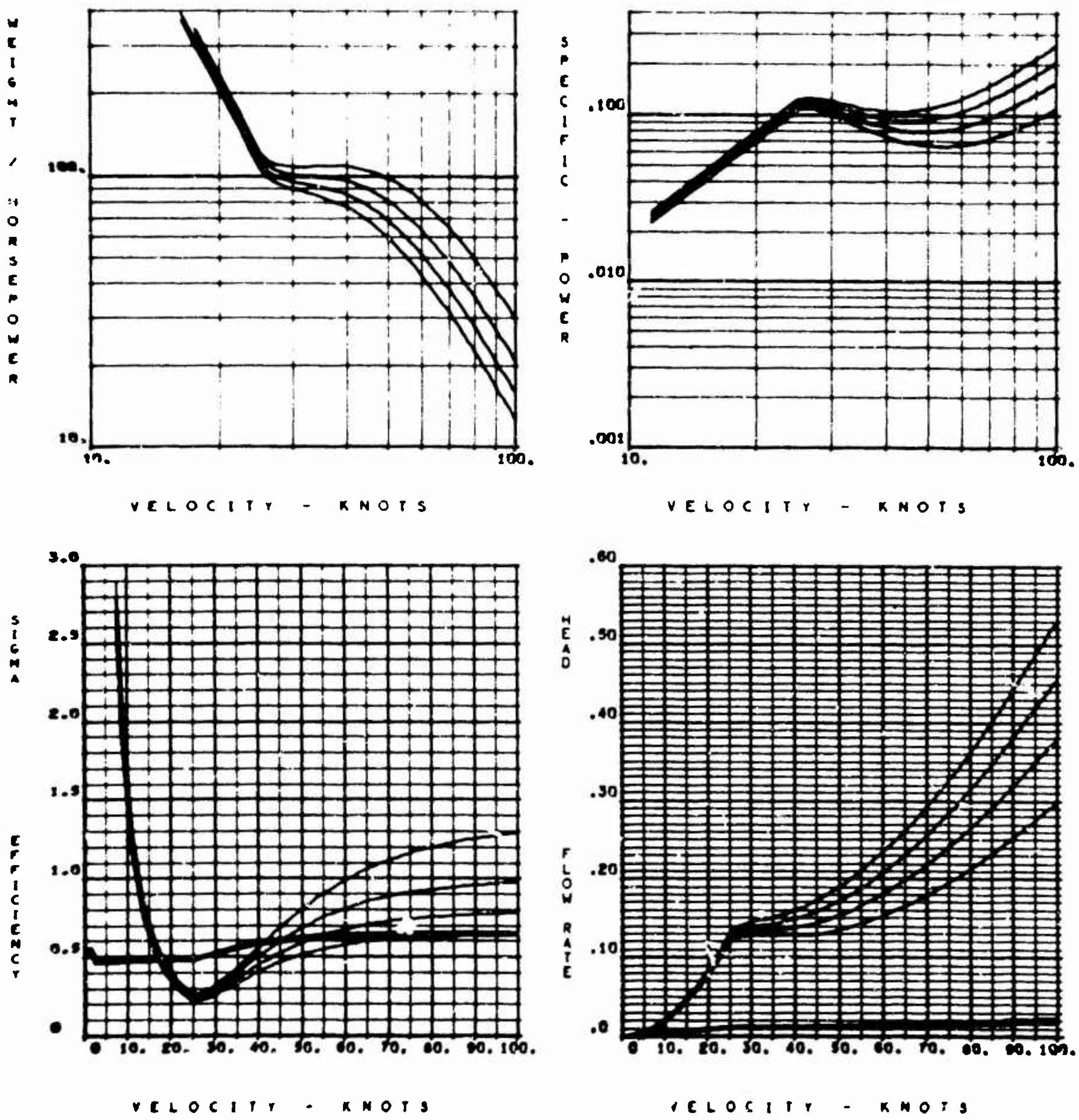

Figure 9 (Continued)

(b) Concluded

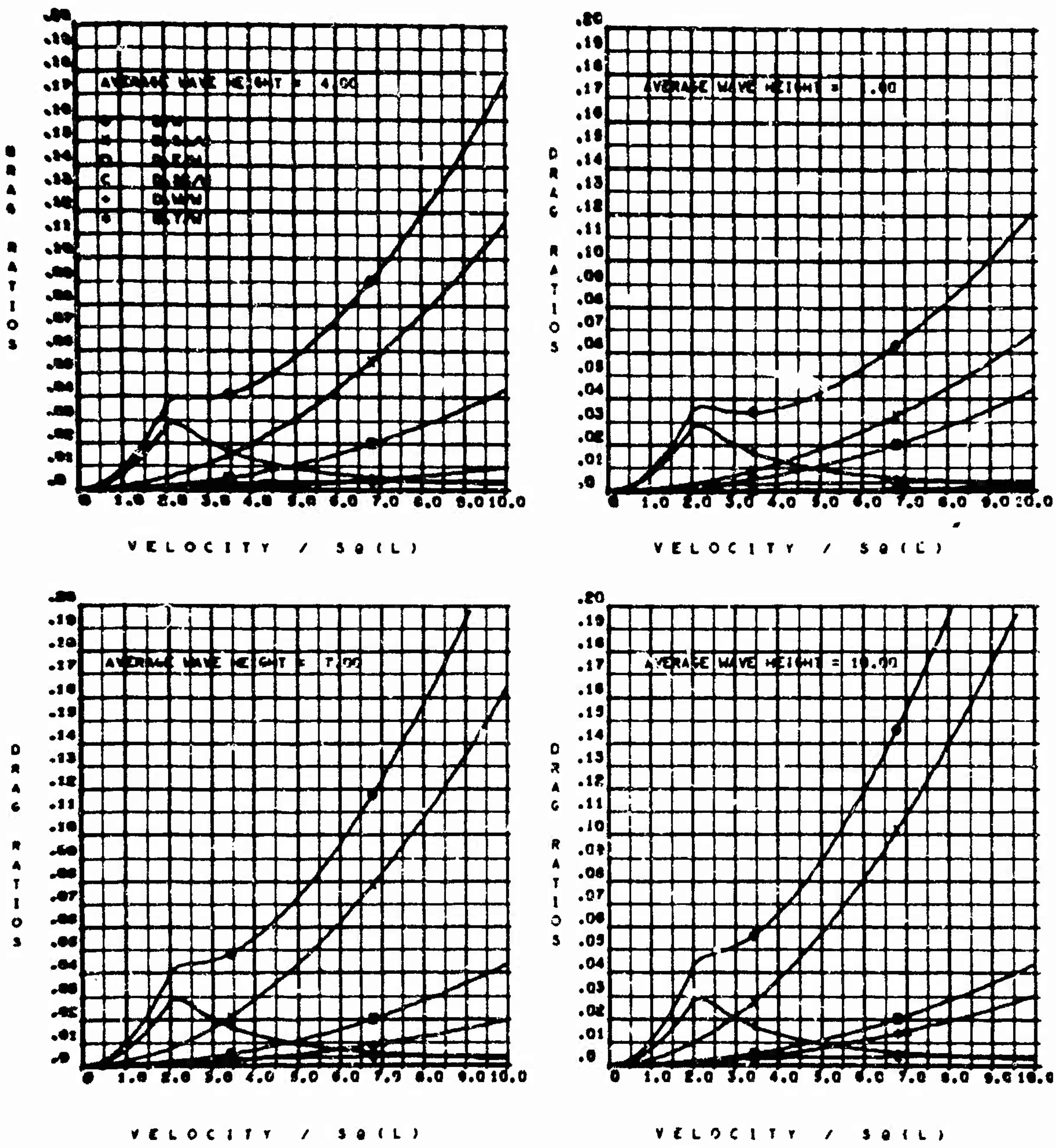

DRAG RATIOS VERSUS VELOCITY / SQ(L)

Figure 9 (Continued)

(c) $K_{D_D} = 0.08$, $K_{D_s} = 0.16$, $w/\sqrt{S} = 1.1$

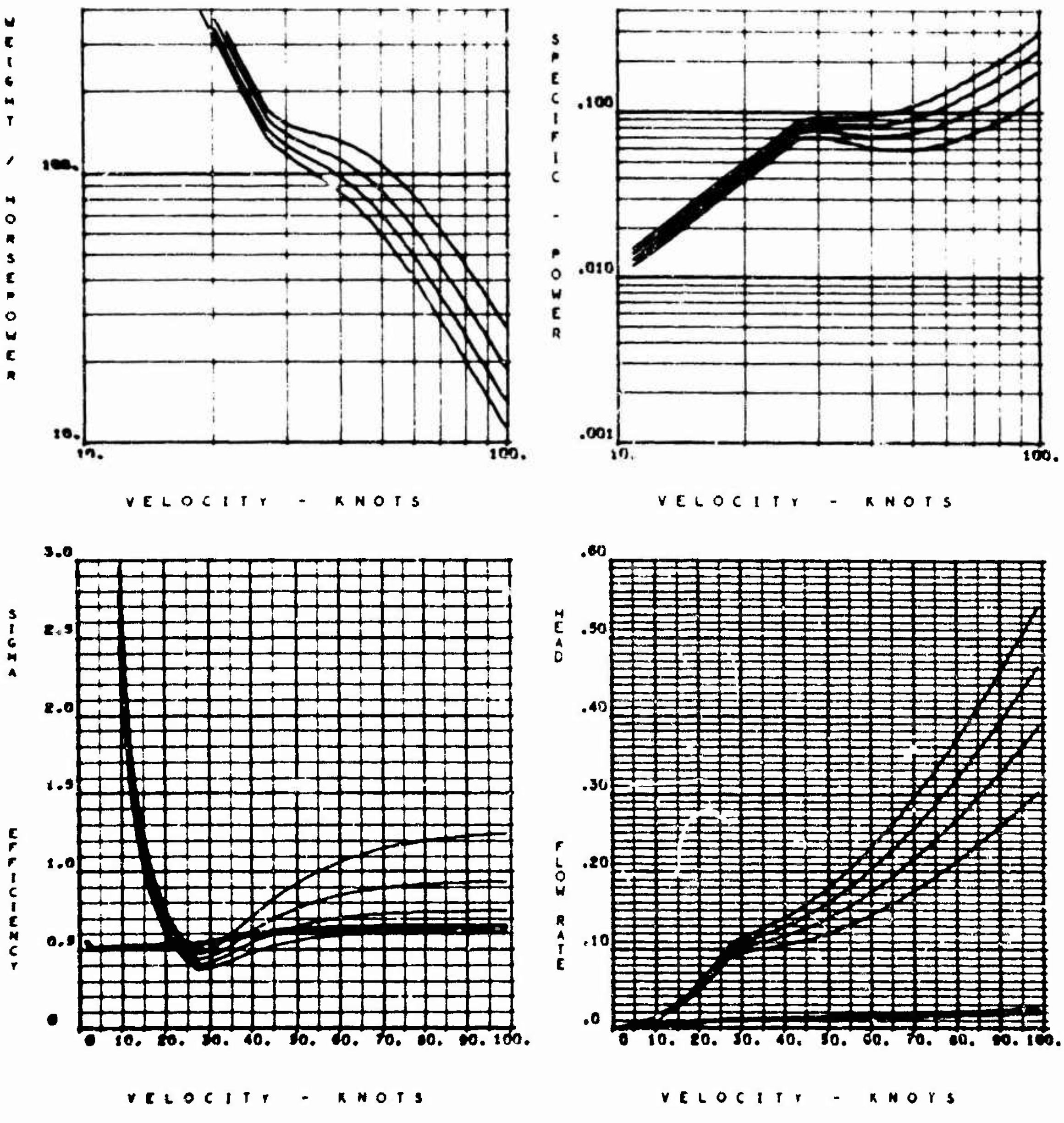

Figure 9 (Continued)
(c) Concluded

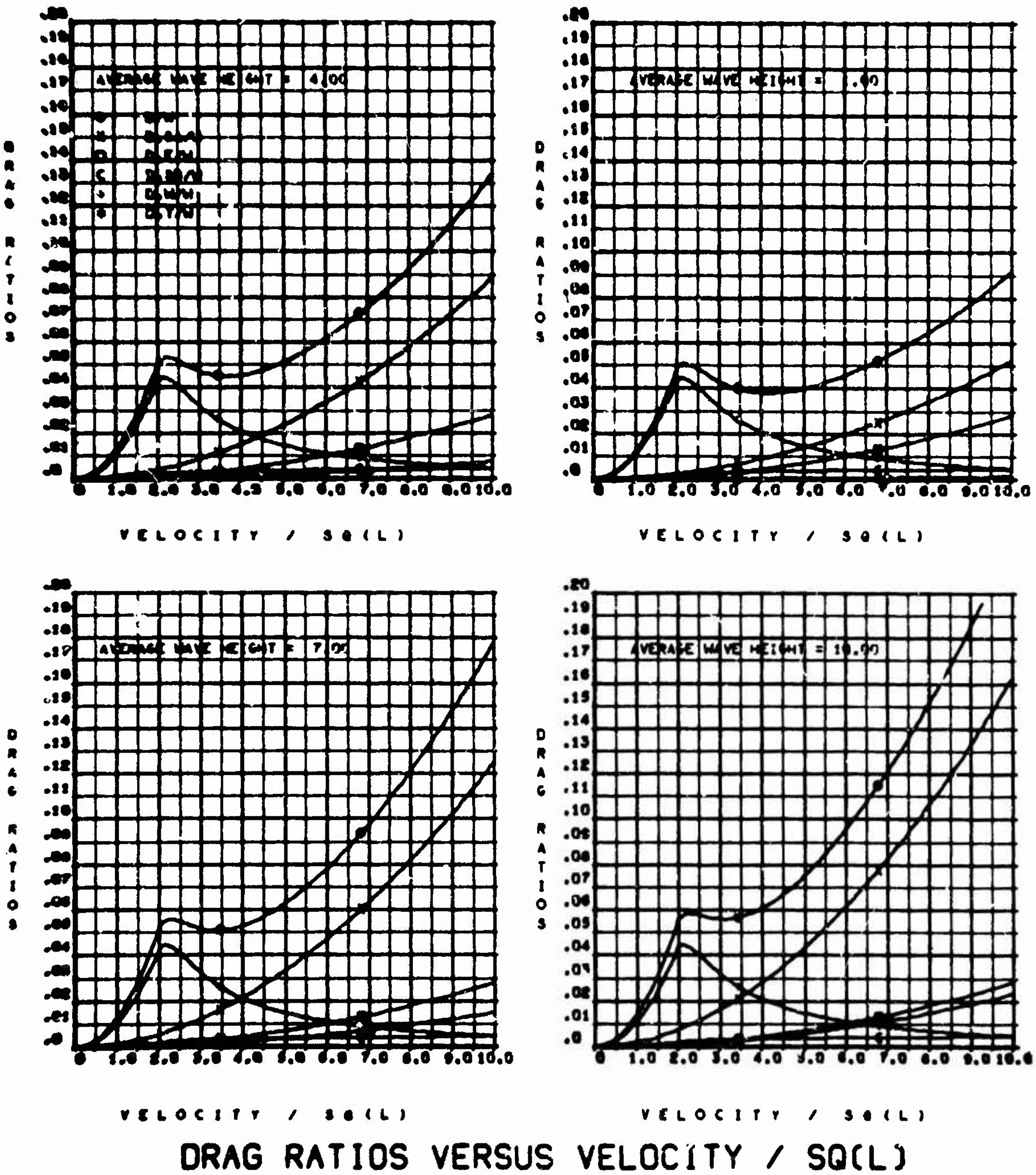

Figure 9 (Continued)

(d) $K_{D_D} = 0.08$, $K_{D_S} = 0.16$, $w/\sqrt{S} = 1.7$

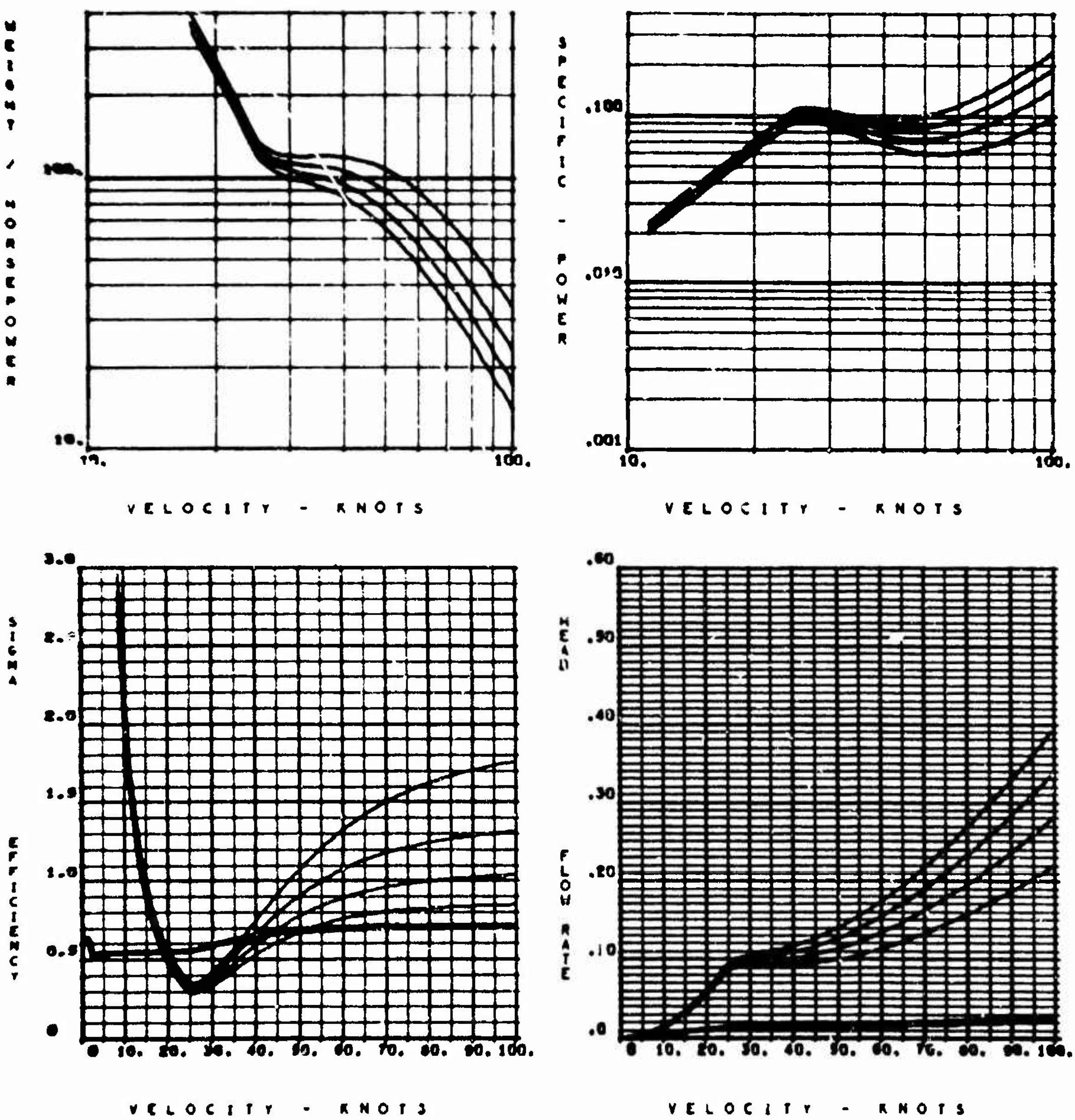

Figure 9 (Concluded)

(d) Concluded

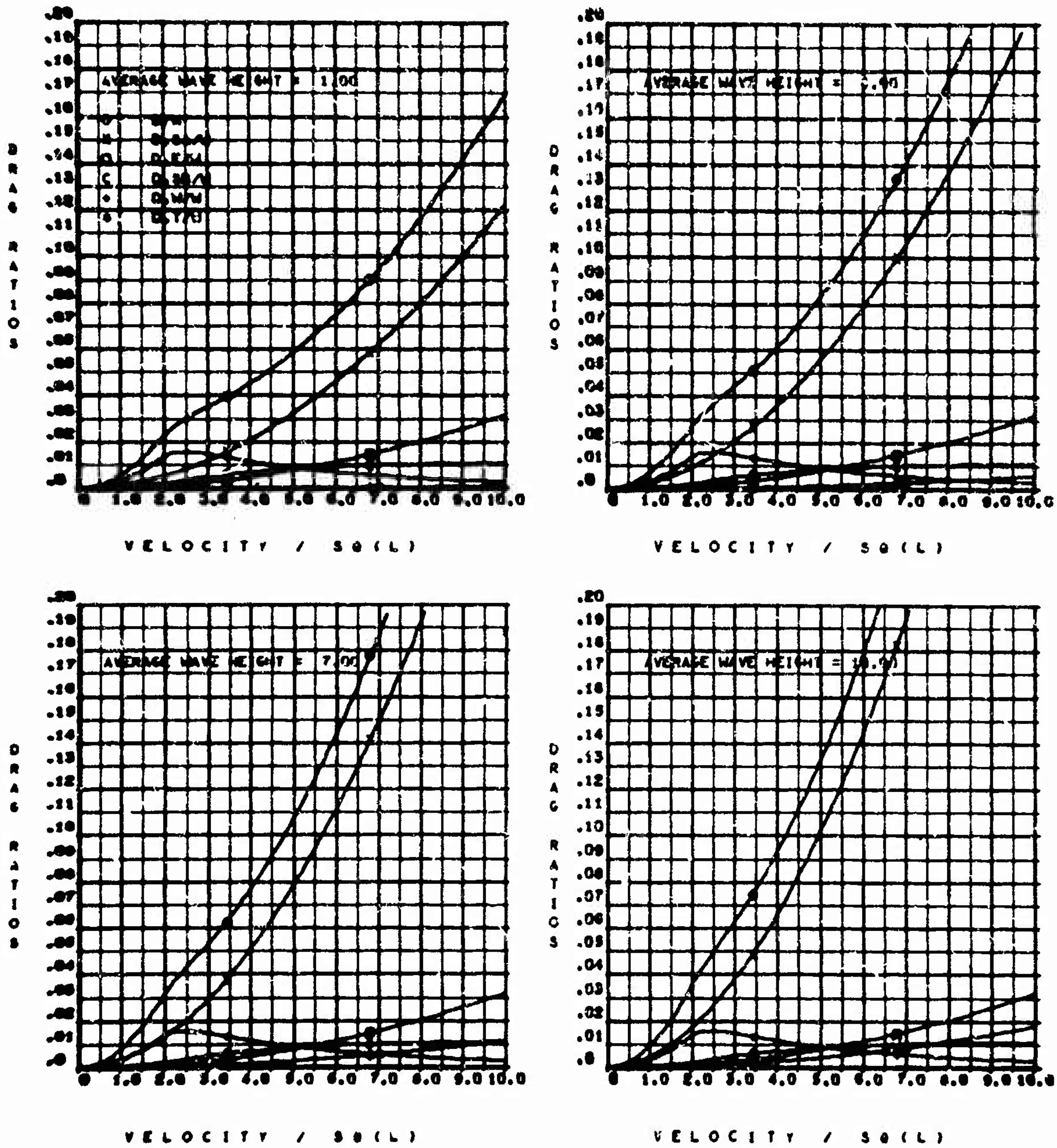

DRAG RATIOS VERSUS VELOCITY / SQ(L)

Figure 10 - General Performance Parameters of 1000 Ton CAB With $\ell/b = 3.74$

(a) $K_{D_D} = 0.04$, $K_{D_s} = 0.08$, $w/\sqrt{S} = 1.1$

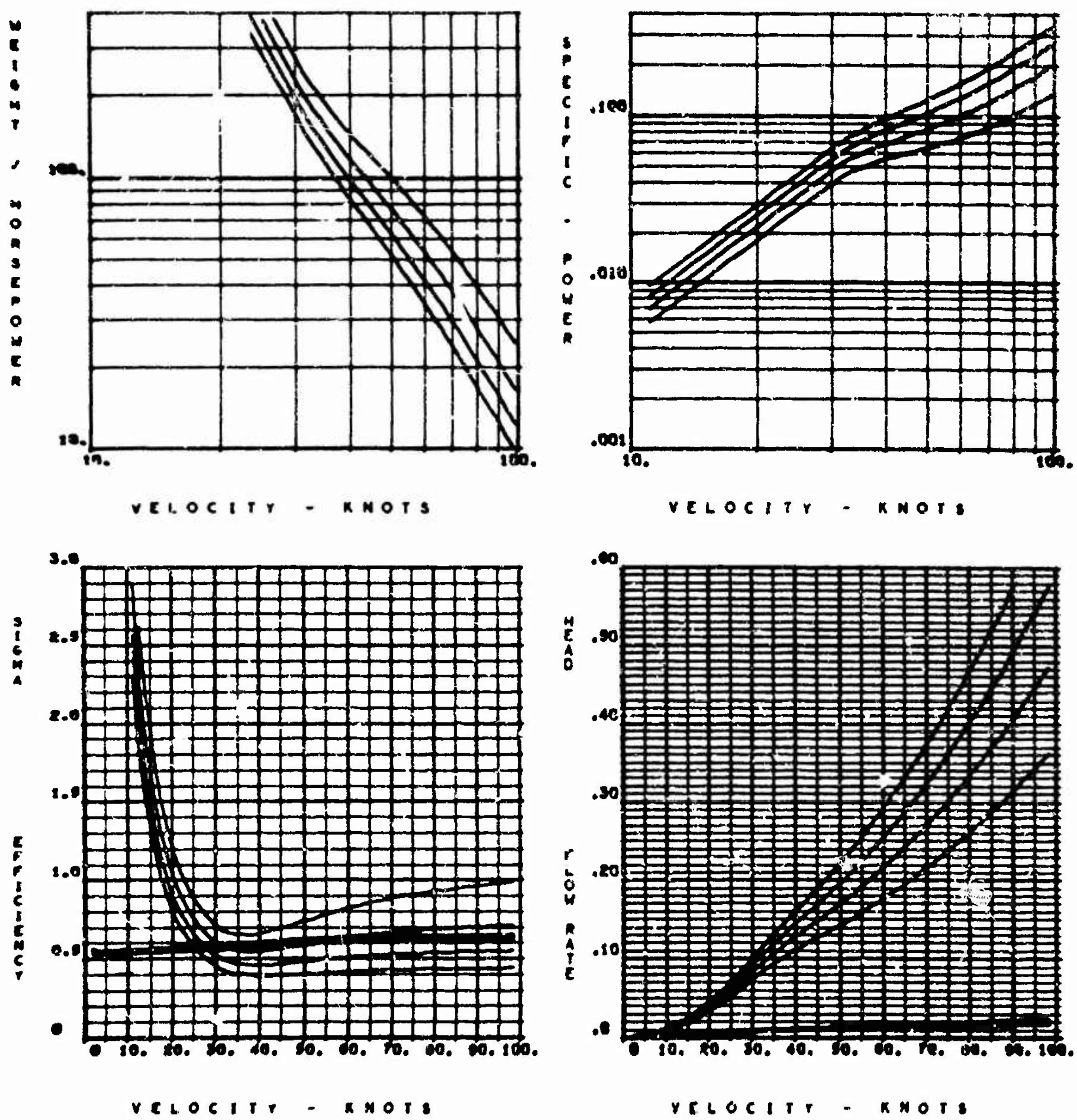

Figure 10 (Continued)

(a) Concluded

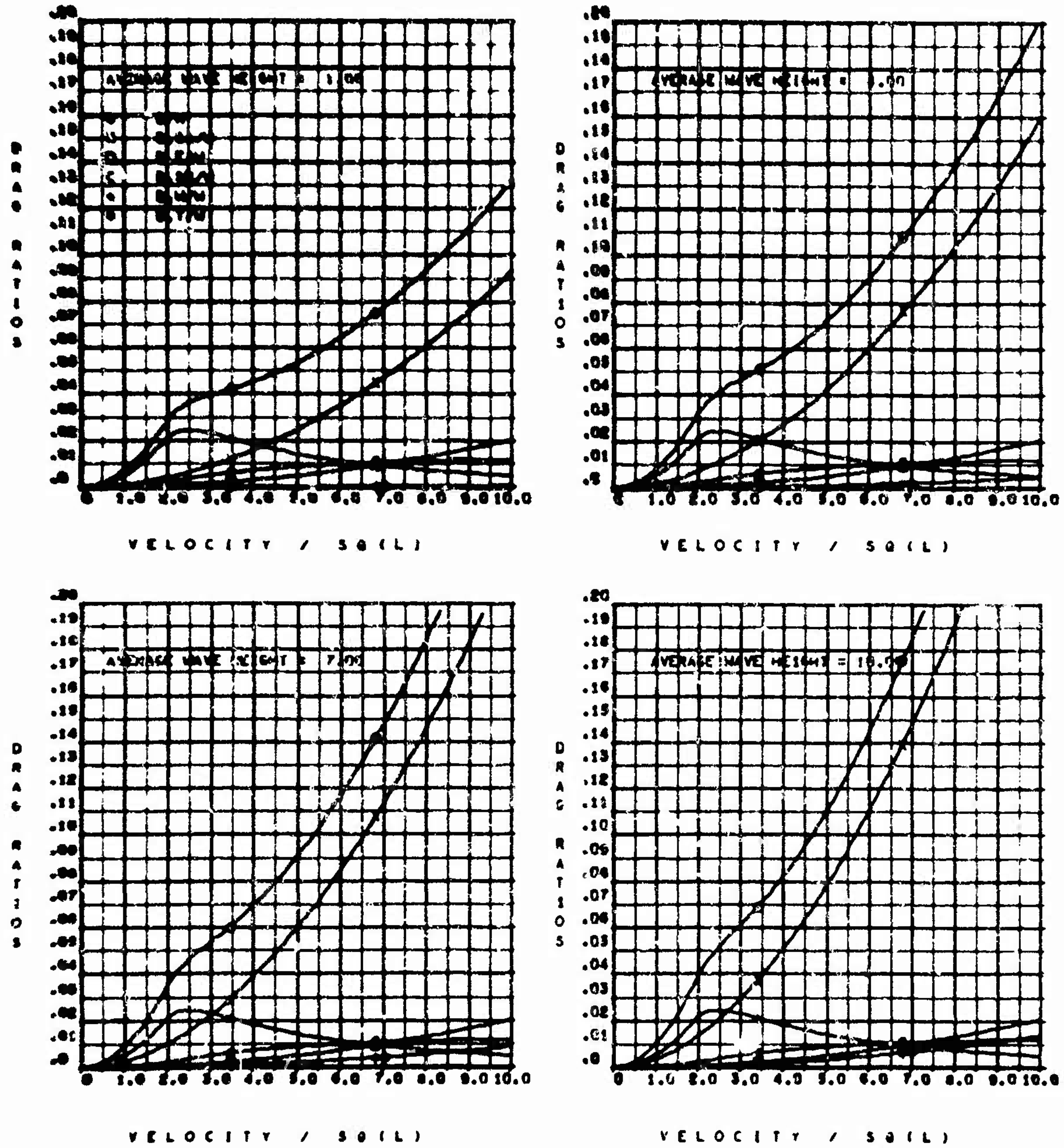

DRAG RATIOS VERSUS VELOCITY / SQ(L)

Figure 10 (Continued)

(b) $K_{D_D} = 0.04$, $K_{D_s} = 0.08$, $w/\sqrt{S} = 1.7$

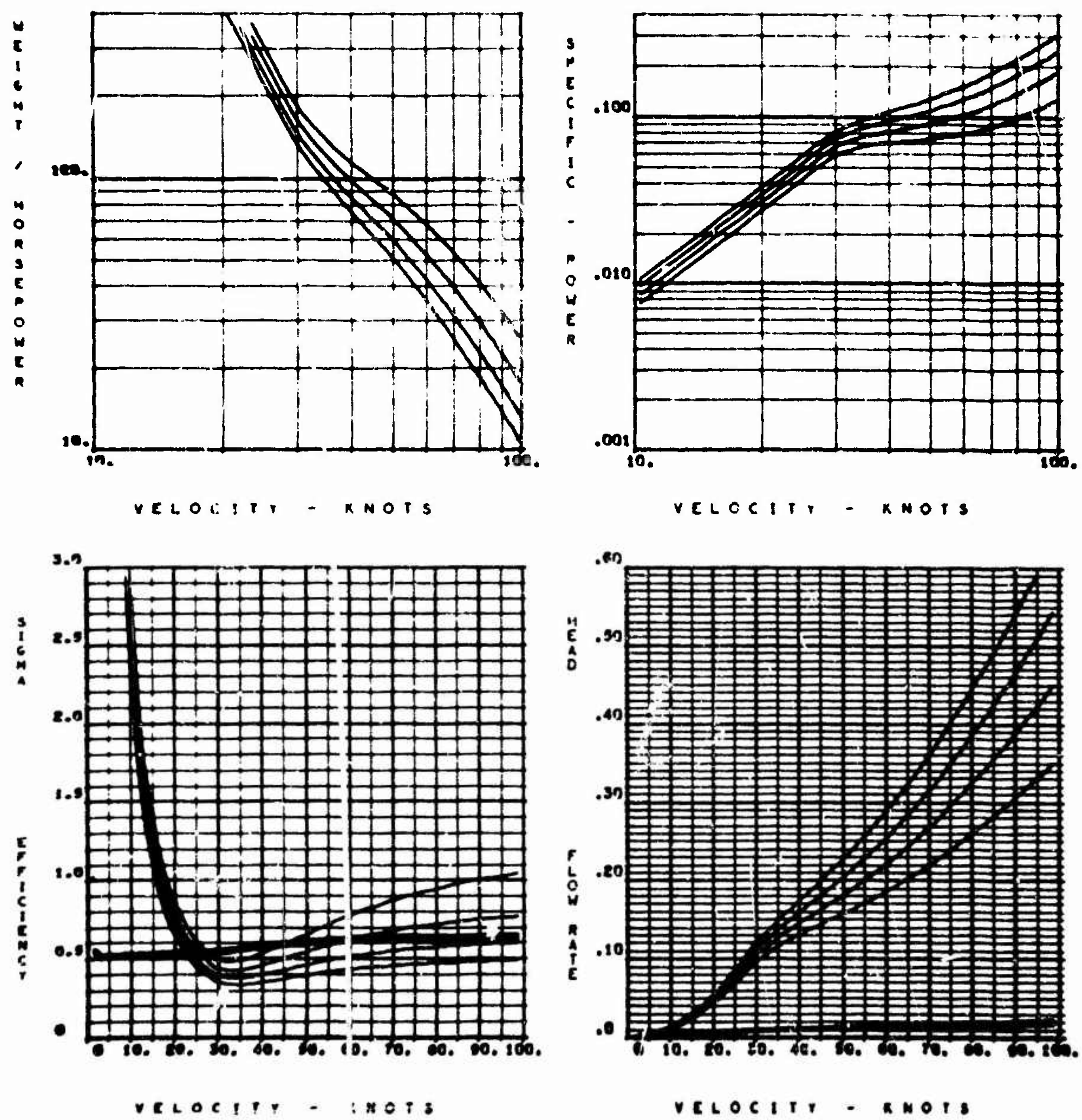

Figure 10 (Continued)

(b) Concluded

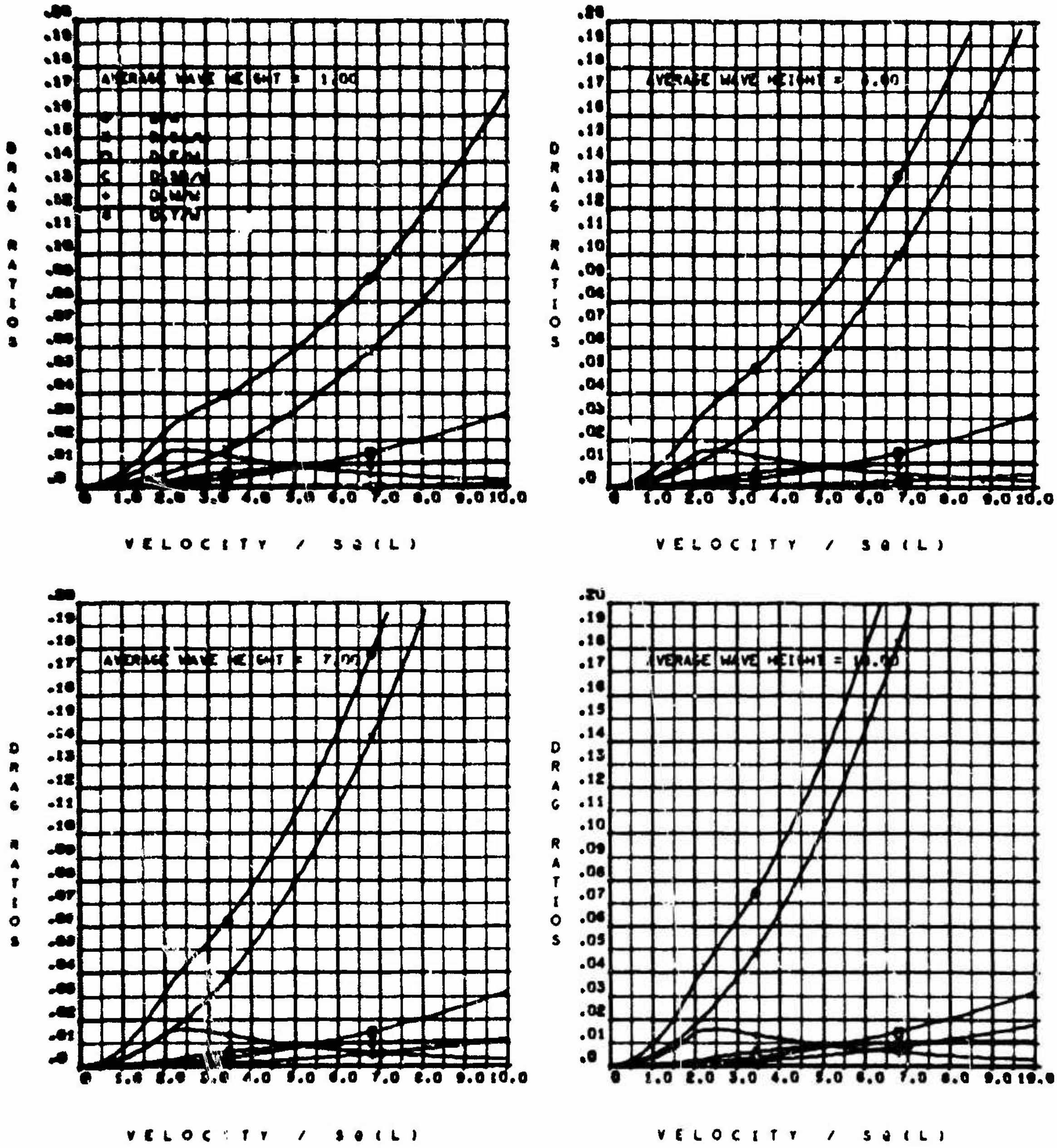

DRAG RATIOS VERSUS VELOCITY / SQ(L)

Figure 10 (Continued)

(c) $K_{D_D} = 0.08$, $K_{D_S} = 0.16$, $w/\sqrt{S} = 1.1$

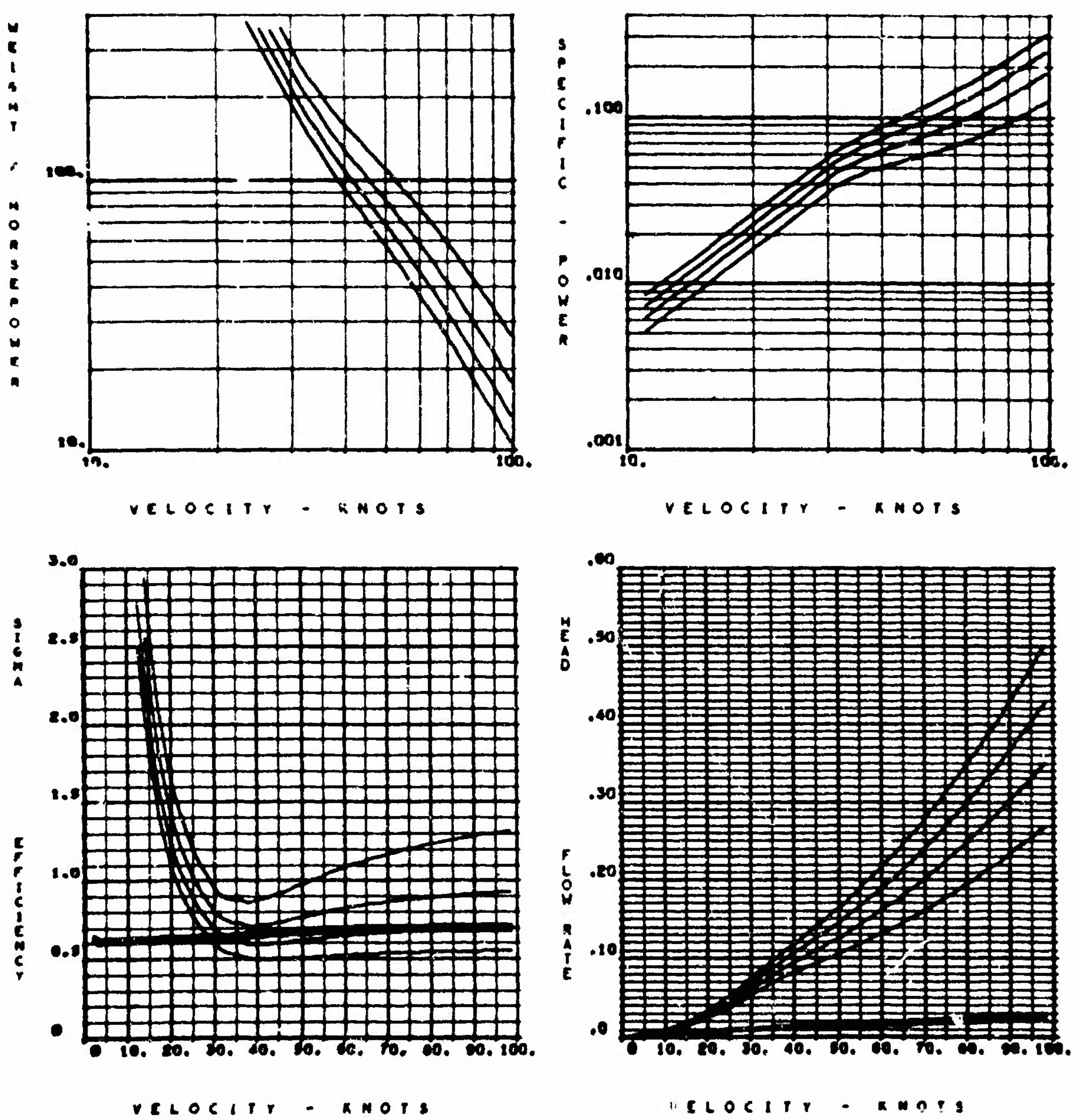

Figure 10 (Continued)

(c) Concluded

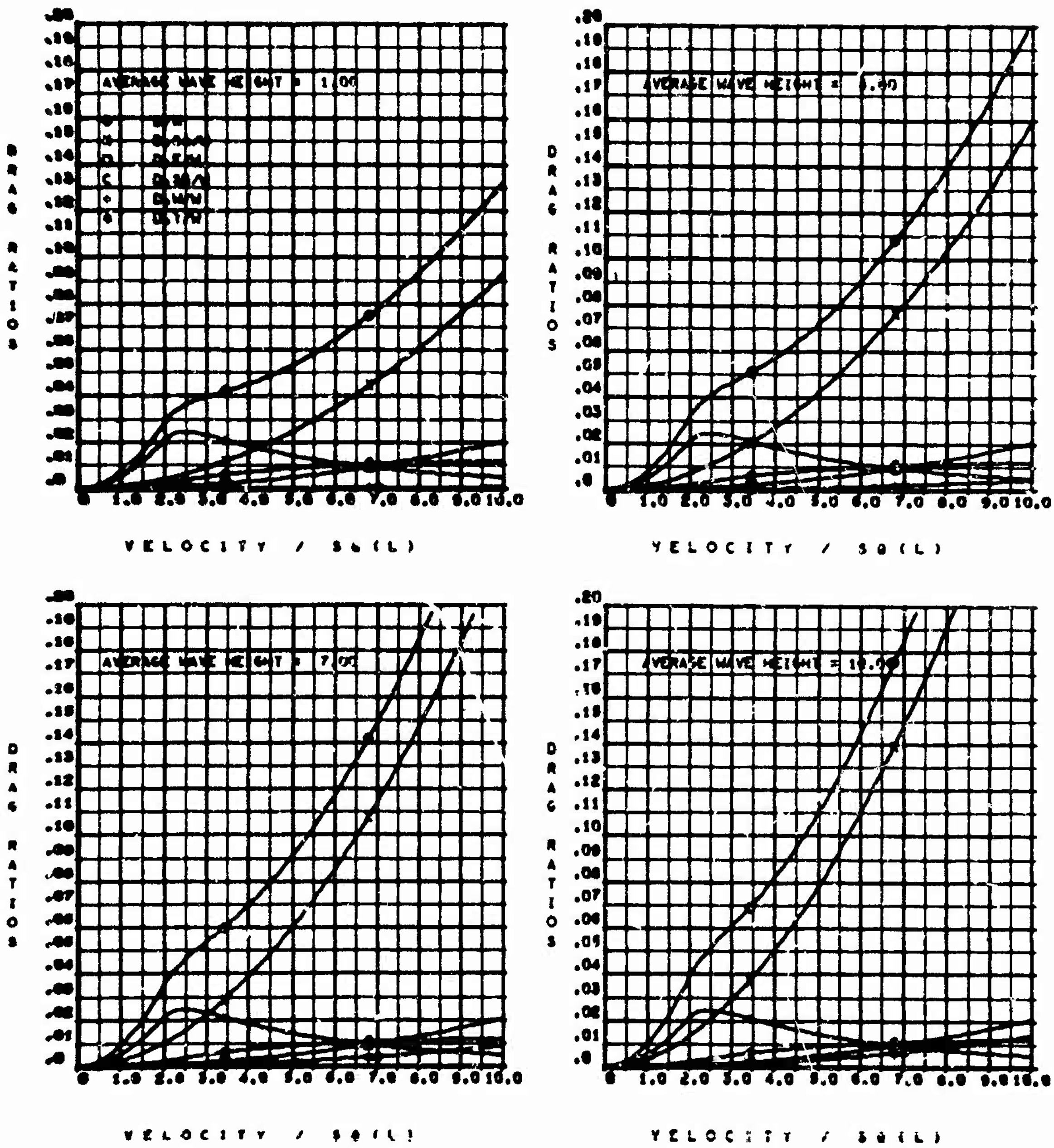

DRAG RATIOS VERSUS VELOCITY / SQ(L)

Figure 10 (Continued)

(d) $K_{D_D} = 0.08$, $K_{D_S} = 0.16$, $w/\sqrt{S} = 1.7$

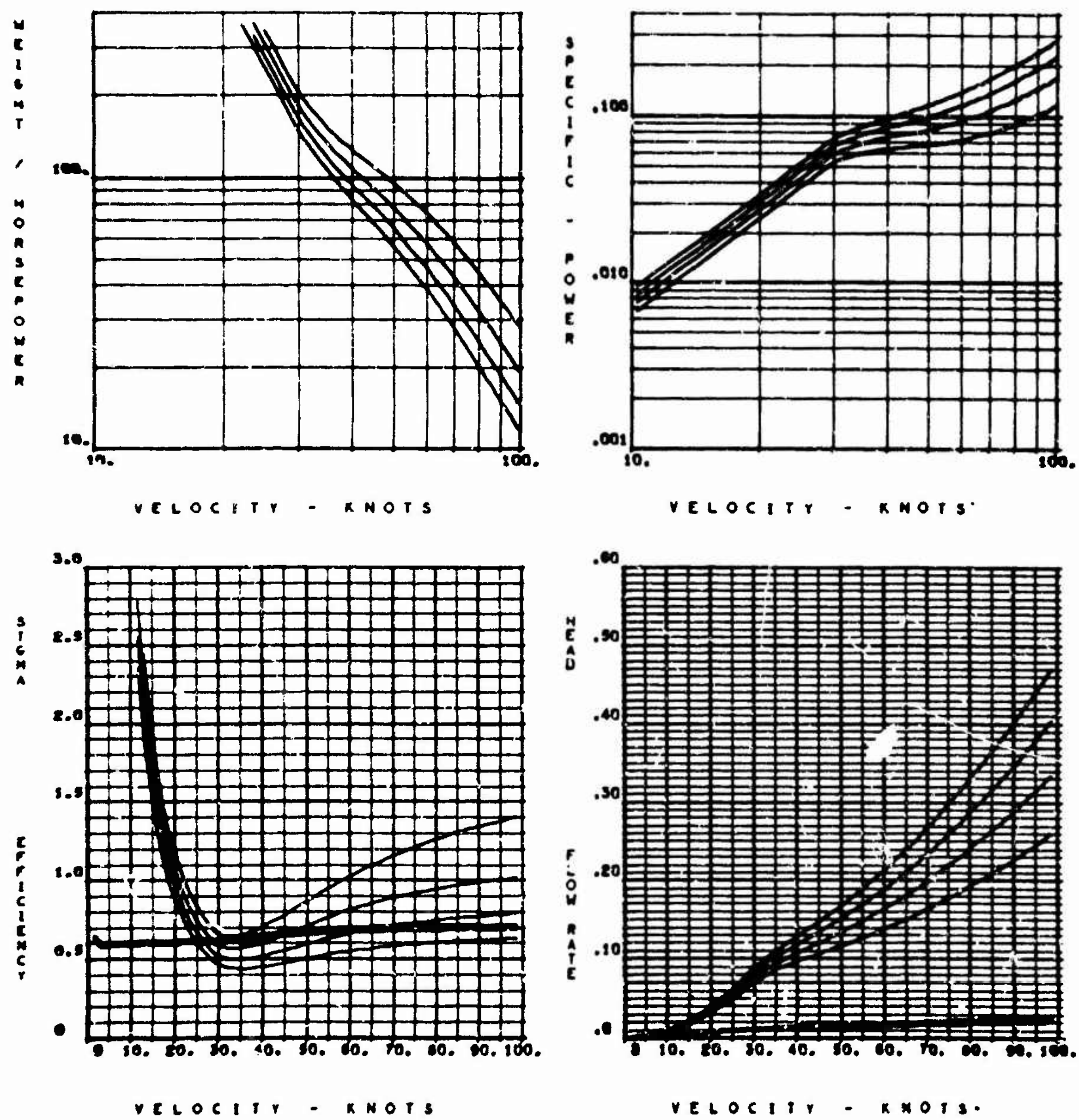

Figure 10 (Concluded)

(d) Concluded

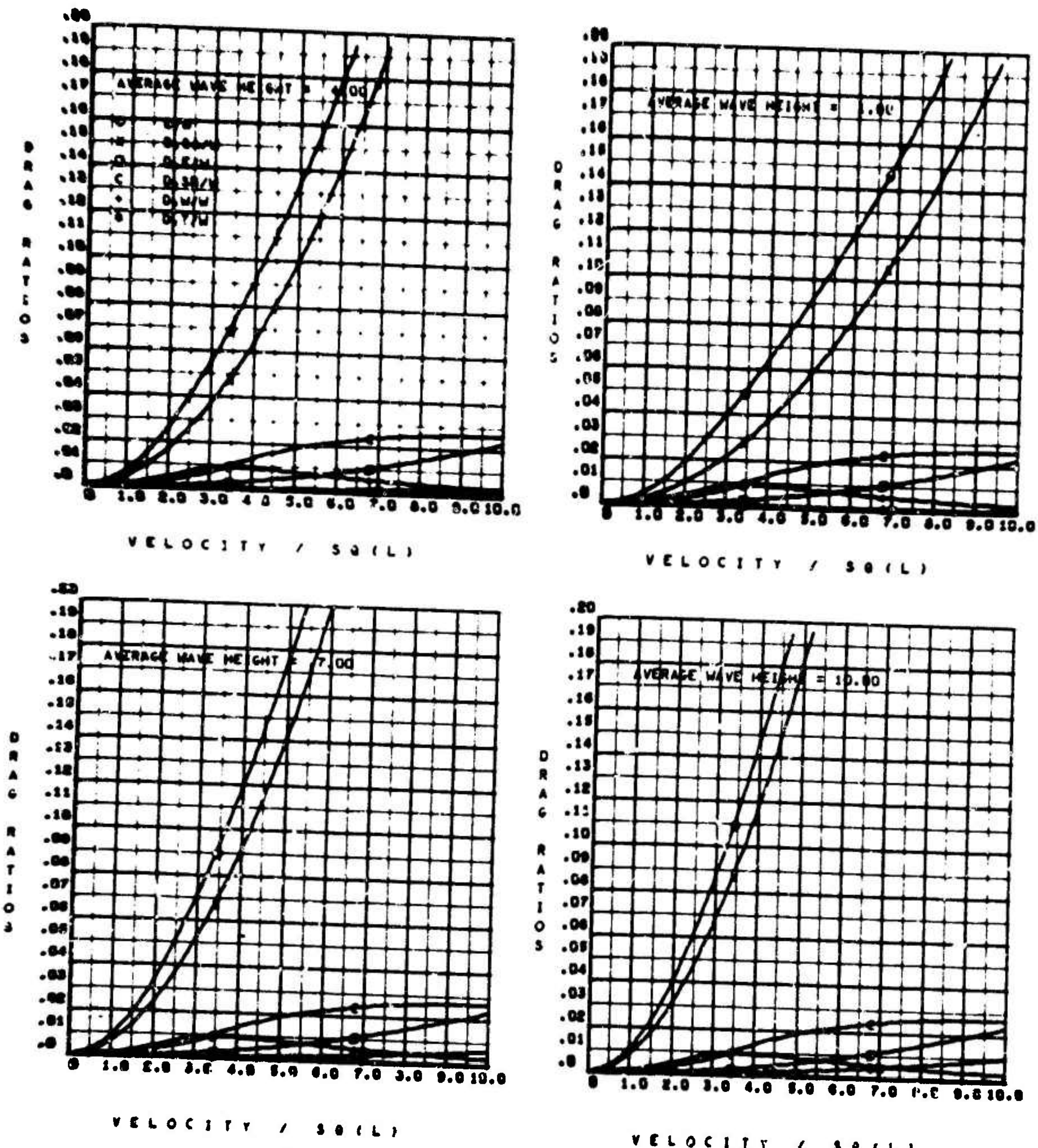

DRAG RATIOS VERSUS VELOCITY / SQ(L)

Figure 11 - General Performance Parameters of 1000 Ton CAB

With $\ell/b = 7.0$

(a) $K_{D_D} = 0.04$, $K_{D_s} = 0.08$, $w/\sqrt{S} = 1.1$

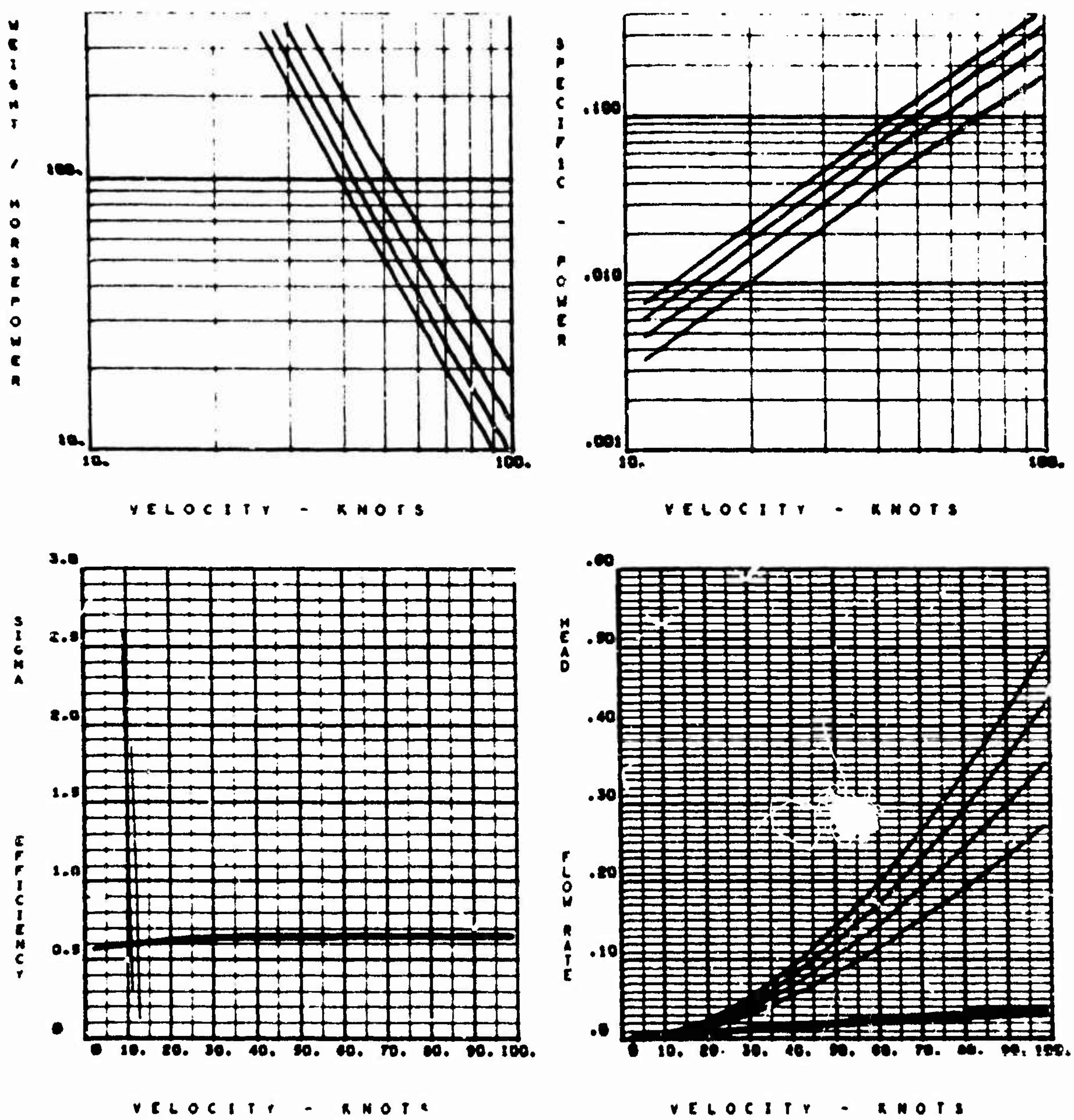

Figure 11 (Continued)
(a) Concluded

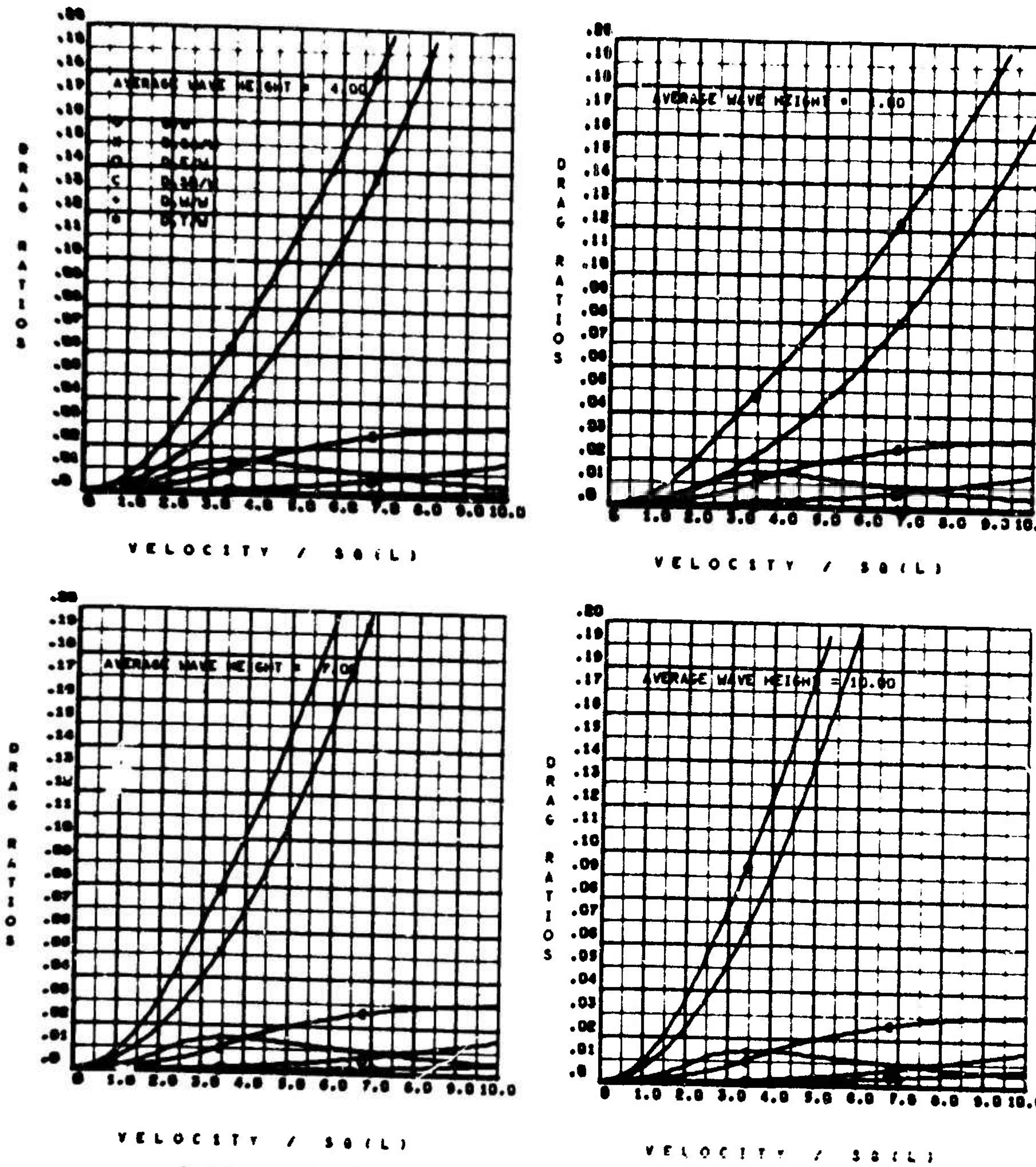

DRAG RATIOS VERSUS VELOCITY / SQ(L)

Figure 11 (Continued)

(b) $K_{D_D} = 0.04$, $K_{D_s} = 0.08$, $w/\sqrt{S} = 1.7$

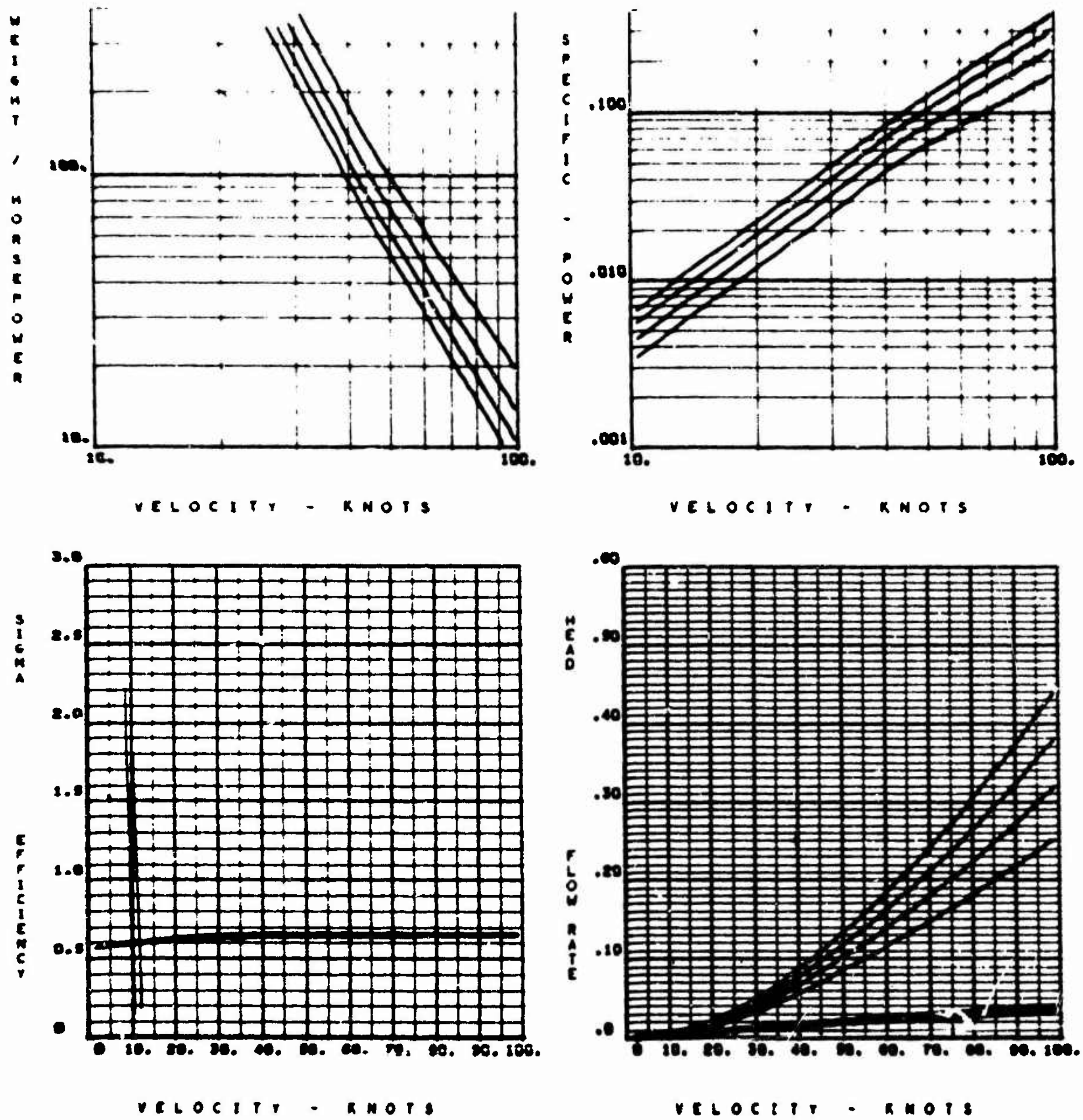

Figure 11 (Continued)
(b) Concluded

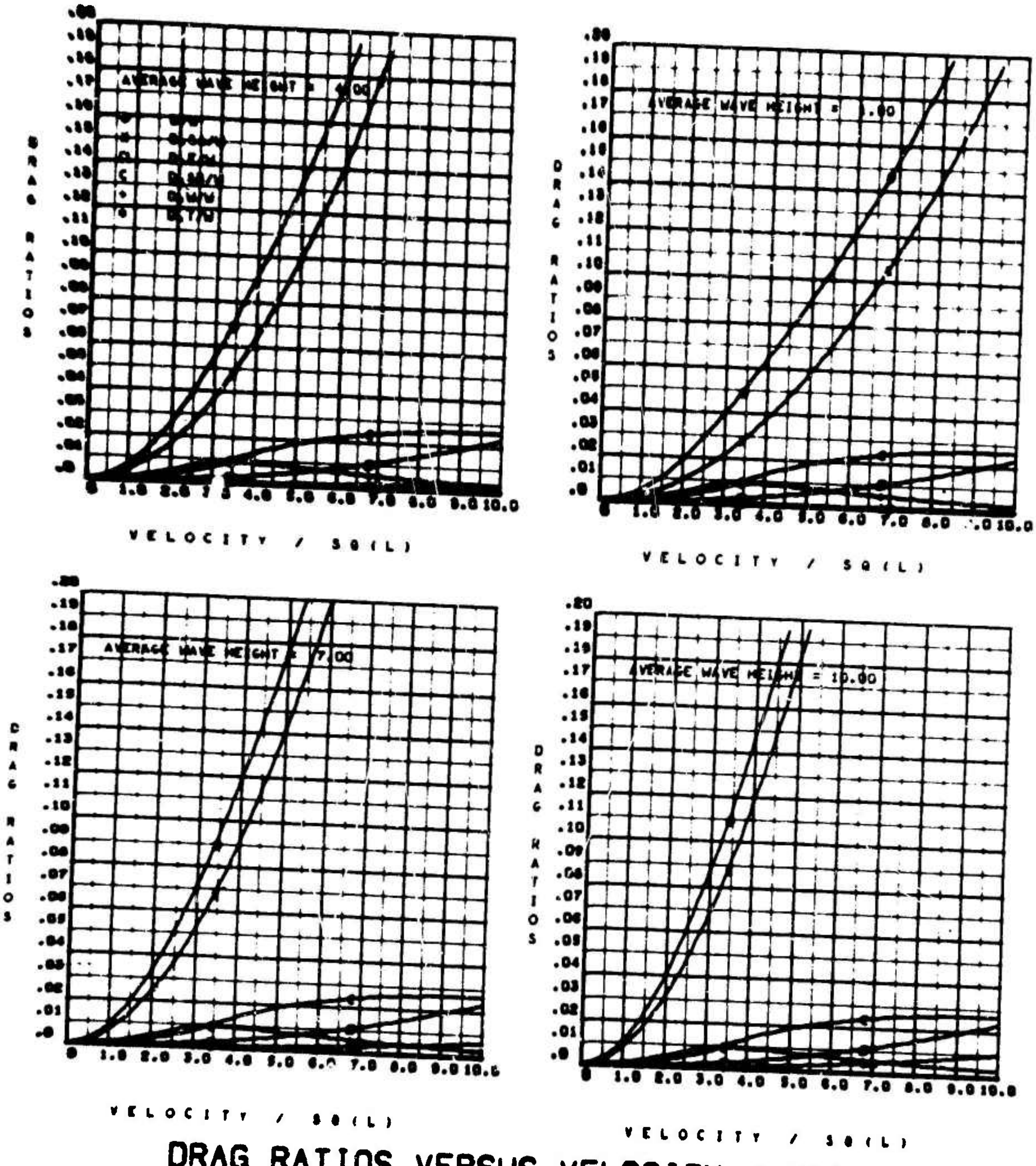

DRAG RATIOS VERSUS VELOCITY / SQ(L)

Figure 11 (Continued)

(c) $K_{D_D} = 0.08$, $K_{D_s} = 0.16$, $w/\sqrt{S} = 1.1$

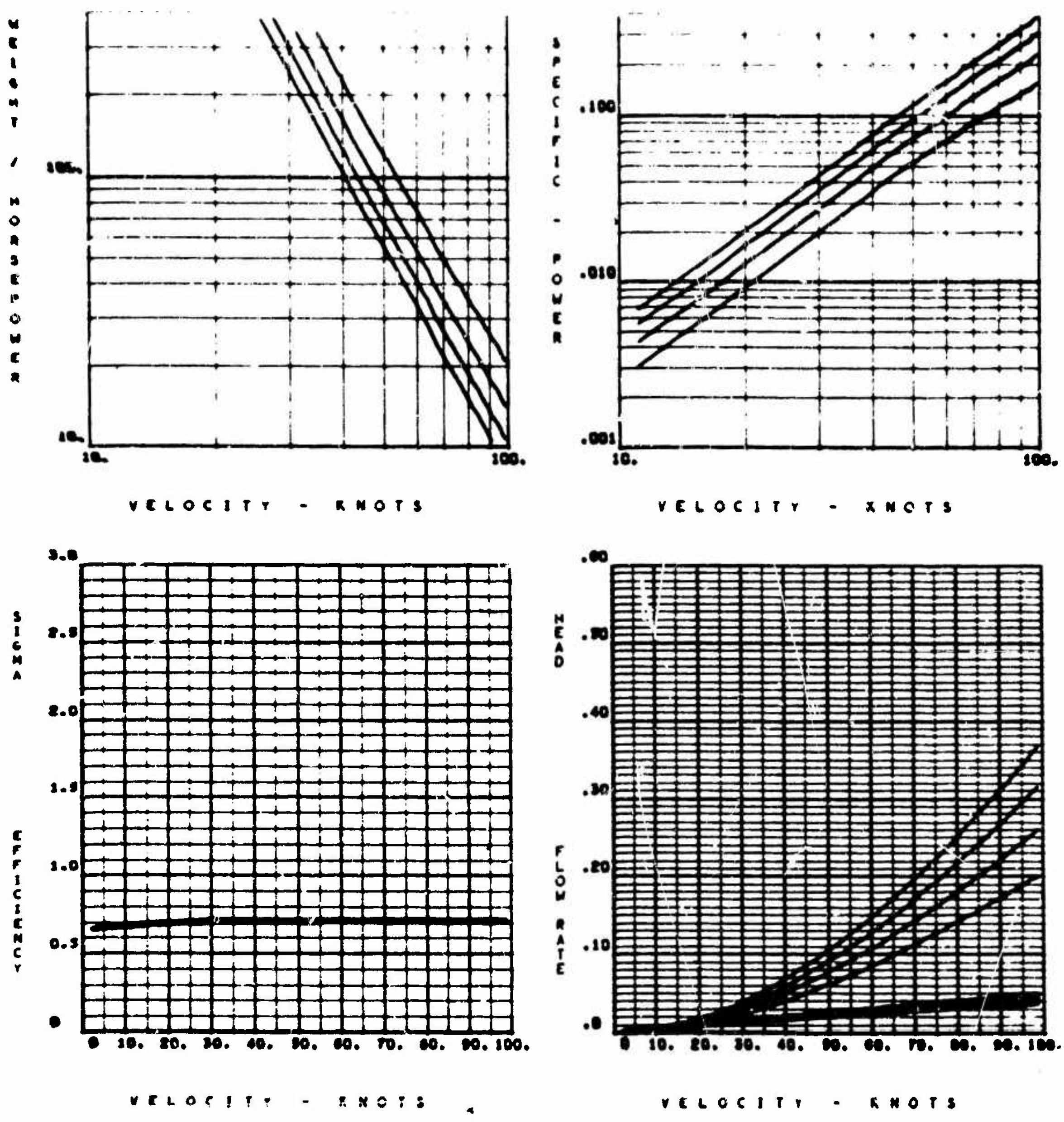

Figure 11 (Continued)
(c) Concluded

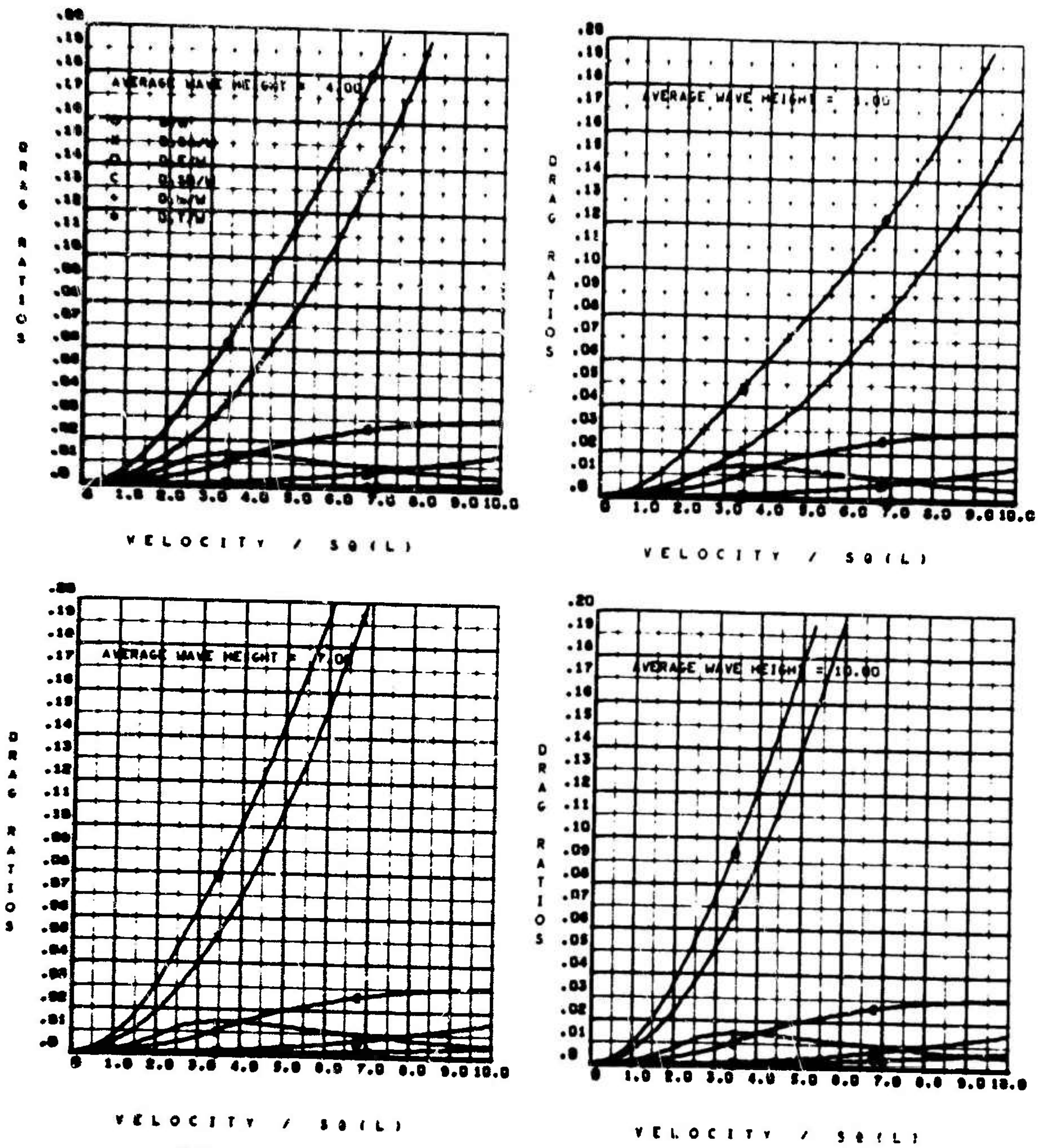

DRAG RATIOS VERSUS VELOCITY / SQ(L)

Figure 11 (Continued)

(d) $K_{D_D} = 0.08$, $K_{D_s} = 0.16$, $w/\sqrt{L} = 1.7$

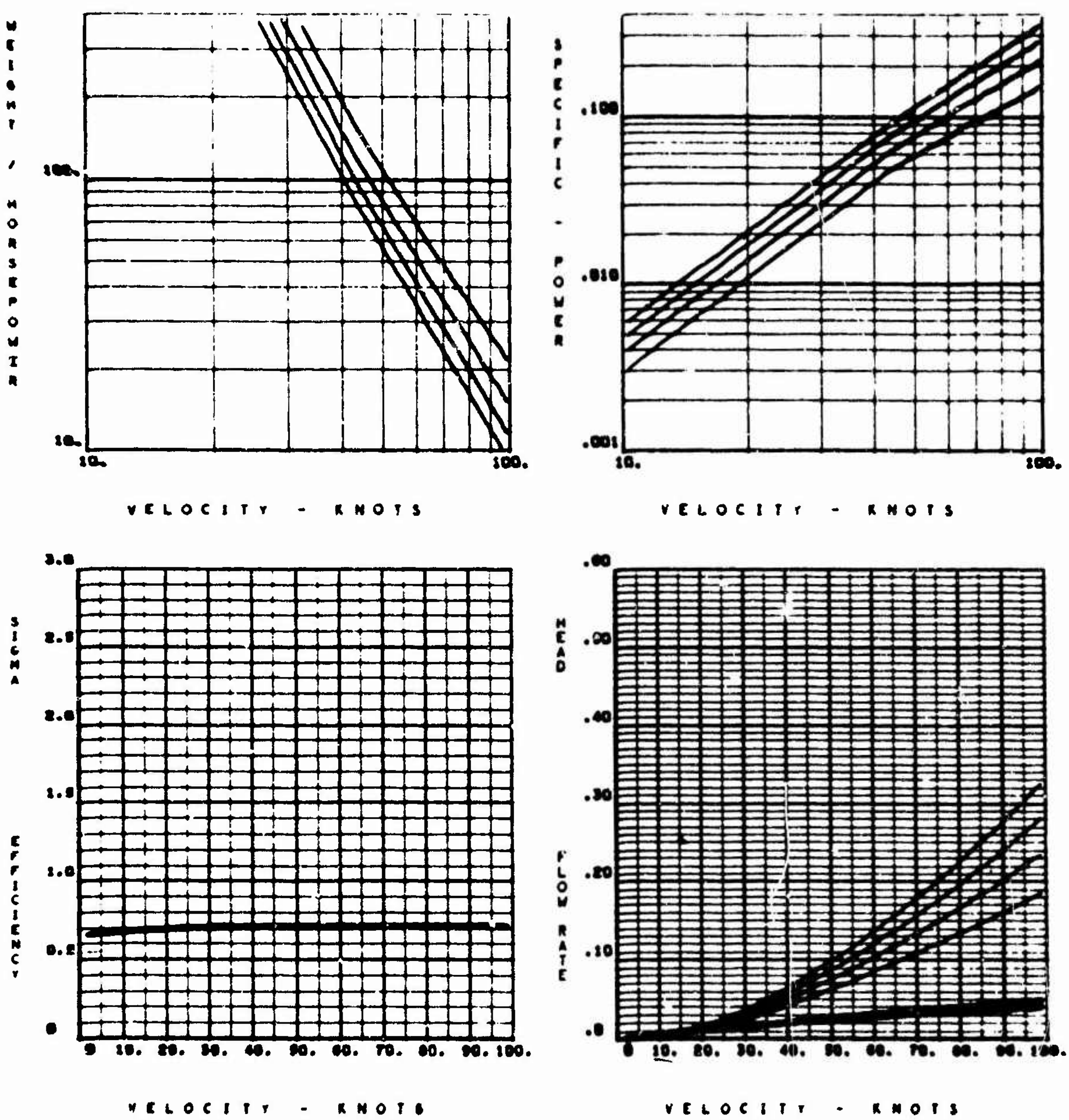

Figure 11 (Concluded)
(d) Concluded

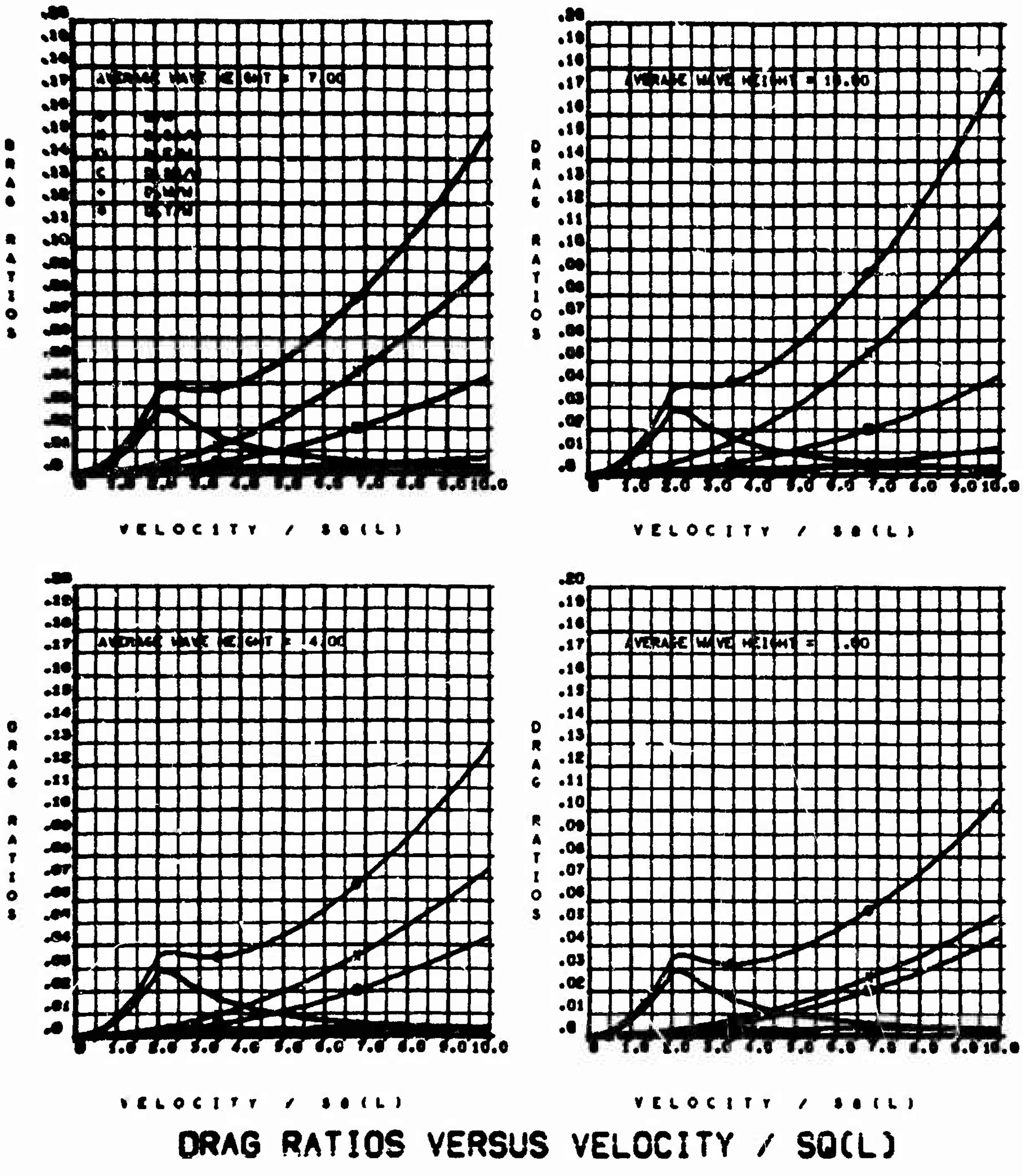

Figure 12 - General Performance Parameters of 10,000 Ton CAB With ℓ/b = 2.0

(a) K_{D_D} = 0.04, K_{D_s} = 0.08, $w/\sqrt{S}$ = 1.1

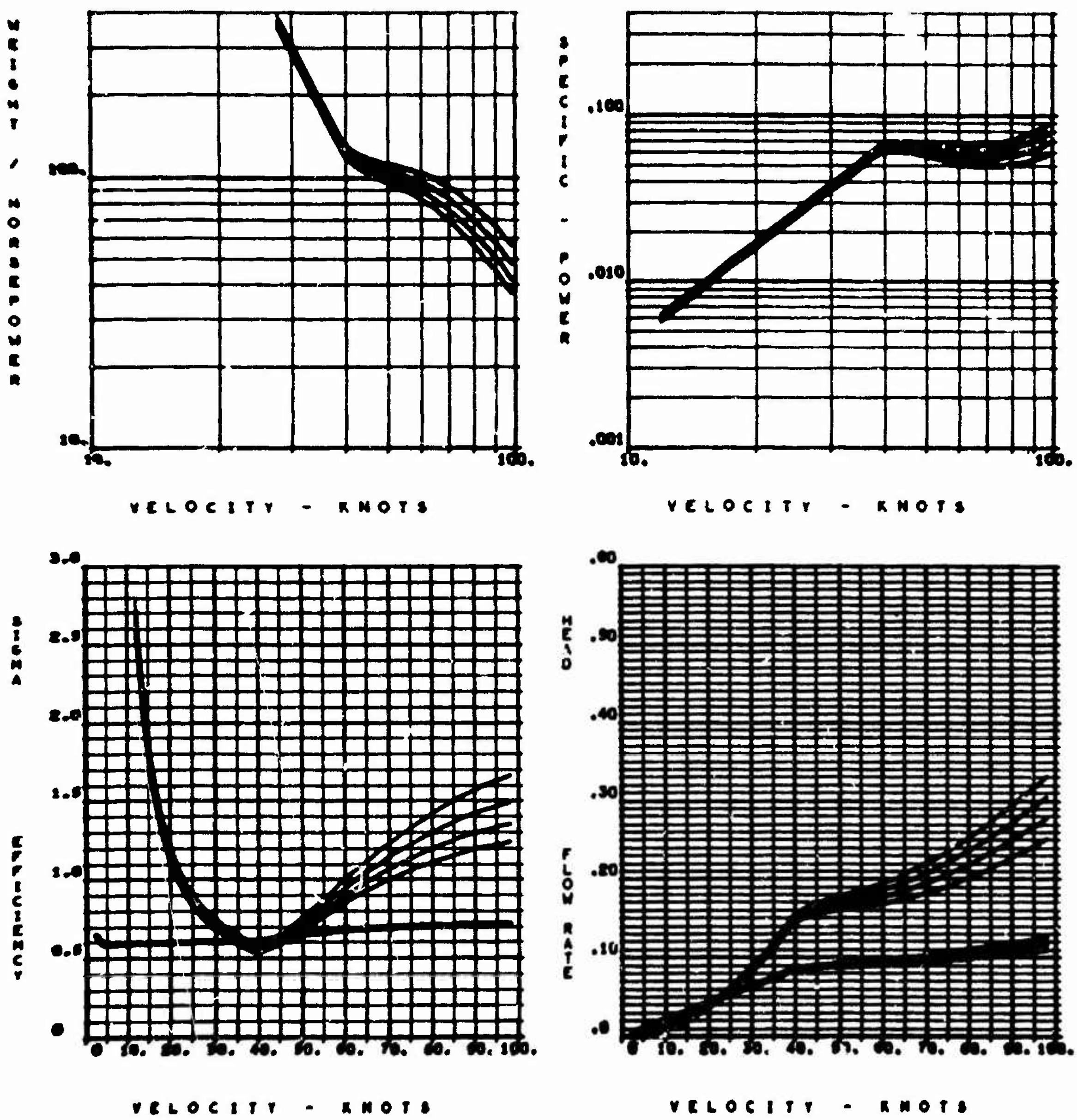

Figure 12 (Continued)
(a) Concluded

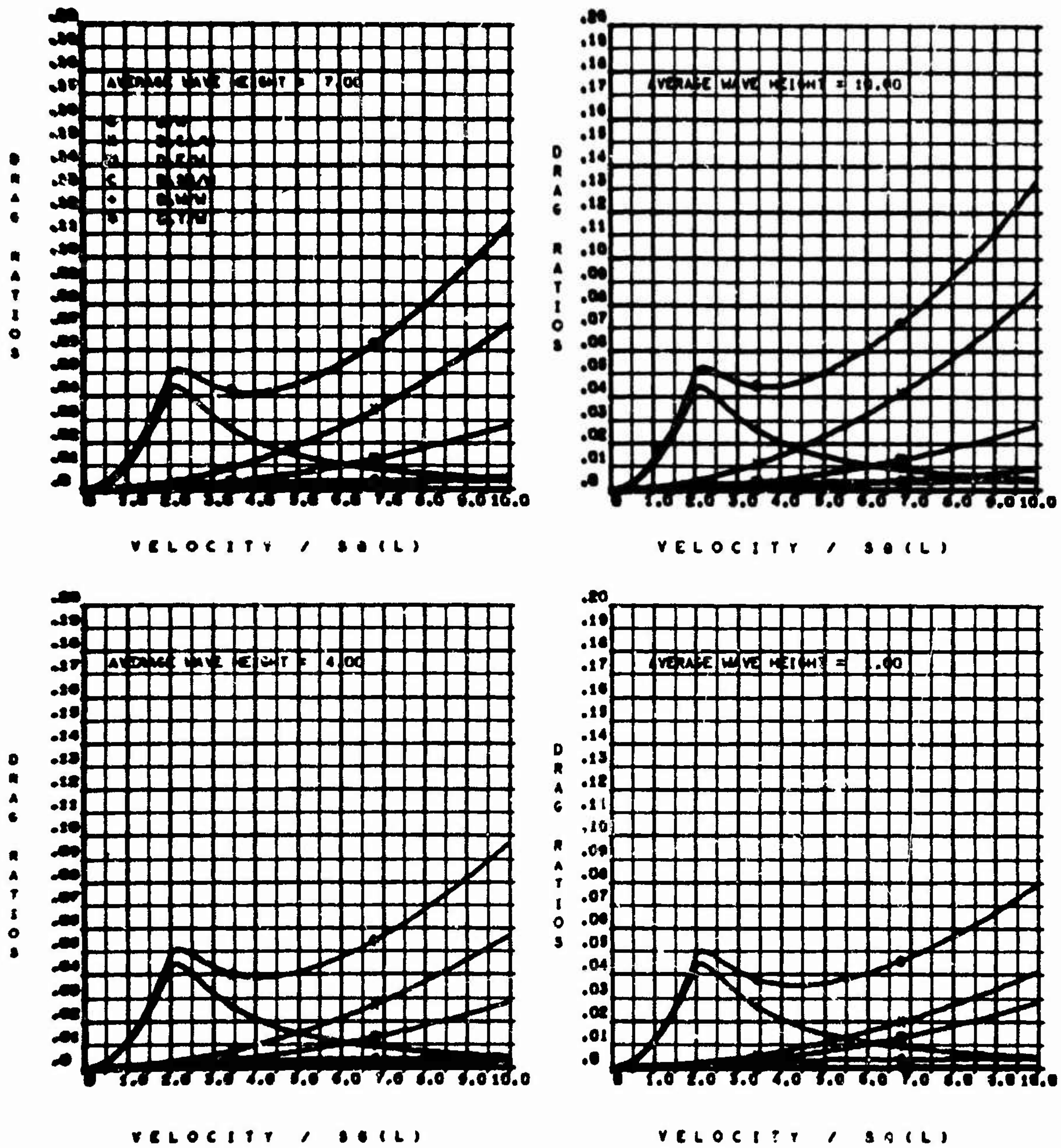

DRAG RATIOS VERSUS VELOCITY / SQ(L)

Figure 12 (Continued)

(b) $K_{D_D} = 0.04$, $K_{D_S} = 0.08$, $w/\sqrt{S} = 1.7$

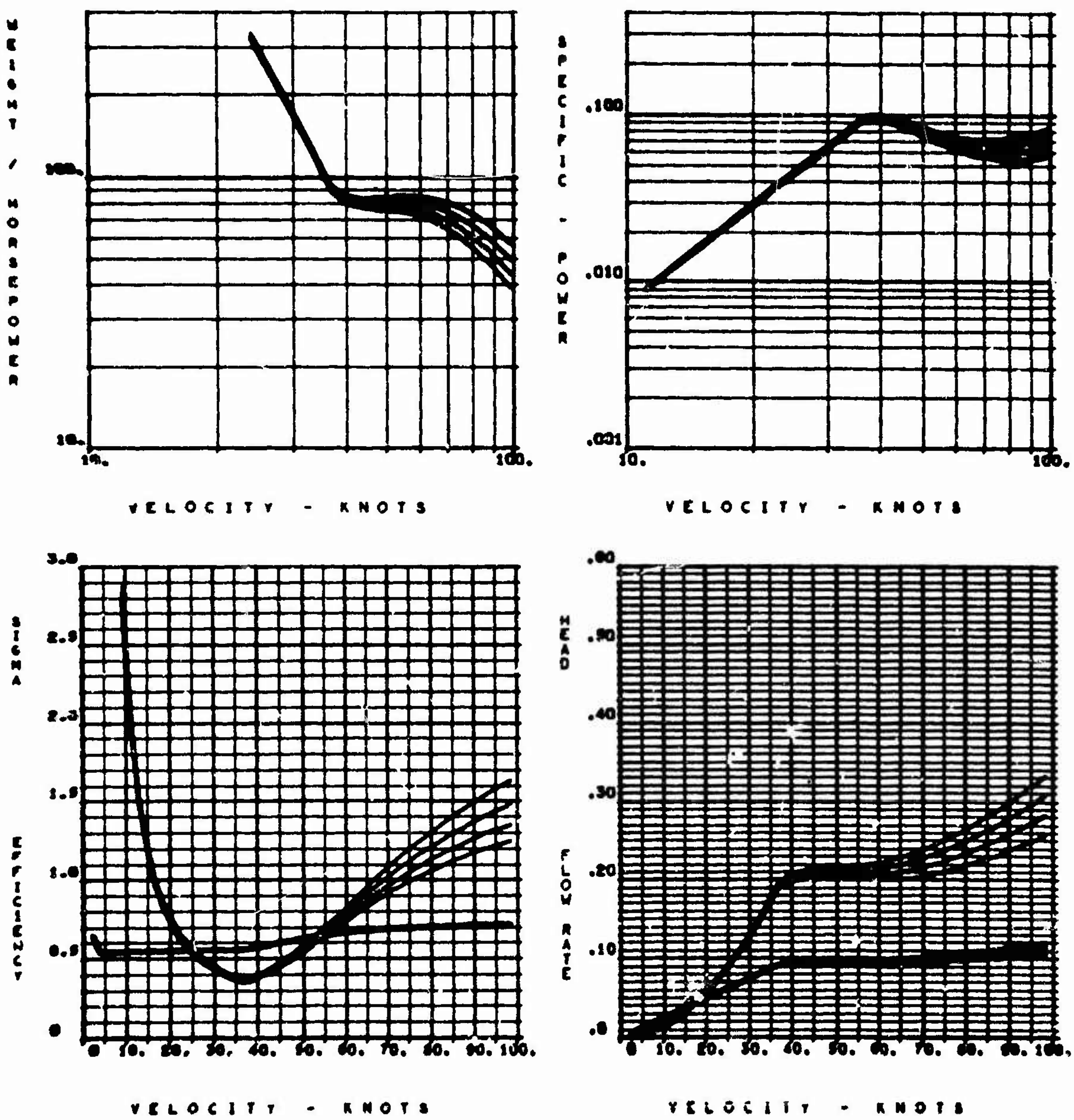

Figure 12 (Continued)

(b) Concluded

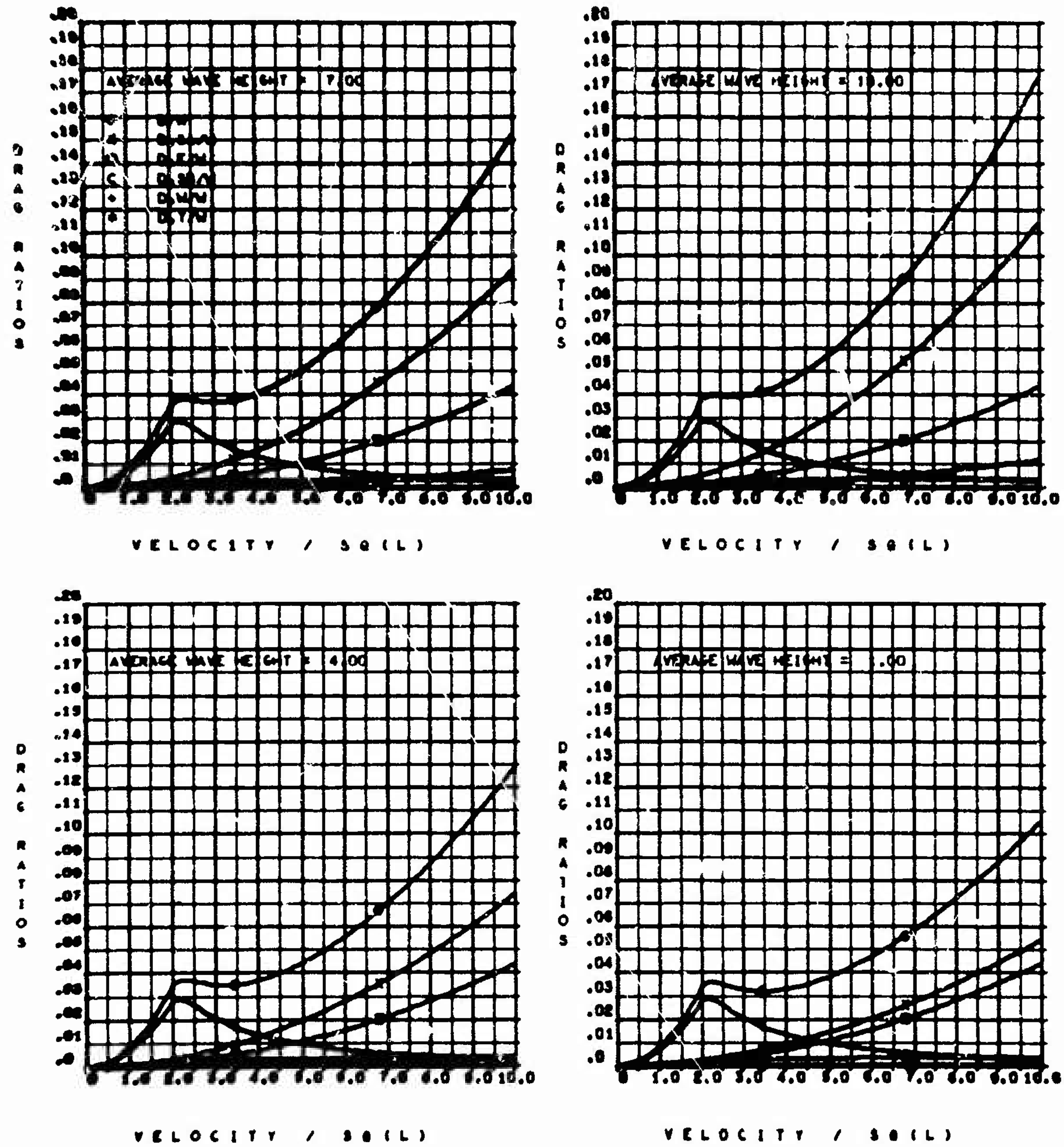

DRAG RATIOS VERSUS VELOCITY / SQ(L)

Figure 12 (Continued)

(c) $K_{D_D} = 0.08$, $K_{D_S} = 0.16$, $w/\sqrt{S} = 1.1$

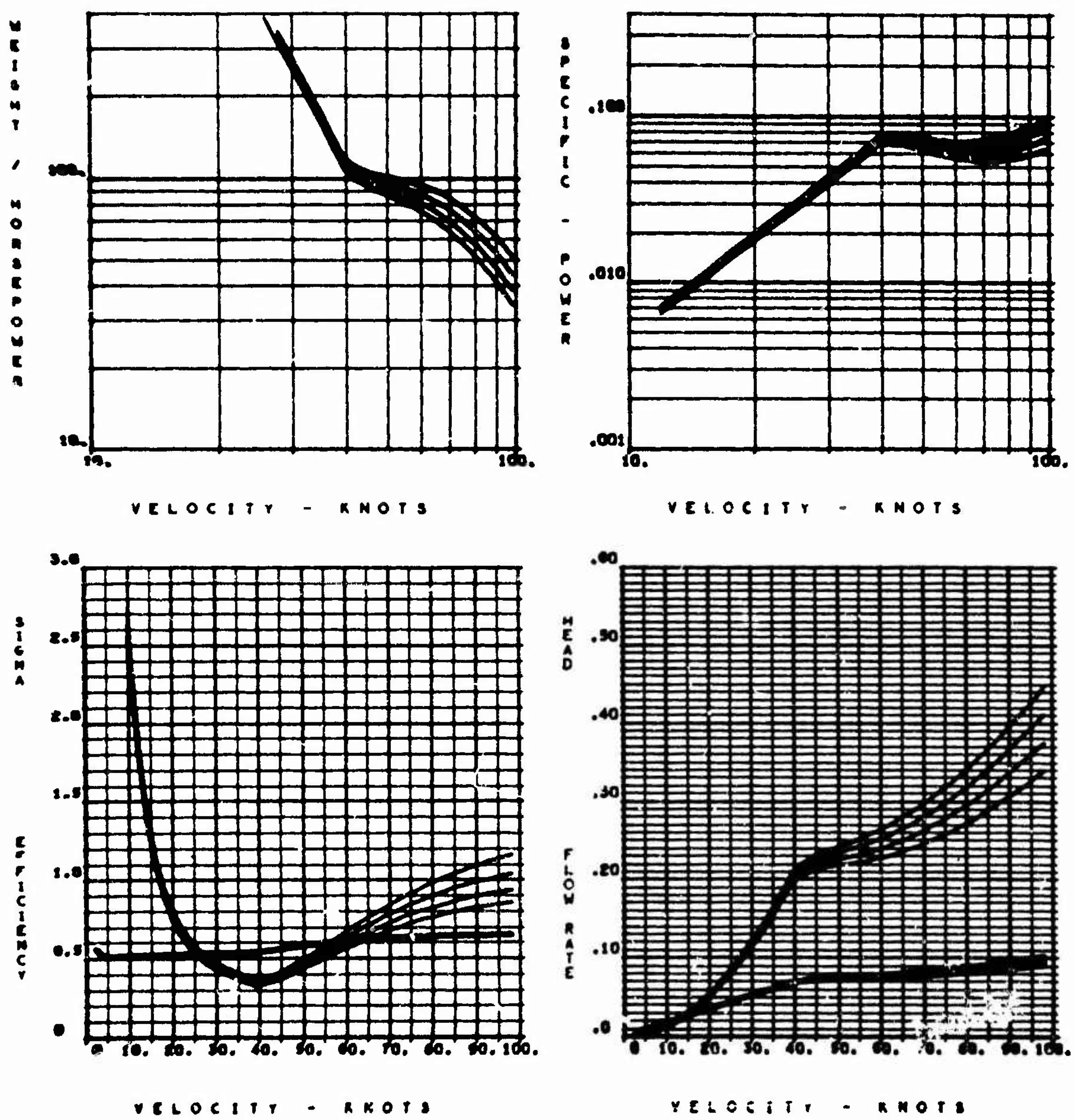

Figure 12 (Continued)

(c) Concluded

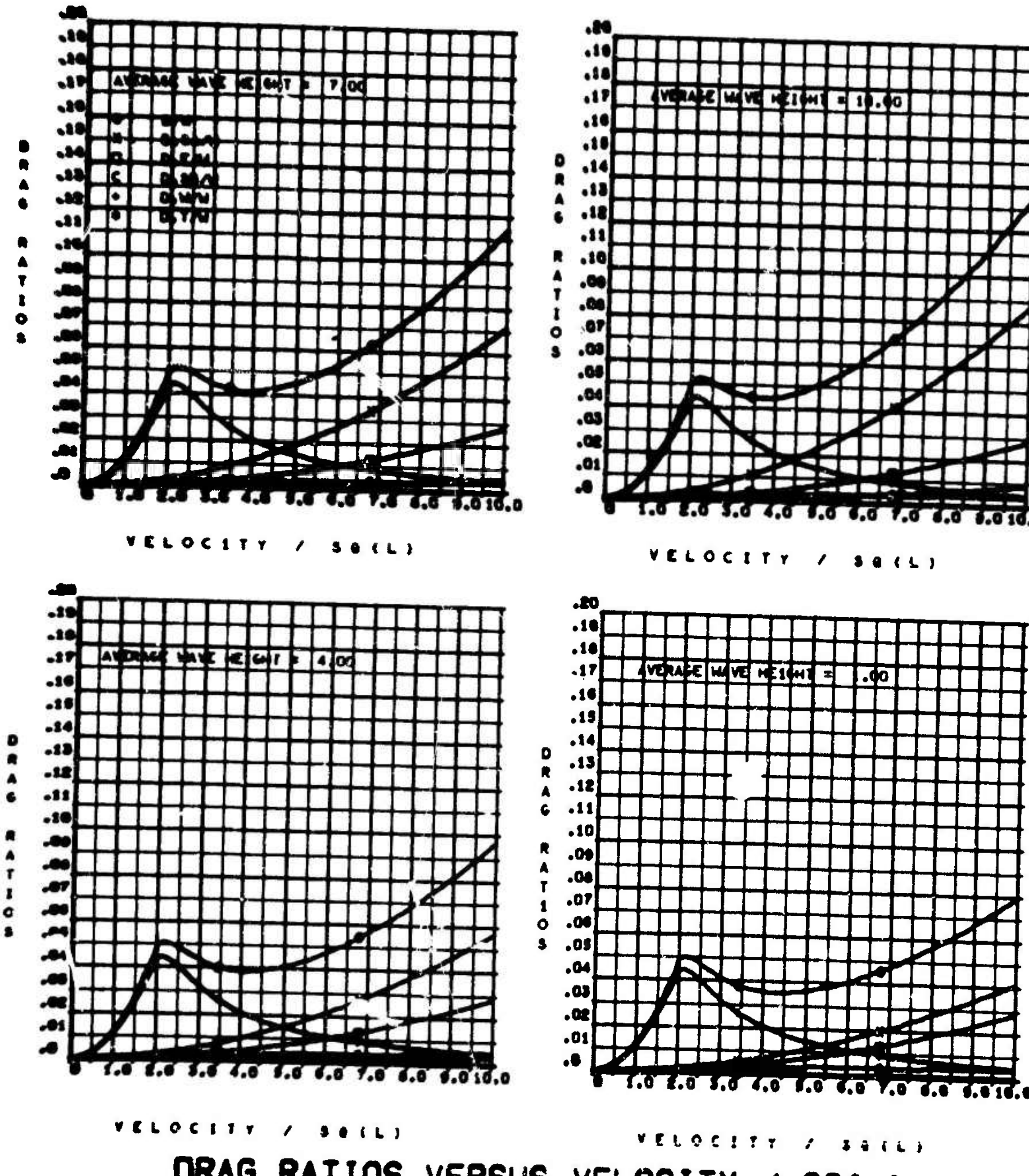

DRAG RATIOS VERSUS VELOCITY / SQ(L)

Figure 12 (Continued)

(d) $K_{D_D} = 0.08$, $K_{D_s} = 0.16$, $w/\sqrt{S} = 1.7$

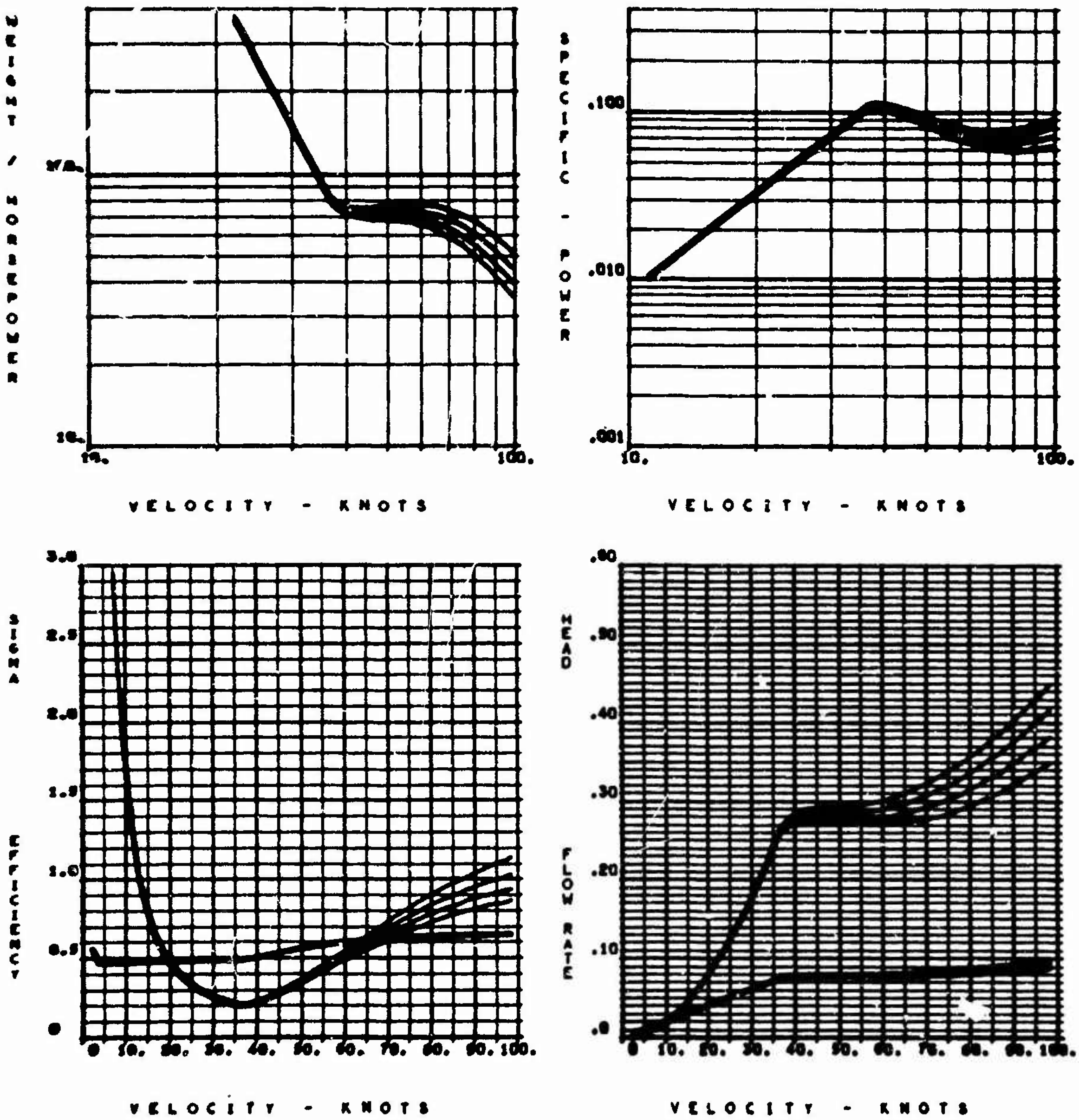

Figure 12 (Concluded)

(d) Concluded

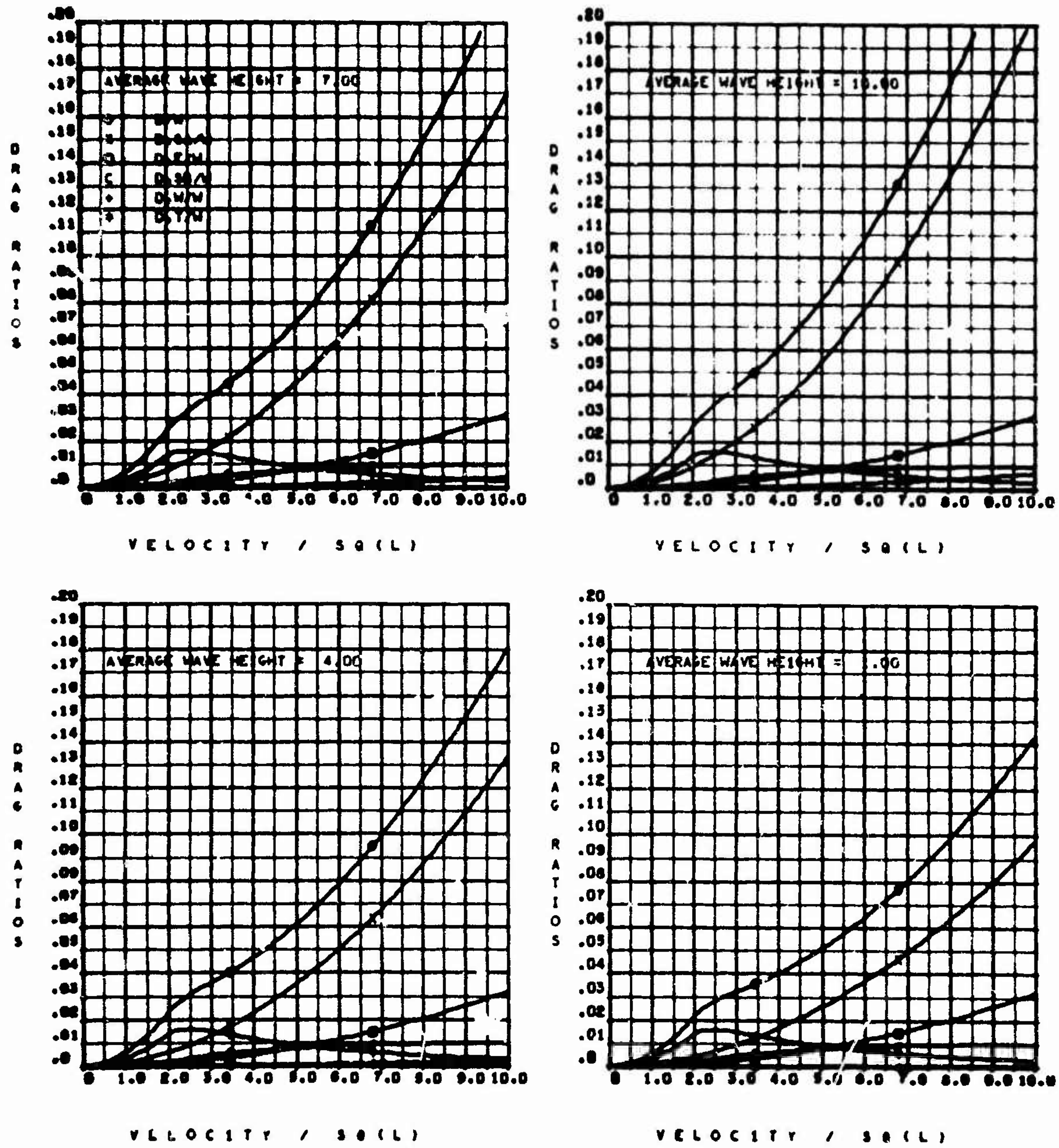

DRAG RATIOS VERSUS VELOCITY / SQ(L)

Figure 13 - General Performance Parameters of 10,000 Ton CAB With $\ell/b = 3.74$

(a) $K_{D_D} = 0.04$, $K_{D_s} = 0.08$, $w/\sqrt{S} = 1.1$

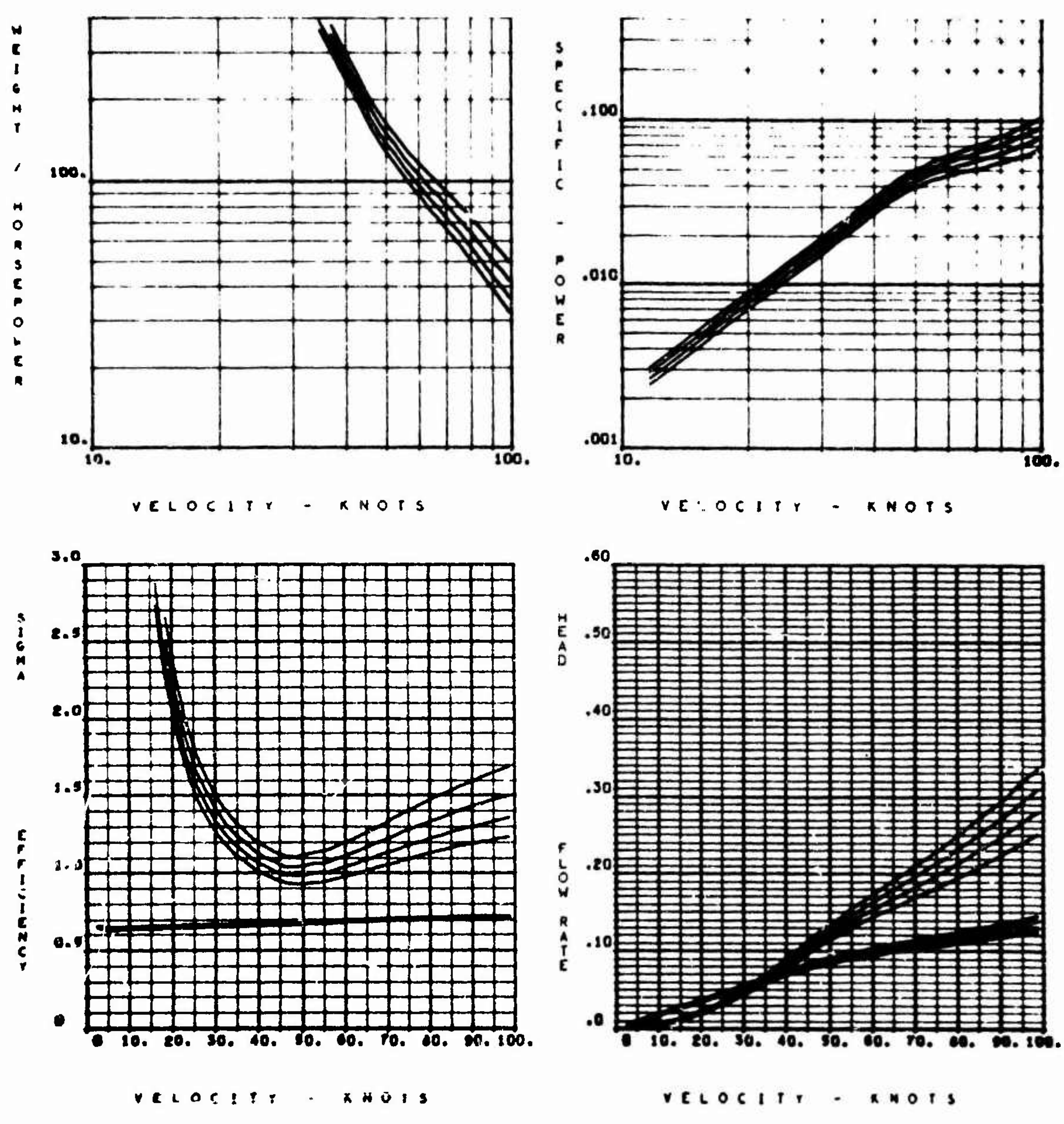

Figure 13 (Continued)

(a) Concluded

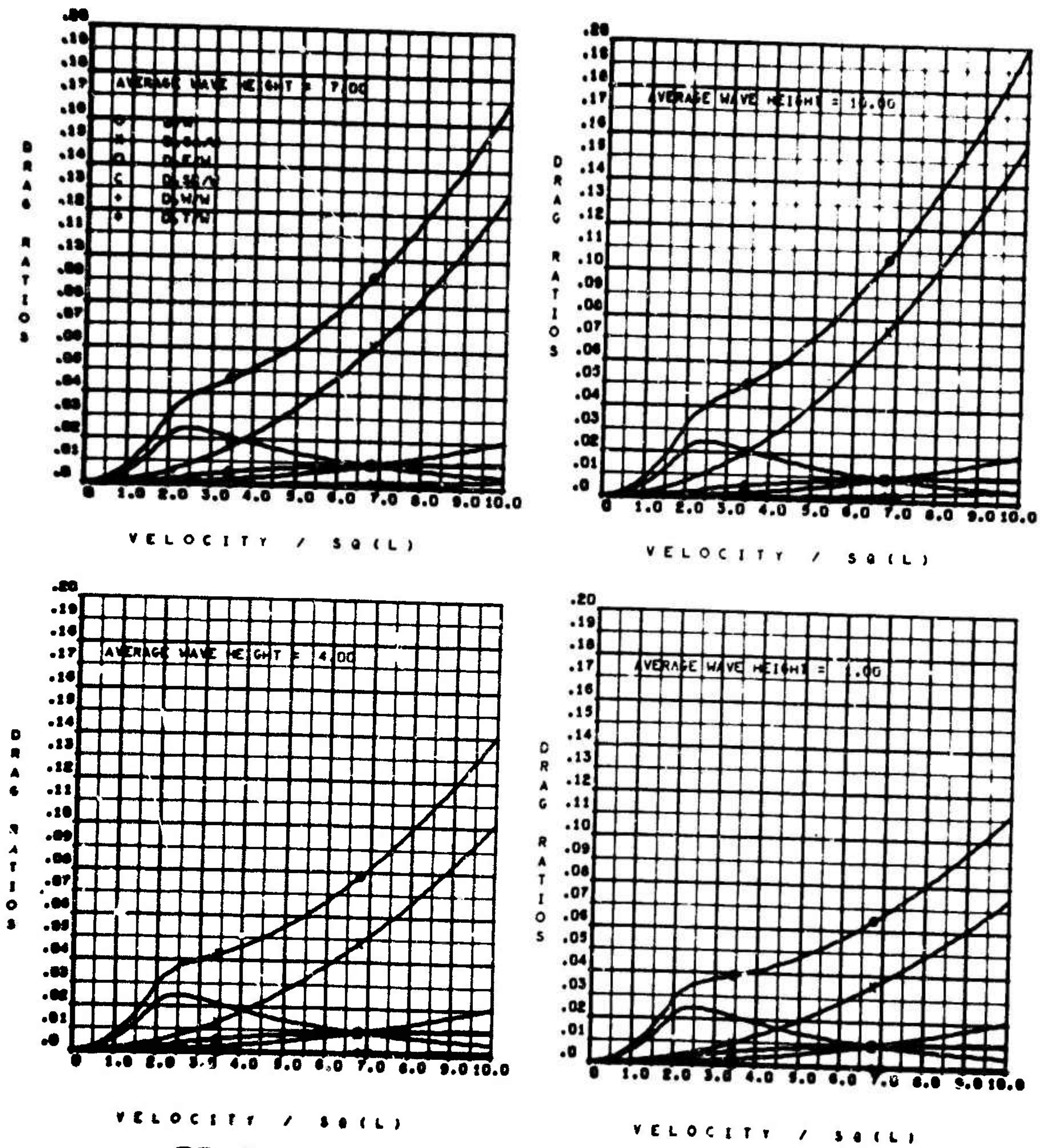

DRAG RATIOS VERSUS VELOCITY / SQ(L)

Figure 13 (Continued)

(b) $K_{D_D} = 0.04$, $K_{D_s} = 0.08$, $w/\sqrt{S} = 1.7$

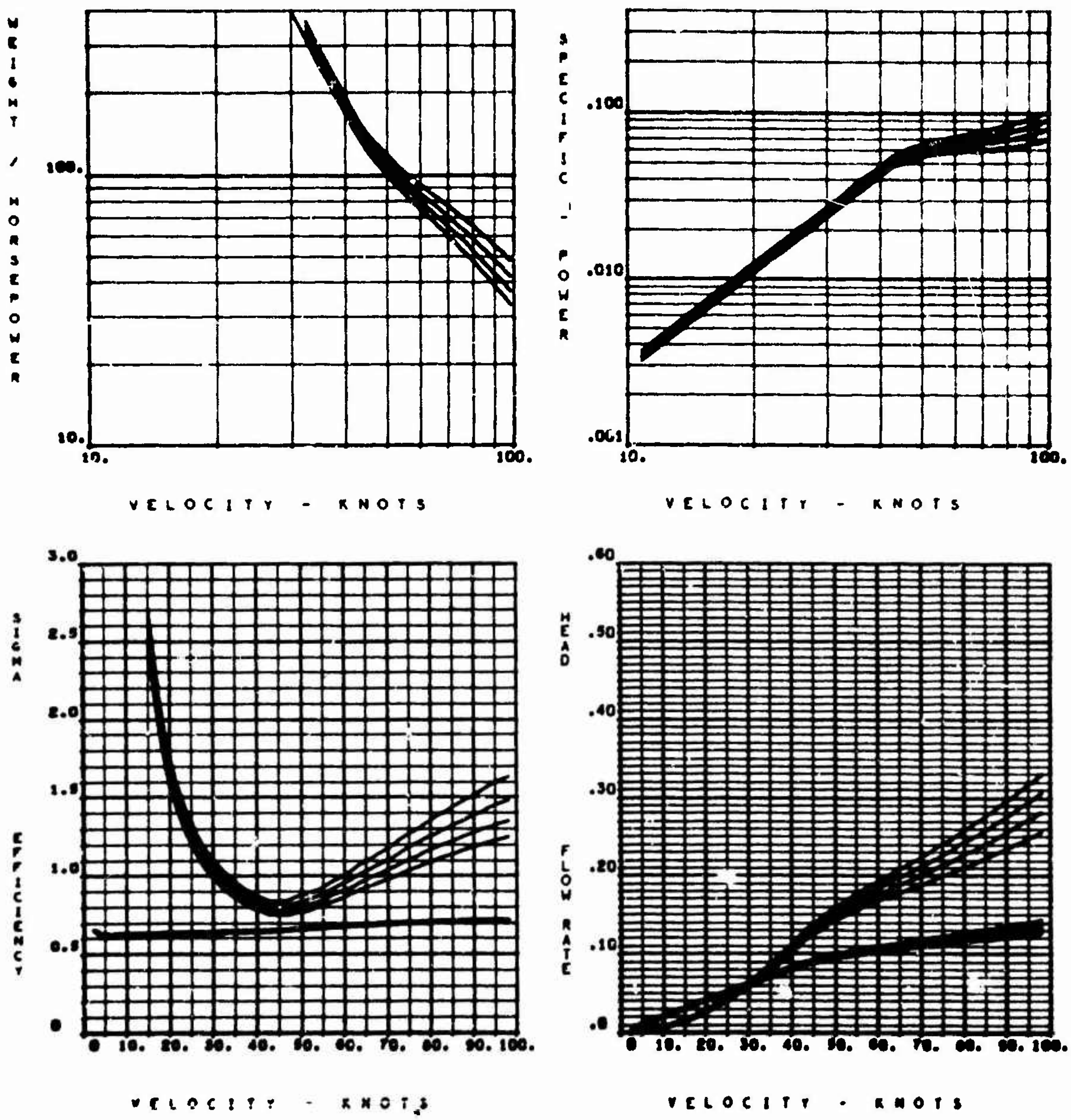

Figure 13 (Continued)

(b) Concluded

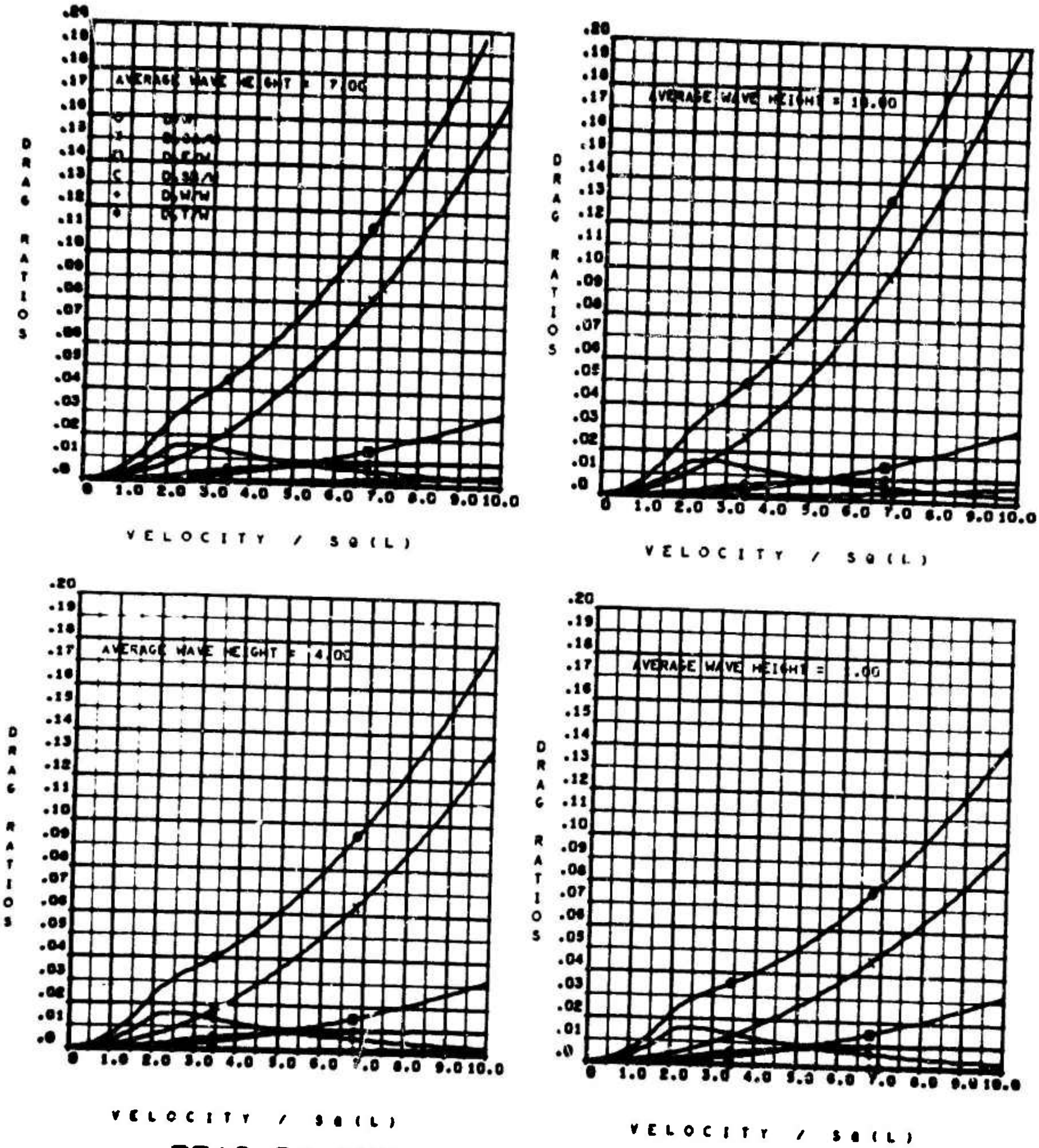

DRAG RATIOS VERSUS VELOCITY / SQ(L)

Figure 13 (Continued)

(c) $K_{D_D} = 0.08$, $K_{D_s} = 0.16$, $w/\sqrt{S} = 1.1$

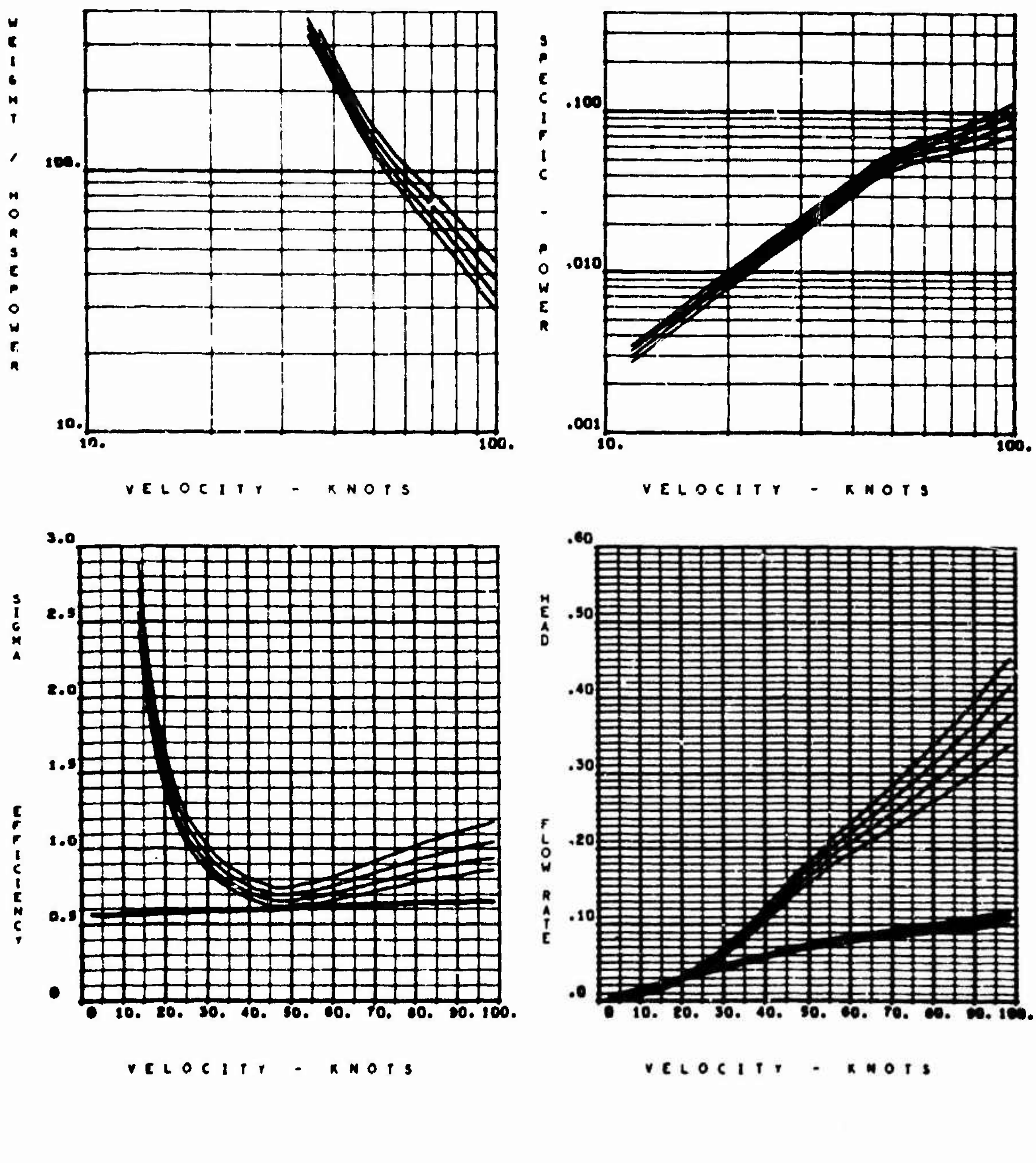

Figure 13 (Continued)

(c) Concluded

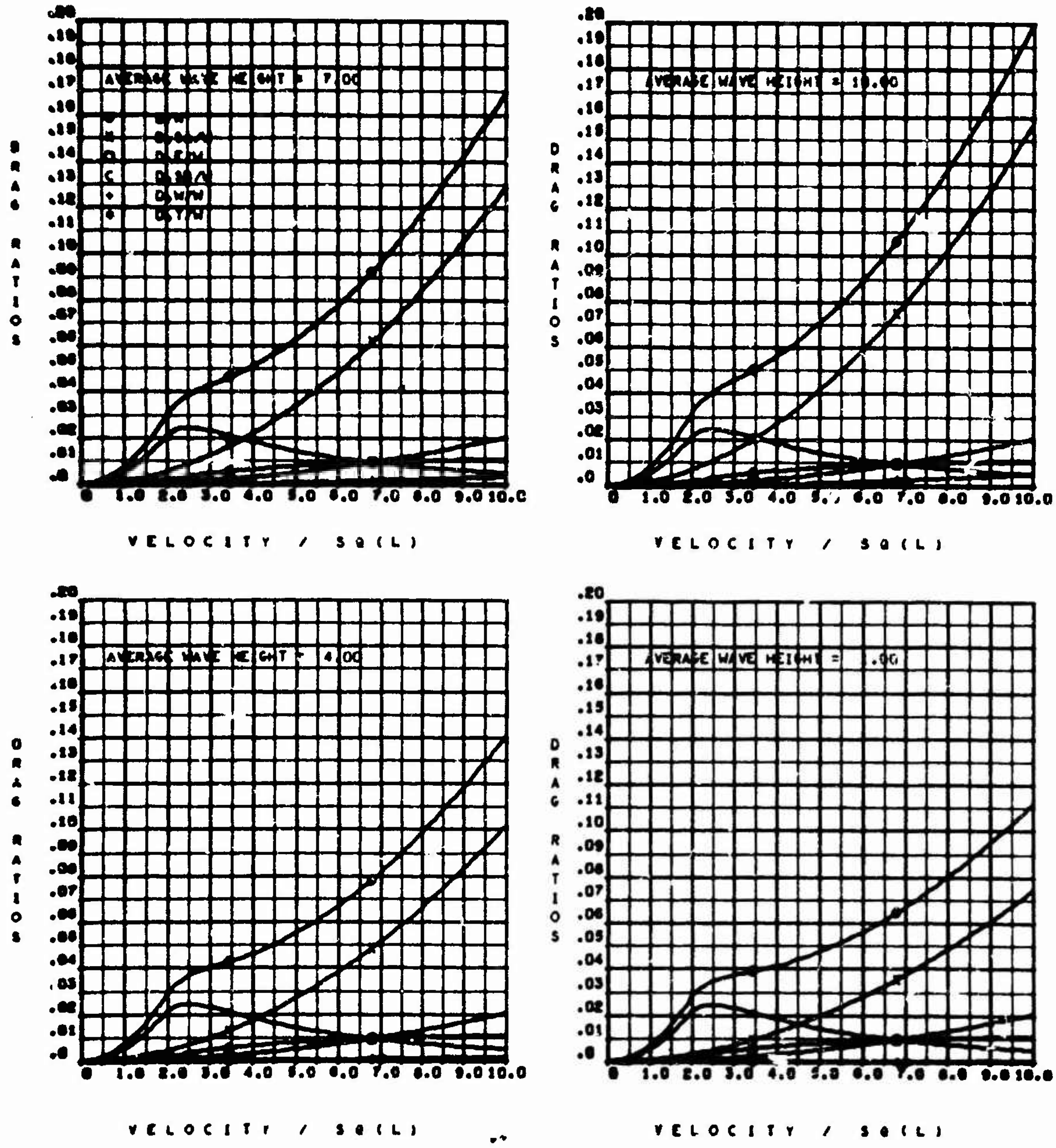

DRAG RATIOS VERSUS VELOCITY / SQ(L)

Figure 13 (Continued)

(d) $K_{D_D} = 0.08$, $K_{D_S} = 0.16$, $w/\sqrt{S} = 1.7$

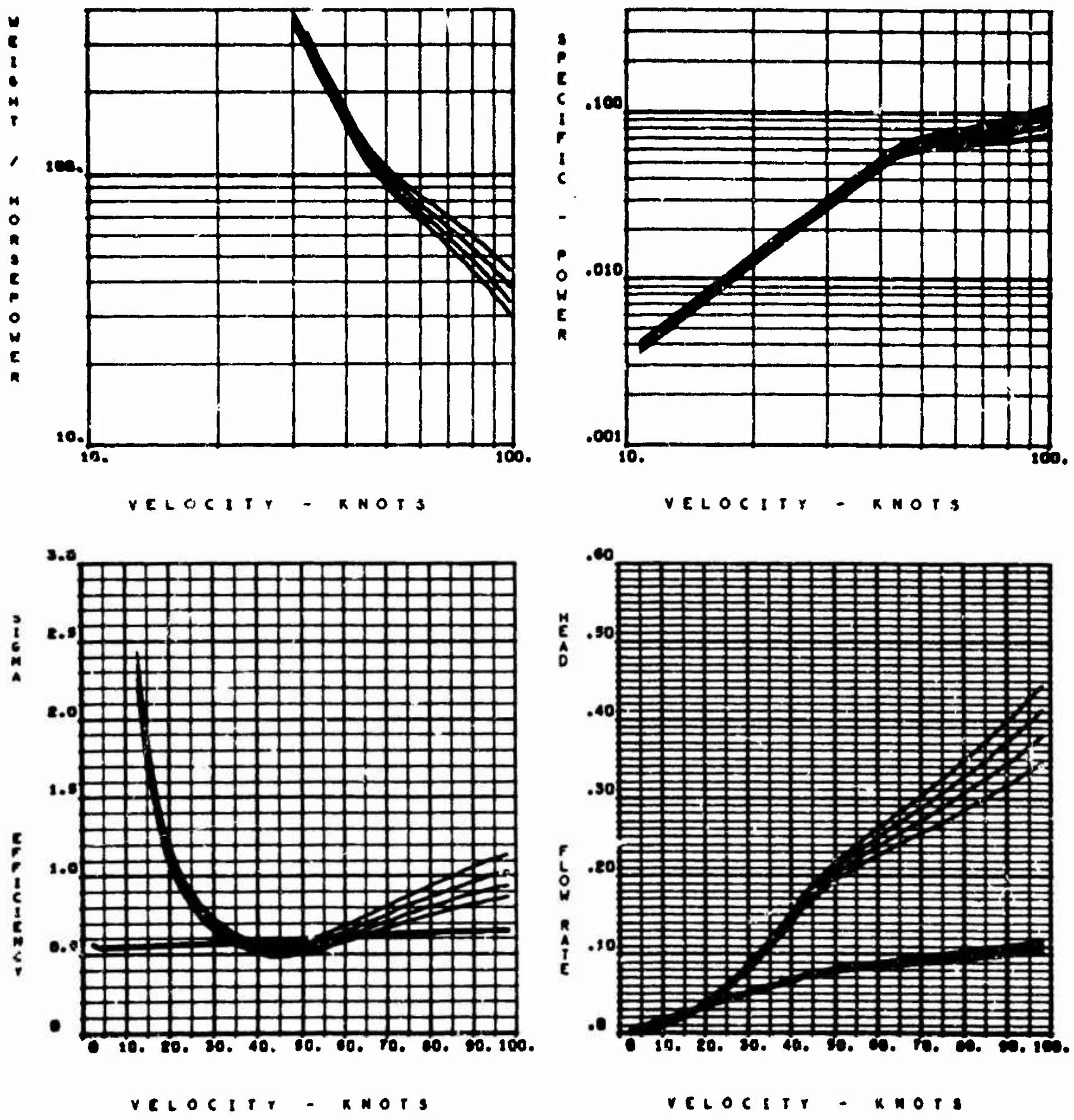

Figure 13 (Concluded)

(d) Concluded

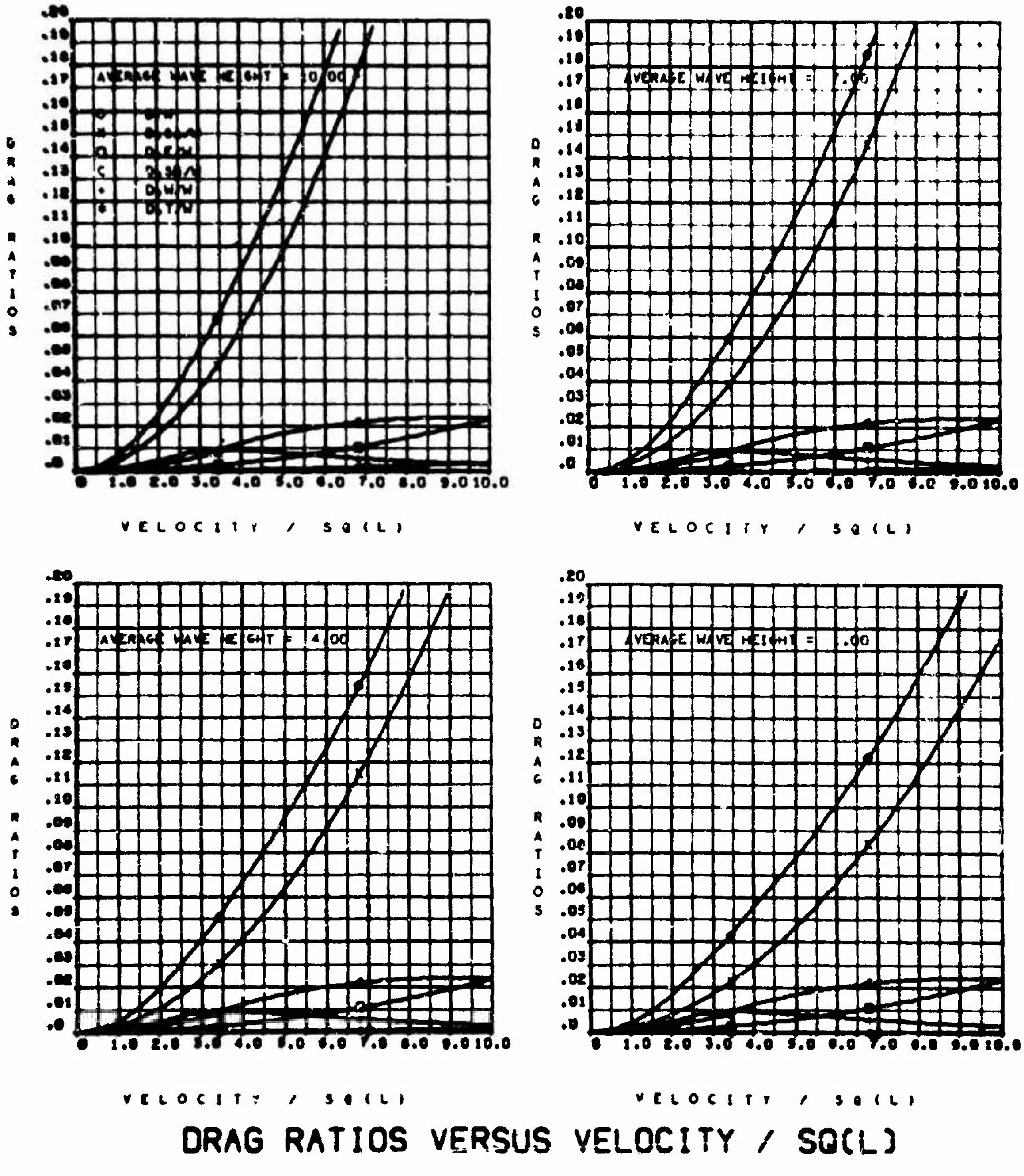

Figure 14 - General Performance Parameters of 10,000 Ton CAB

With $\ell/b = 7.0$

(a) $K_{D_D} = 0.04$, $K_{D_s} = 0.08$, $w/\sqrt{S} = 1.1$

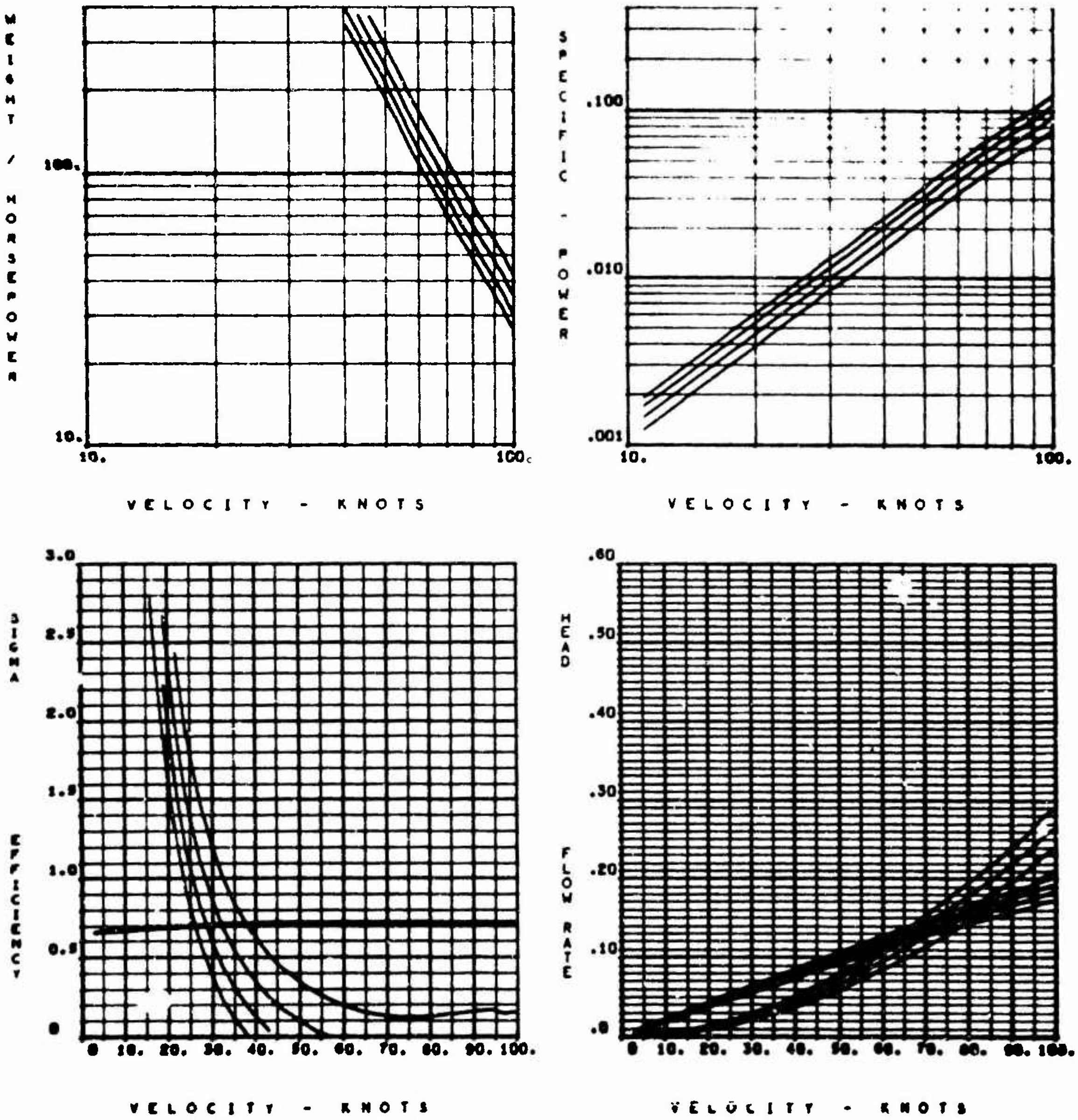

Figure 14 (Continued)

(a) Concluded

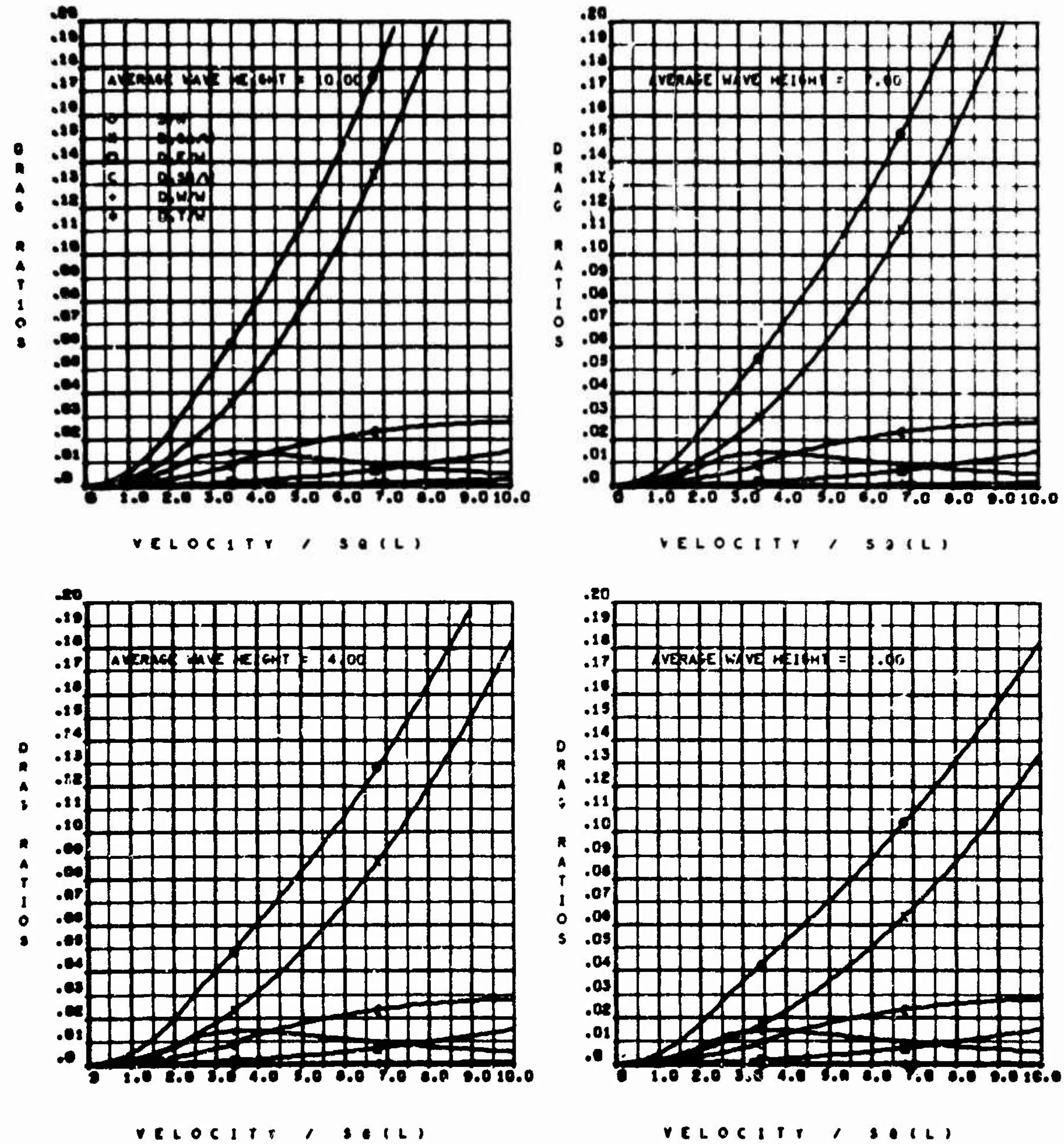

DRAG RATIOS VERSUS VELOCITY / SQ(L)

Figure 14 (Continued)

(b) $K_{D_D} = 0.04$, $K_{D_s} = 0.08$, $w/\sqrt{S} = 1.7$

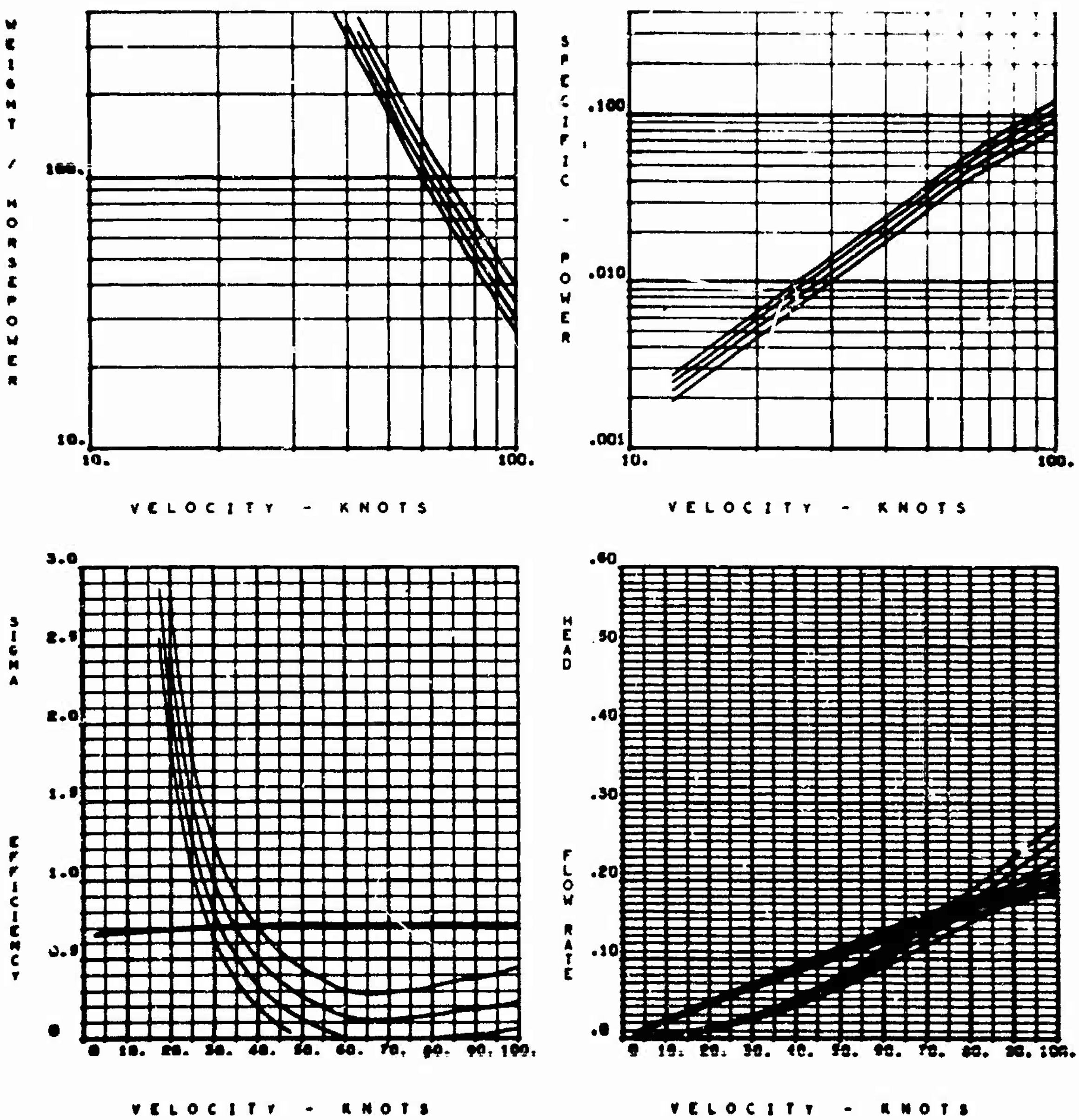

Figure 14 (Continued)

(b) Concluded

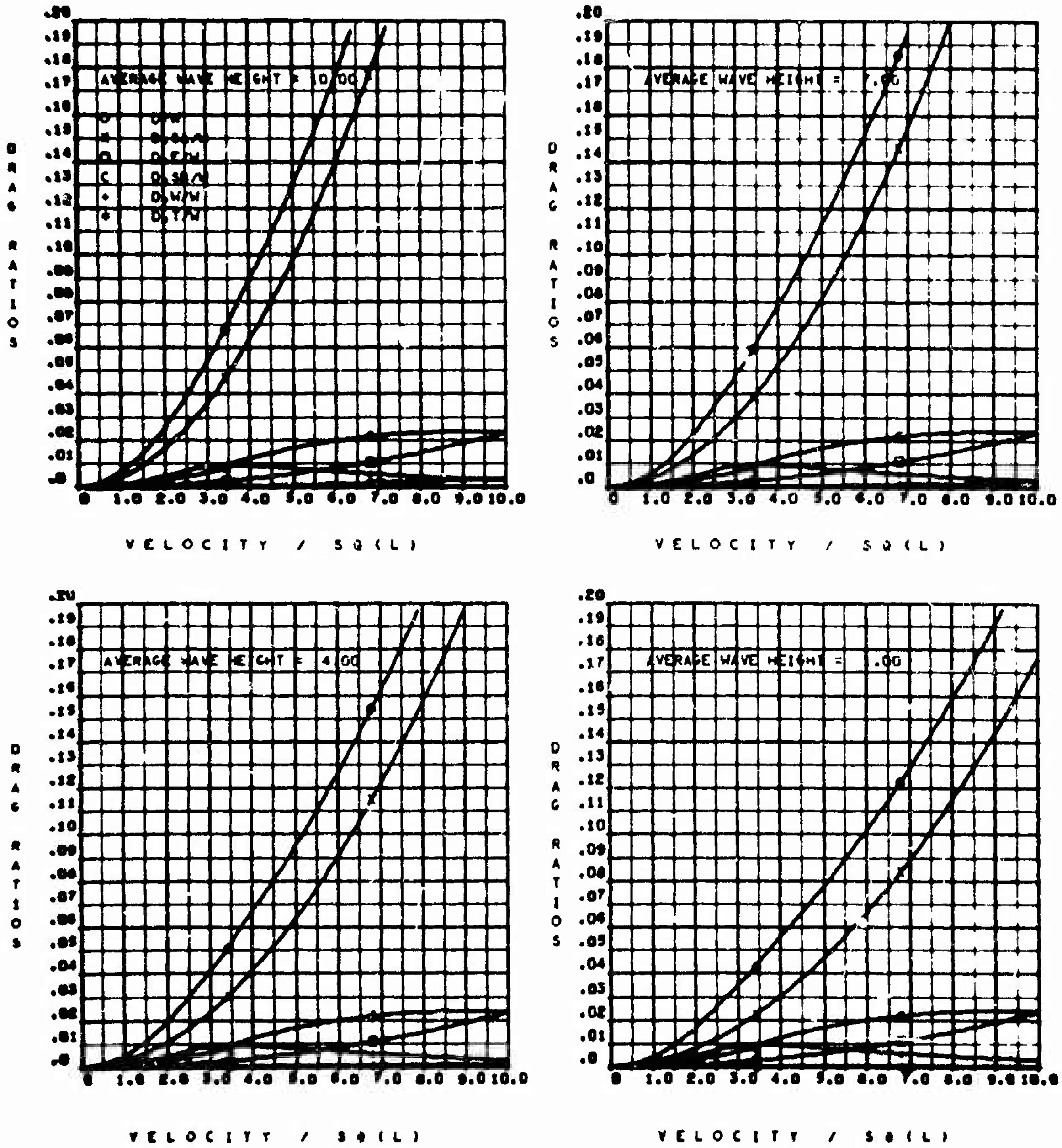

DRAG RATIOS VERSUS VELOCITY / SQ(L)

Figure 14 (Continued)

(c) $K_{D_D} = 0.08$, $K_{D_s} = 0.16$, $w/\sqrt{S} = 1.1$

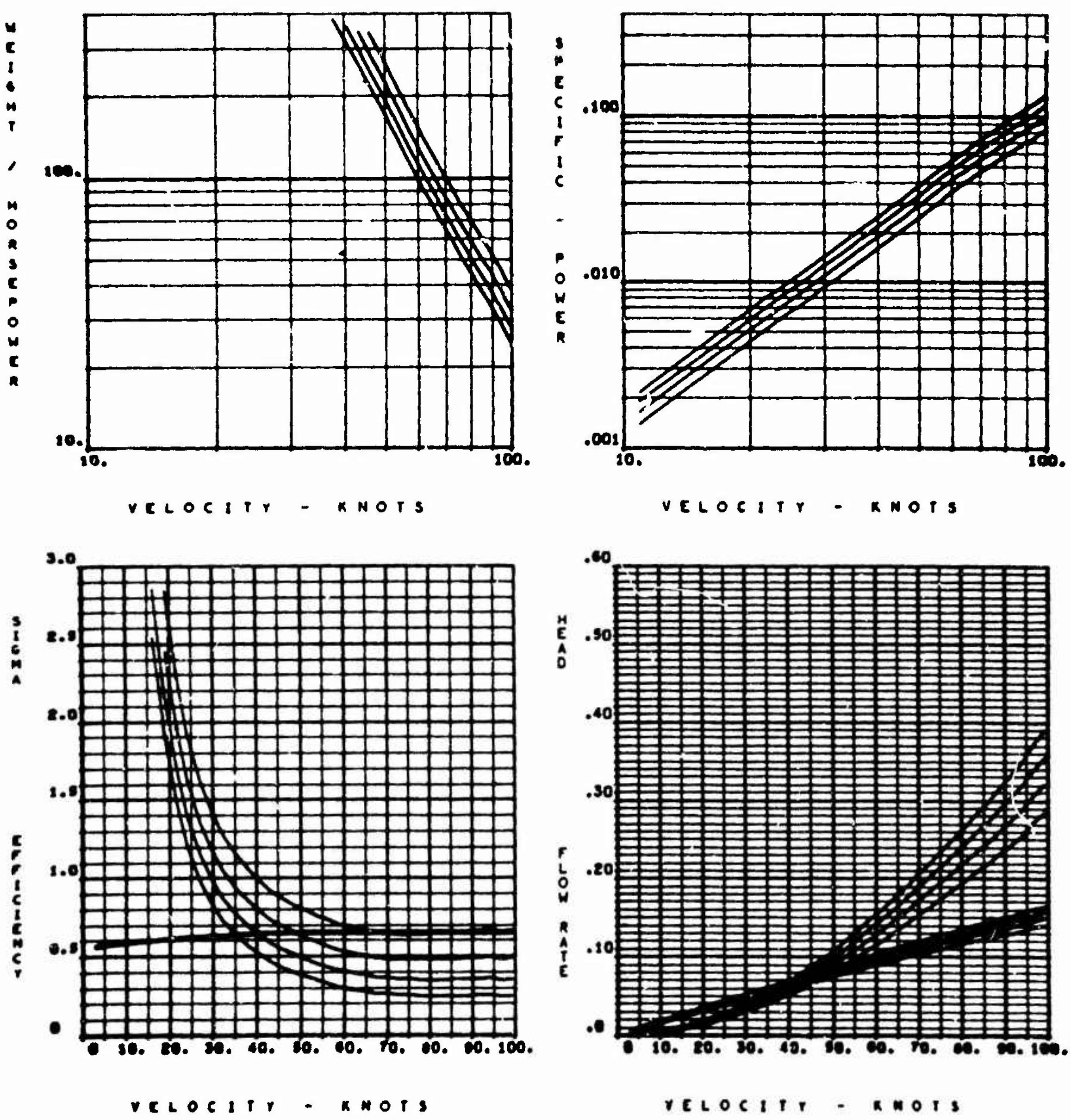

Figure 14 (Continued)
(c) Concluded

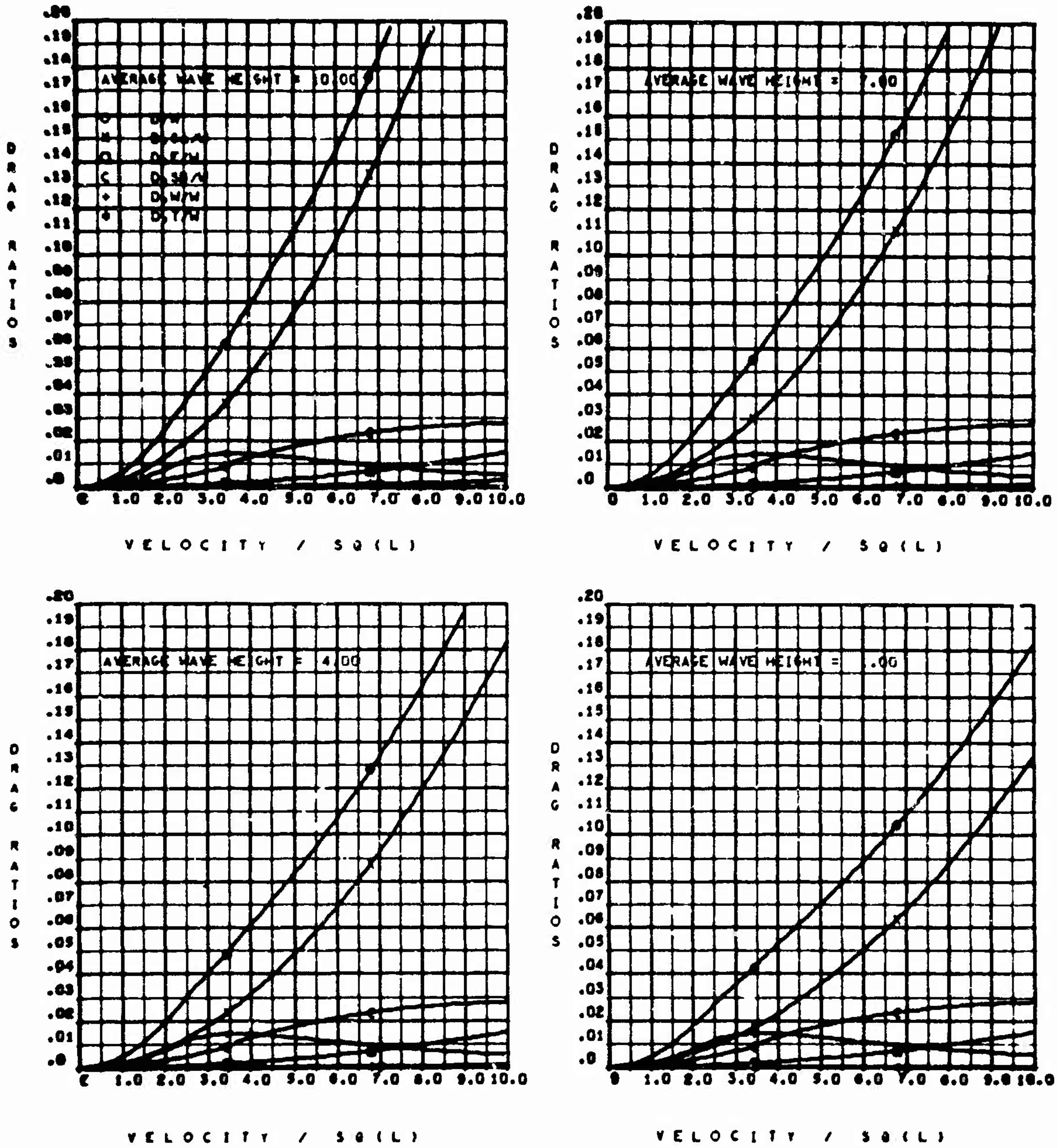

DRAG RATIOS VERSUS VELOCITY / SQ(L)

Figure 14 (Continued)

(d) $K_{D_D} = 0.08$, $K_{D_S} = 0.16$, $w/\sqrt{S} = 1.7$

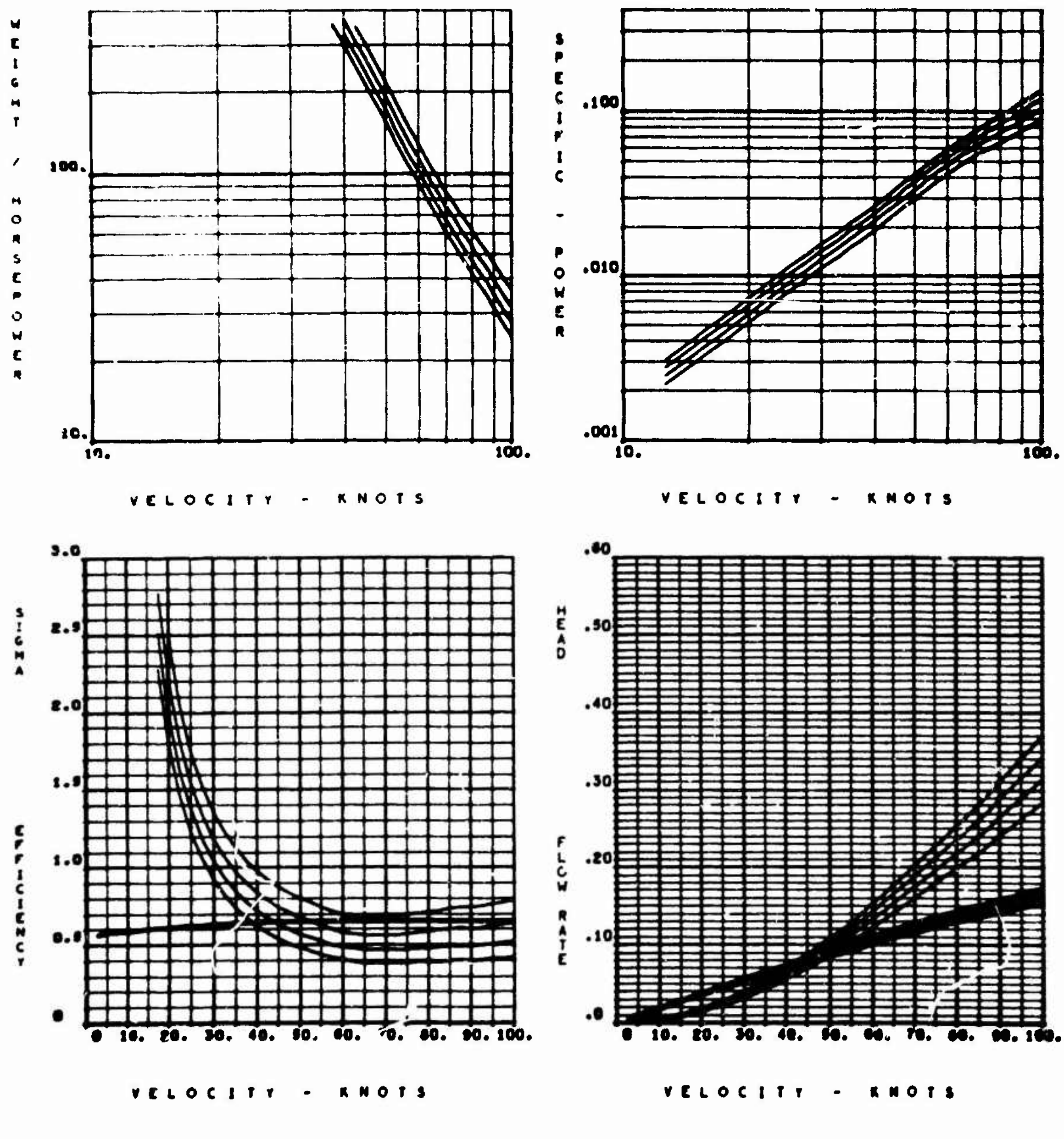

Figure 14 (Concluded)

(d) Concluded

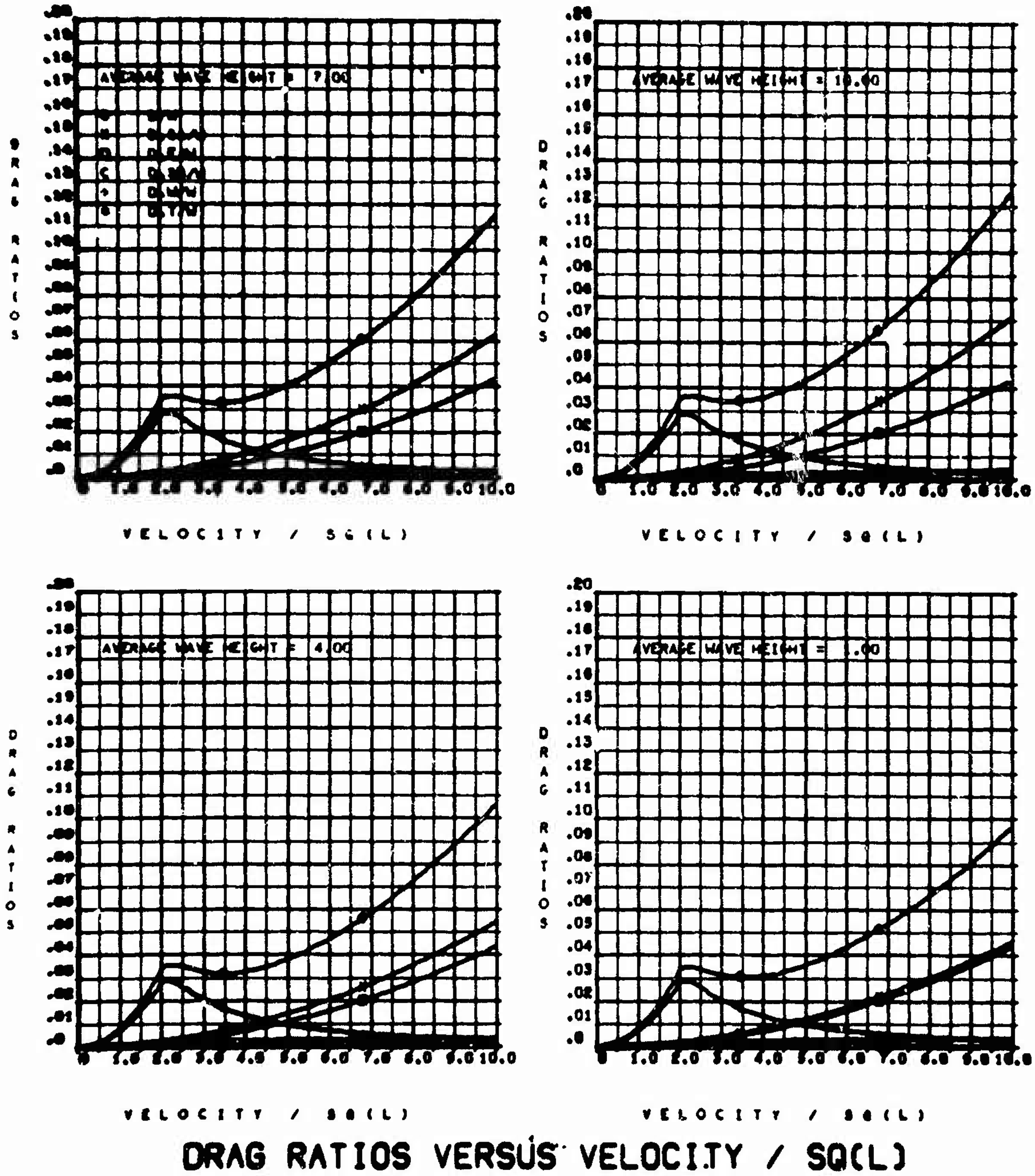

Figure 15 - General Performance Parameters of 100,000 Ton CAB With $\ell/b = 2.0$

(a) $K_{D_D} = 0.04$, $K_{D_s} = 0.08$, $w/\sqrt{S} = 1.1$

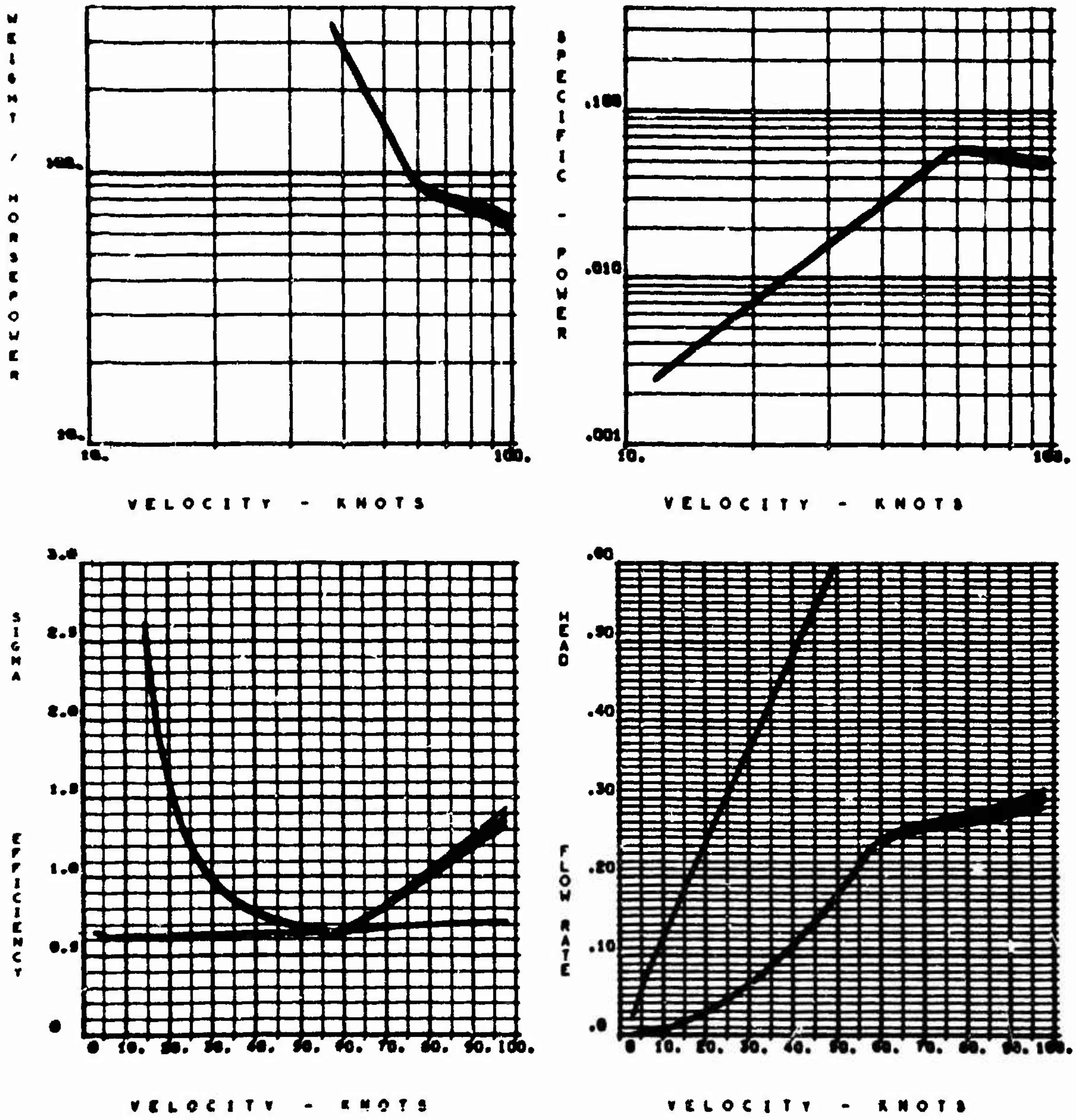

Figure 15 (Continued)

(a) Concluded

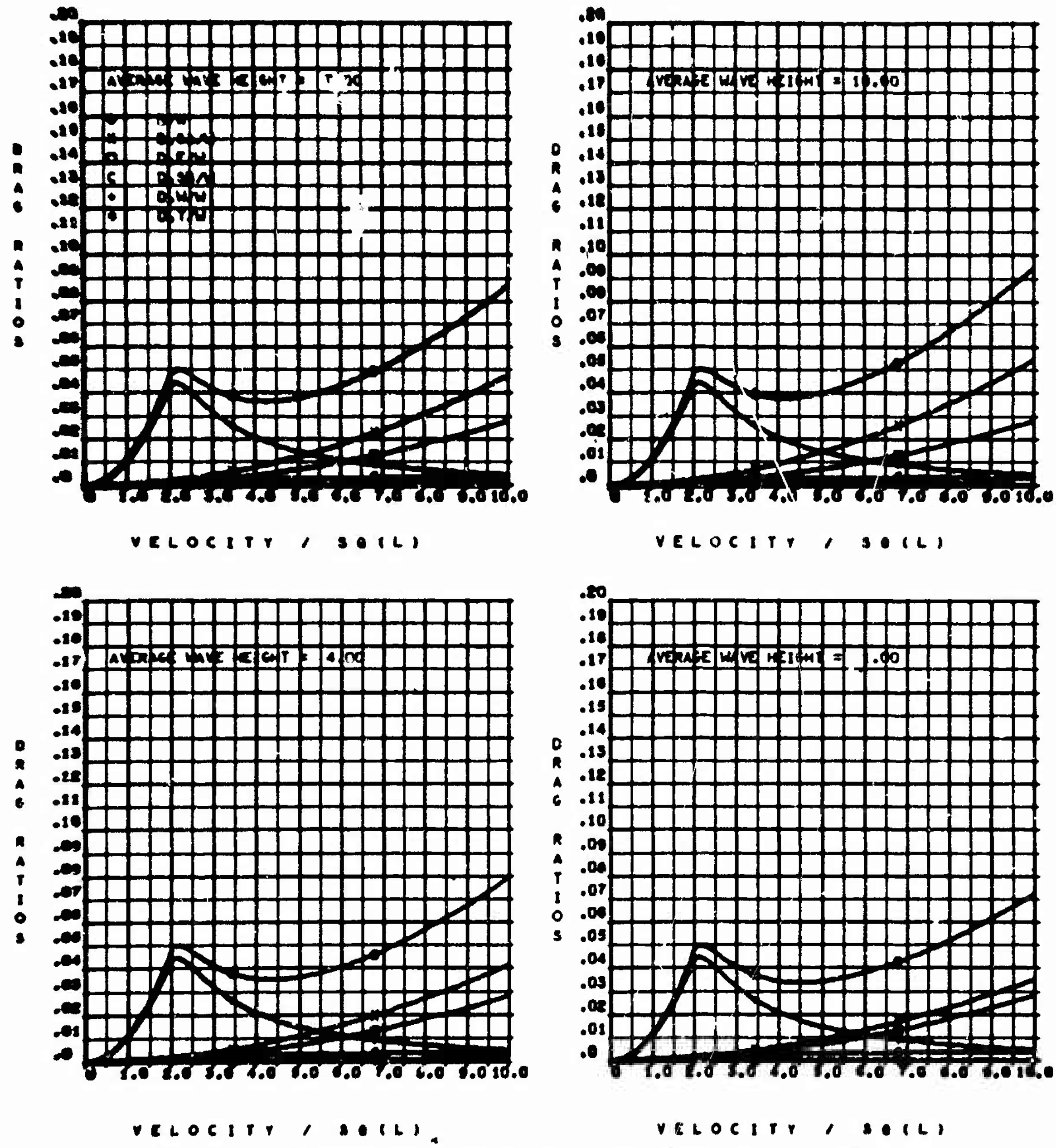

DRAG RATIOS VERSUS VELOCITY / SQ(L)

Figure 15 (Continued)

(b) $K_{D_D} = 0.04$, $K_{D_s} = 0.08$, $w/\sqrt{S} = 1.7$

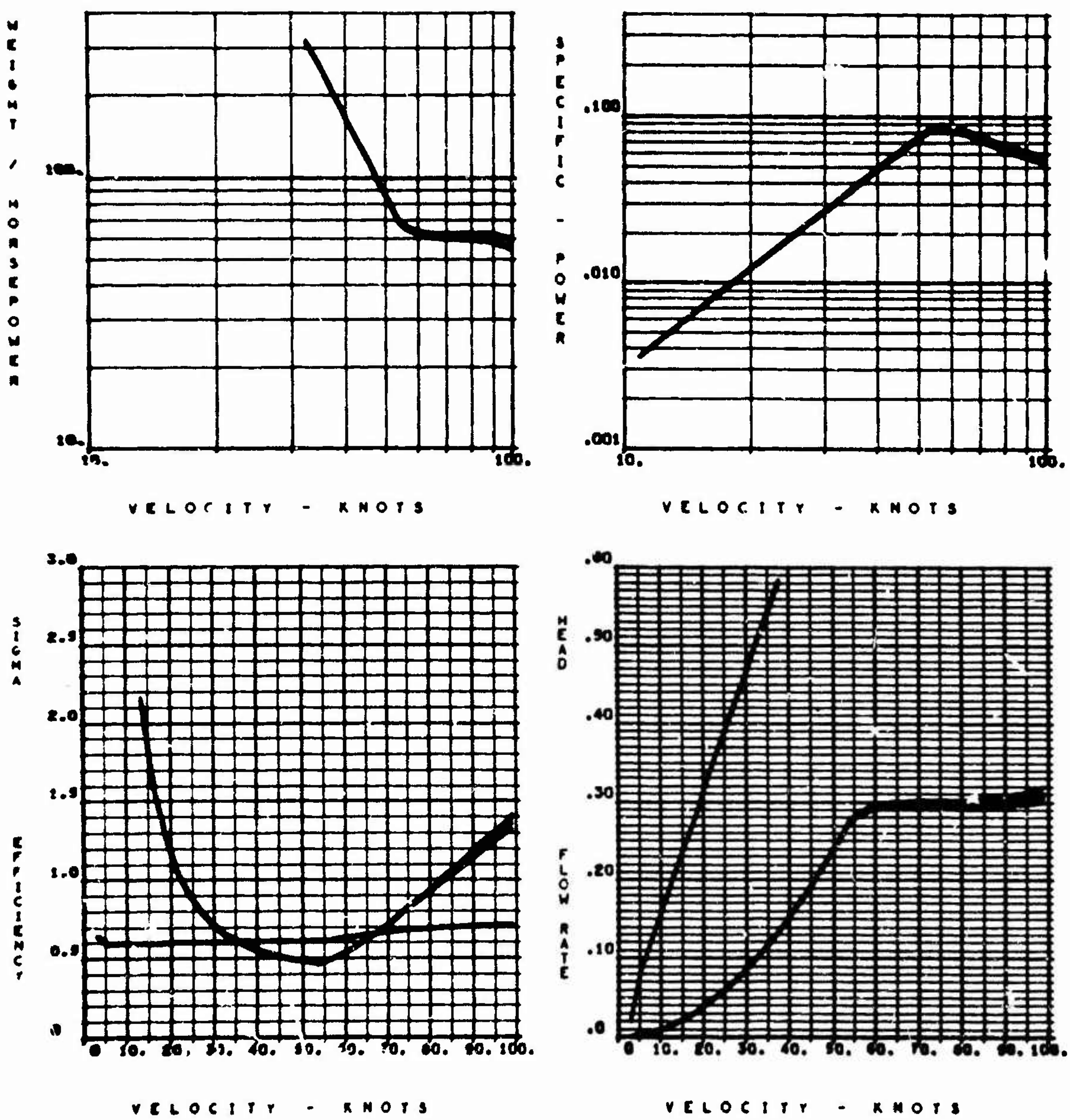

Figure 15 (Continued)

(b) Concluded

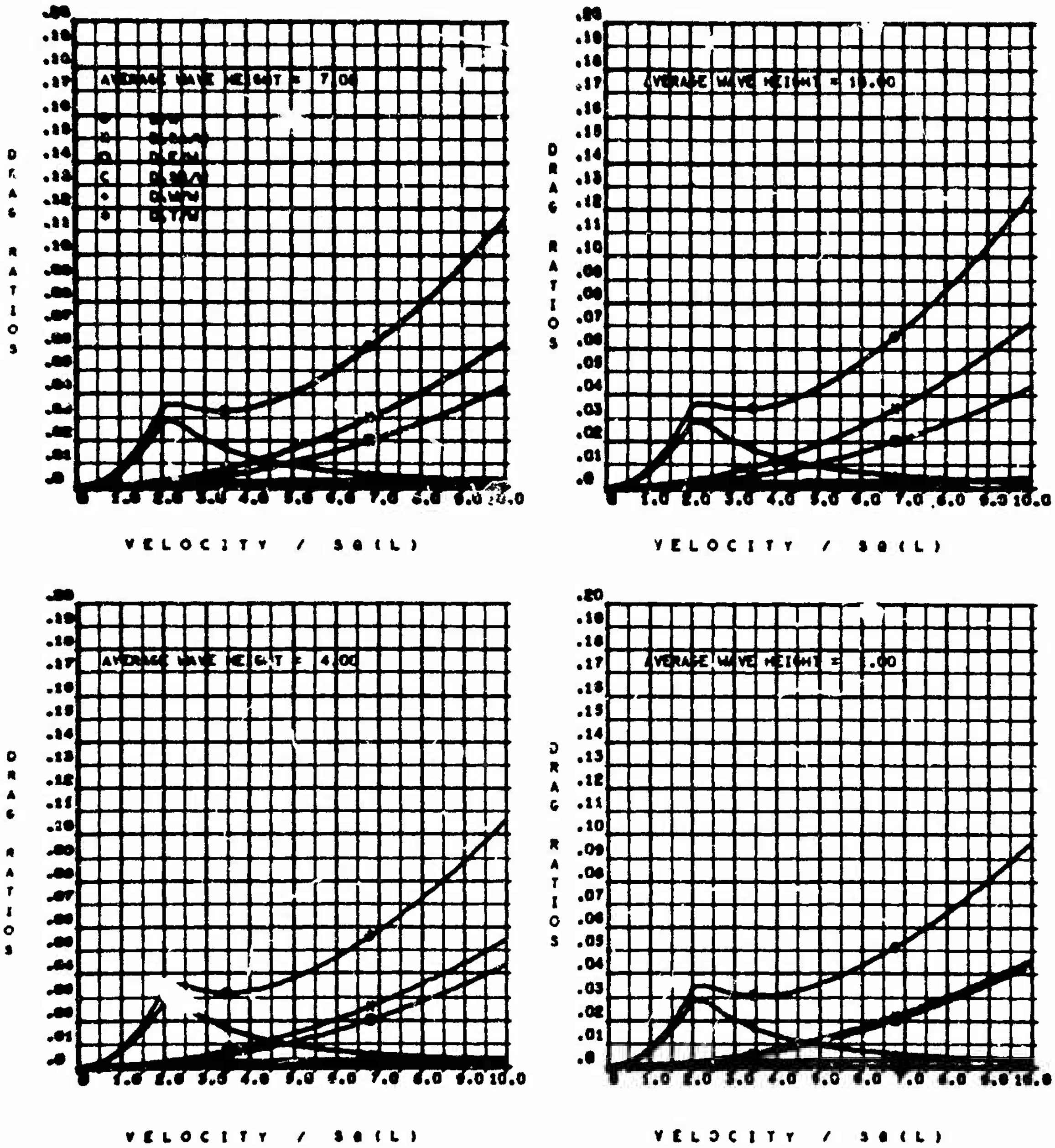

DRAG RATIOS VERSUS VELOCITY / SQ(L)

Figure 15 (Continued)

(c) $K_{D_D} = 0.08$, $K_{D_s} = 0.16$, $w/\sqrt{S} = 1.1$

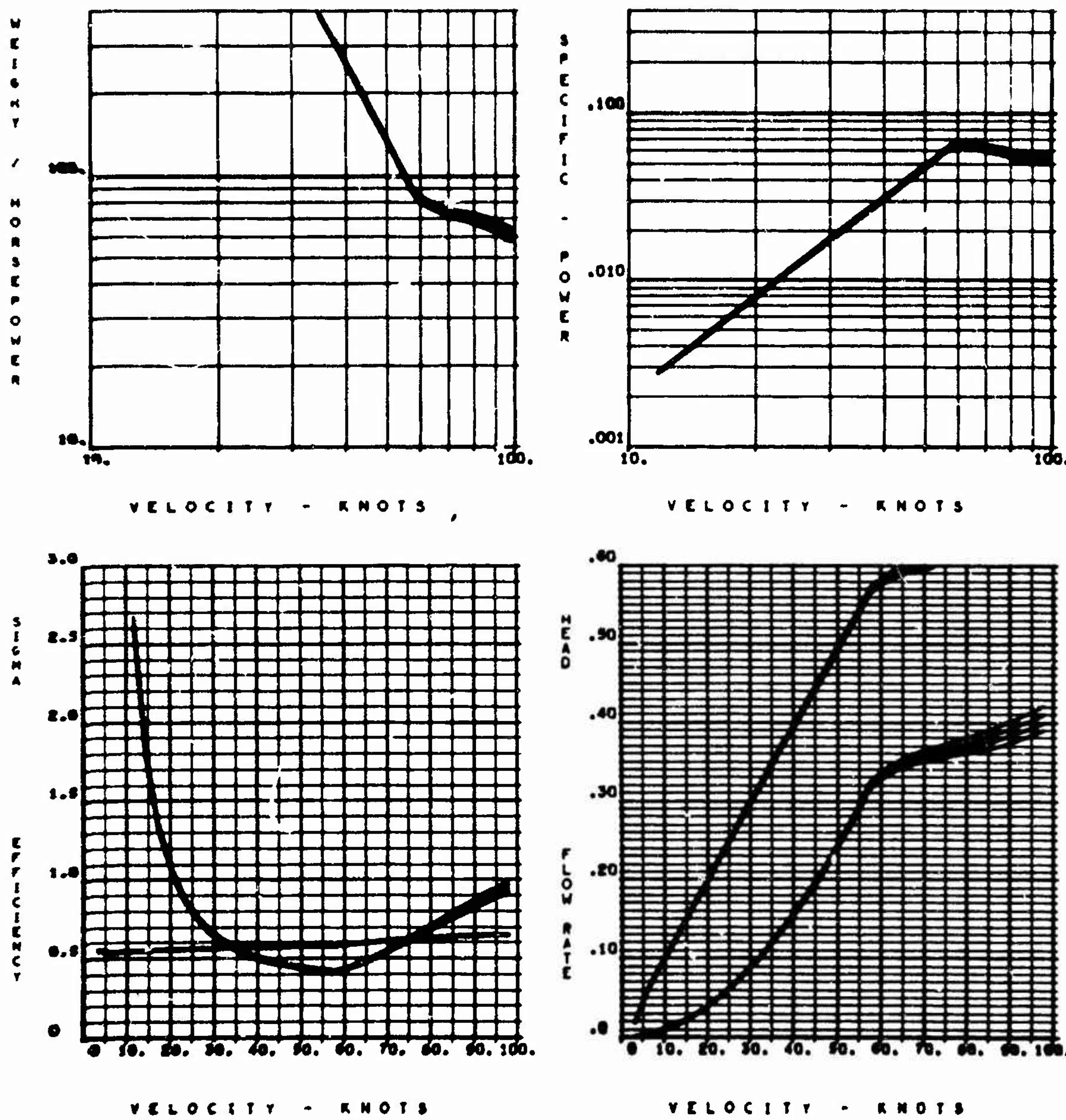

Figure 15 (Continued)

(c) Concluded

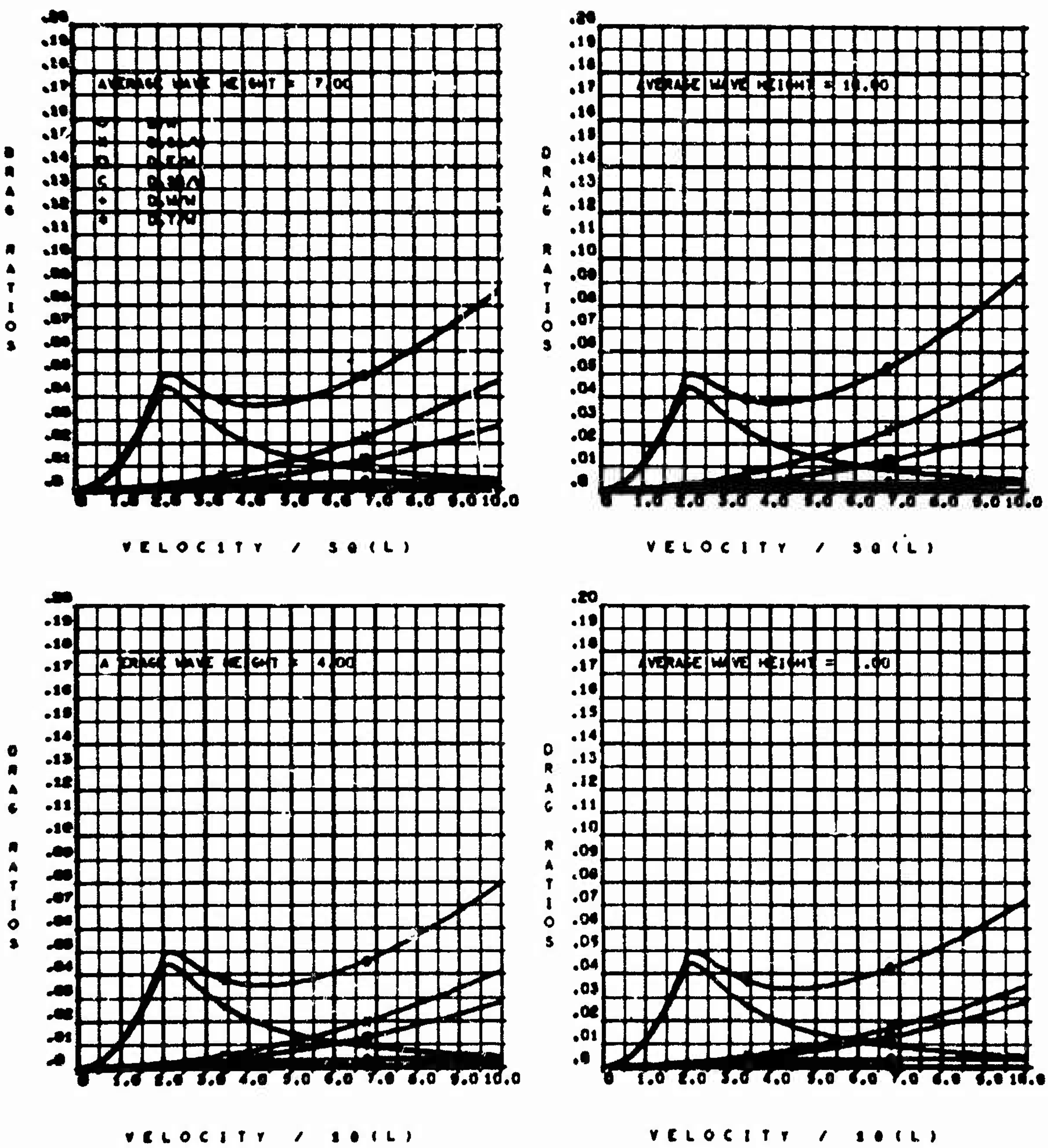

DRAG RATIOS VERSUS VELOCITY / SQ(L)

Figure 15 (Continued)

(d) $K_{D_D} = 0.08$, $K_{D_s} = 0.16$, $w/\sqrt{S} = 1.7$

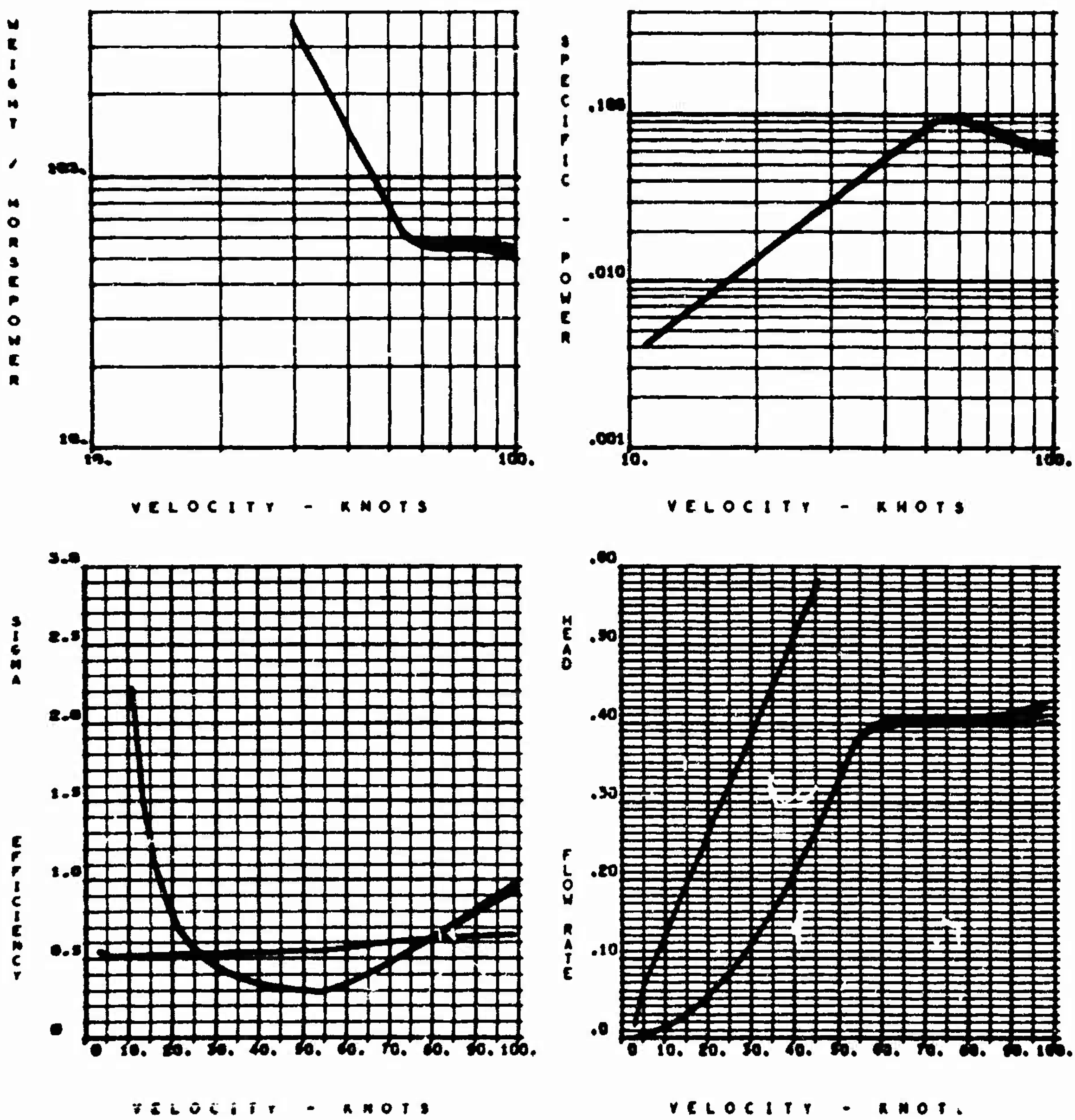

Figure 15 (Concluded)
(d) Concluded

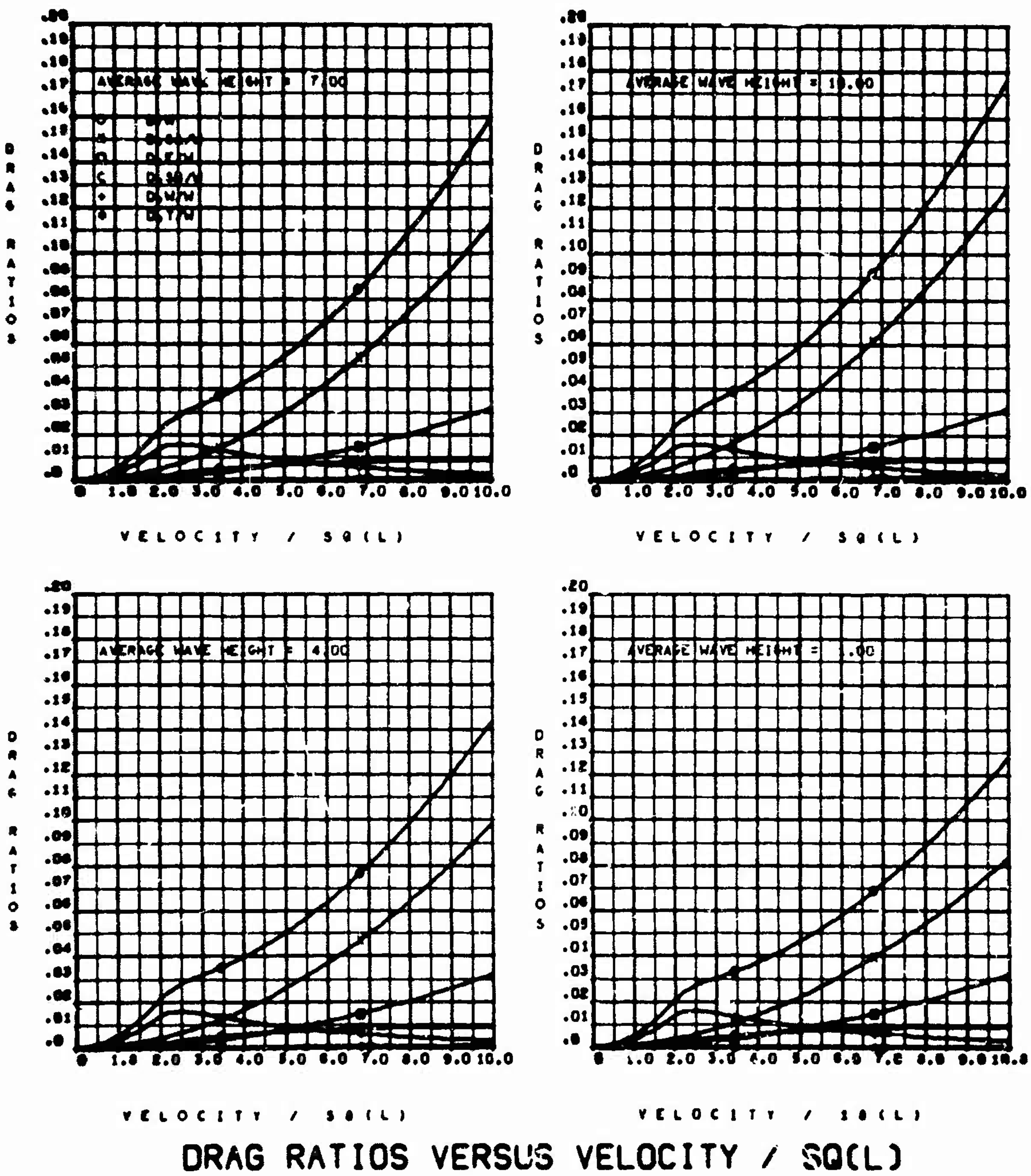

Figure 16 - General Performance Parameters of 100,000 Ton CAB With $\ell/b = 3.74$

(a) $K_{D_D} = 0.04$, $K_{D_s} = 0.08$, $w/\sqrt{S} = 1.1$

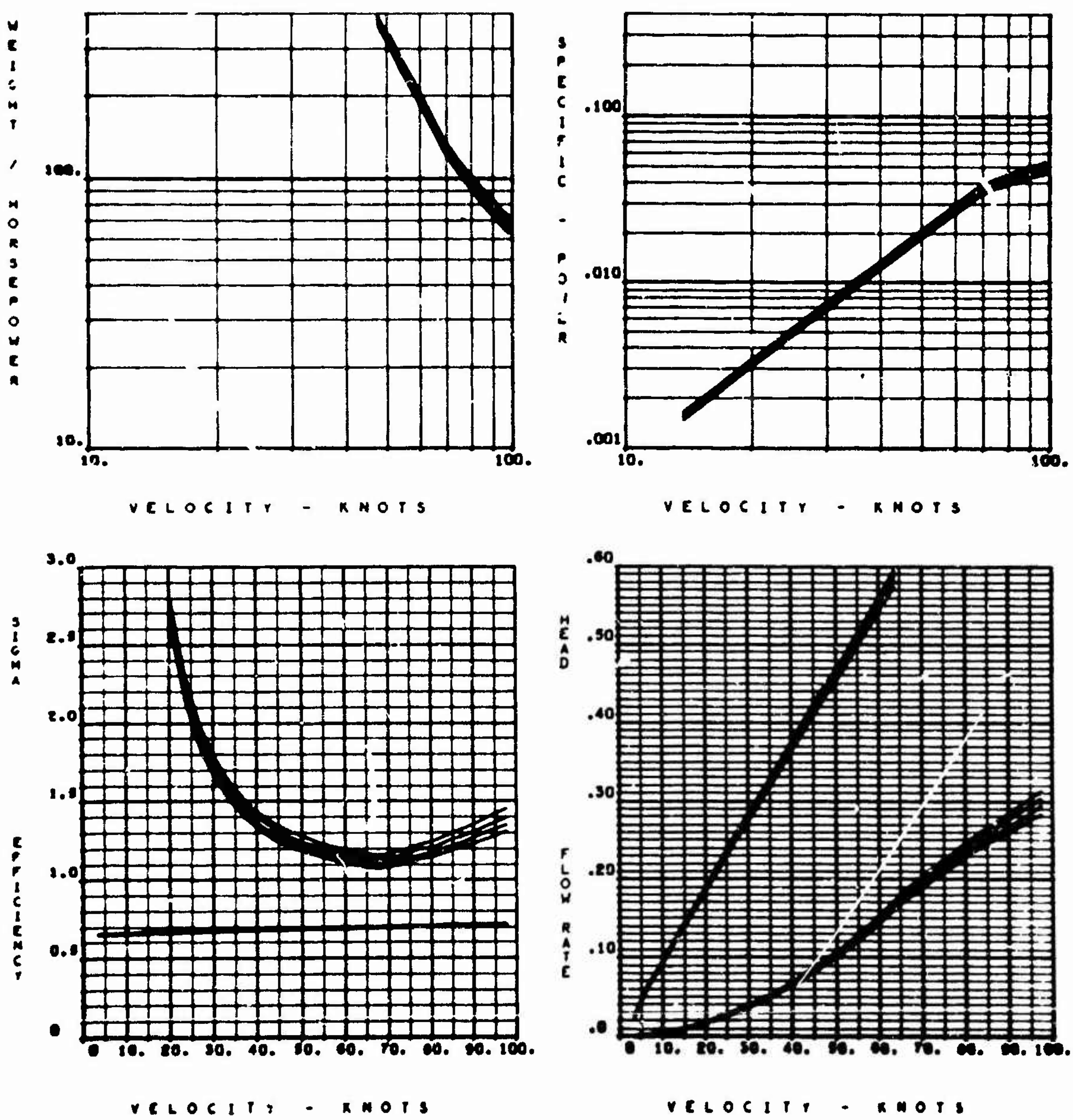

Figure 16 (Continued)

(a) Concluded

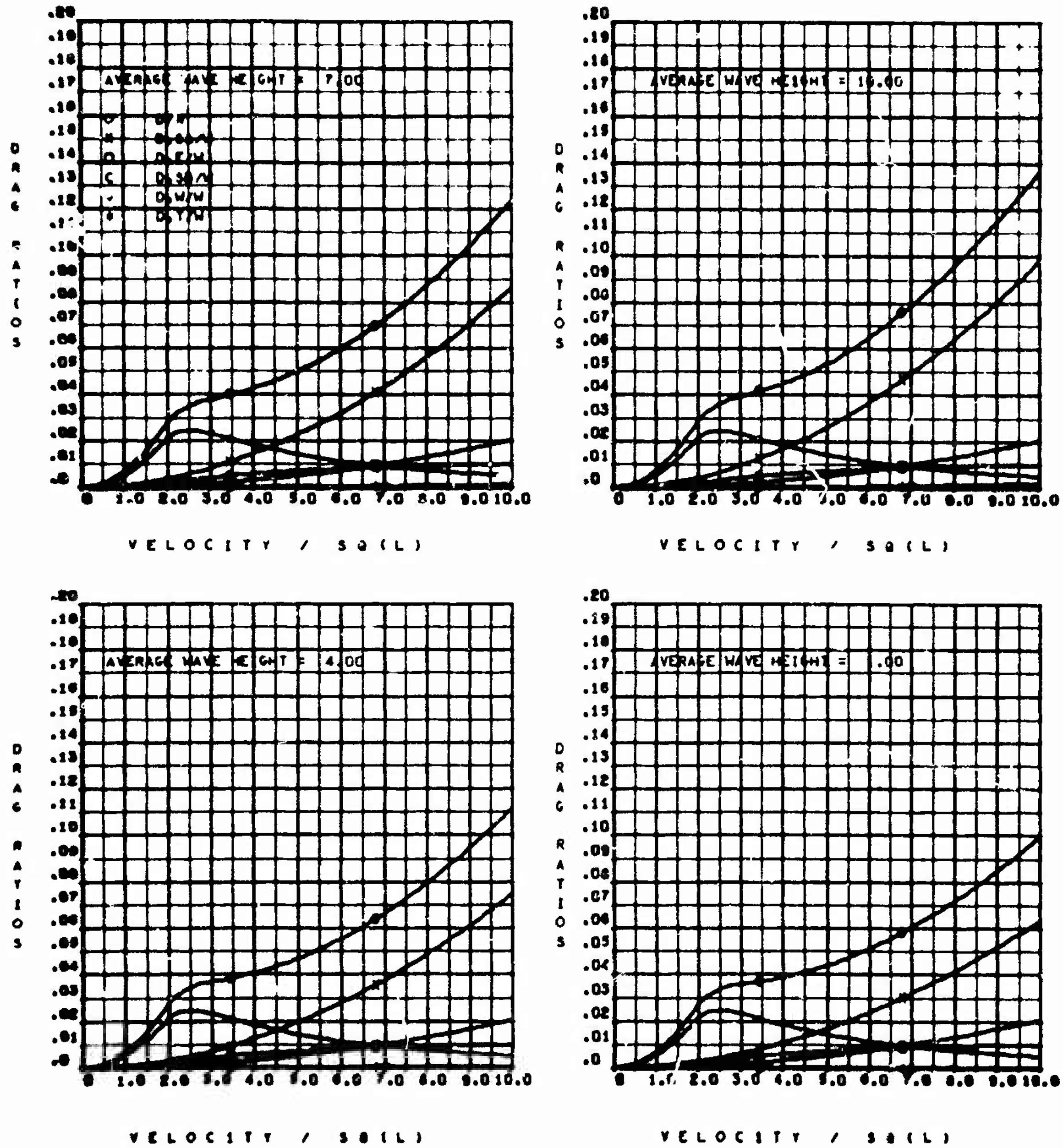

DRAG RATIOS VERSUS VELOCITY / SQ(L)

Figure 16 (Continued)

(b) $K_{D_D} = 0.04$, $K_{D_s} = 0.08$, $w/\sqrt{S} = 1.7$

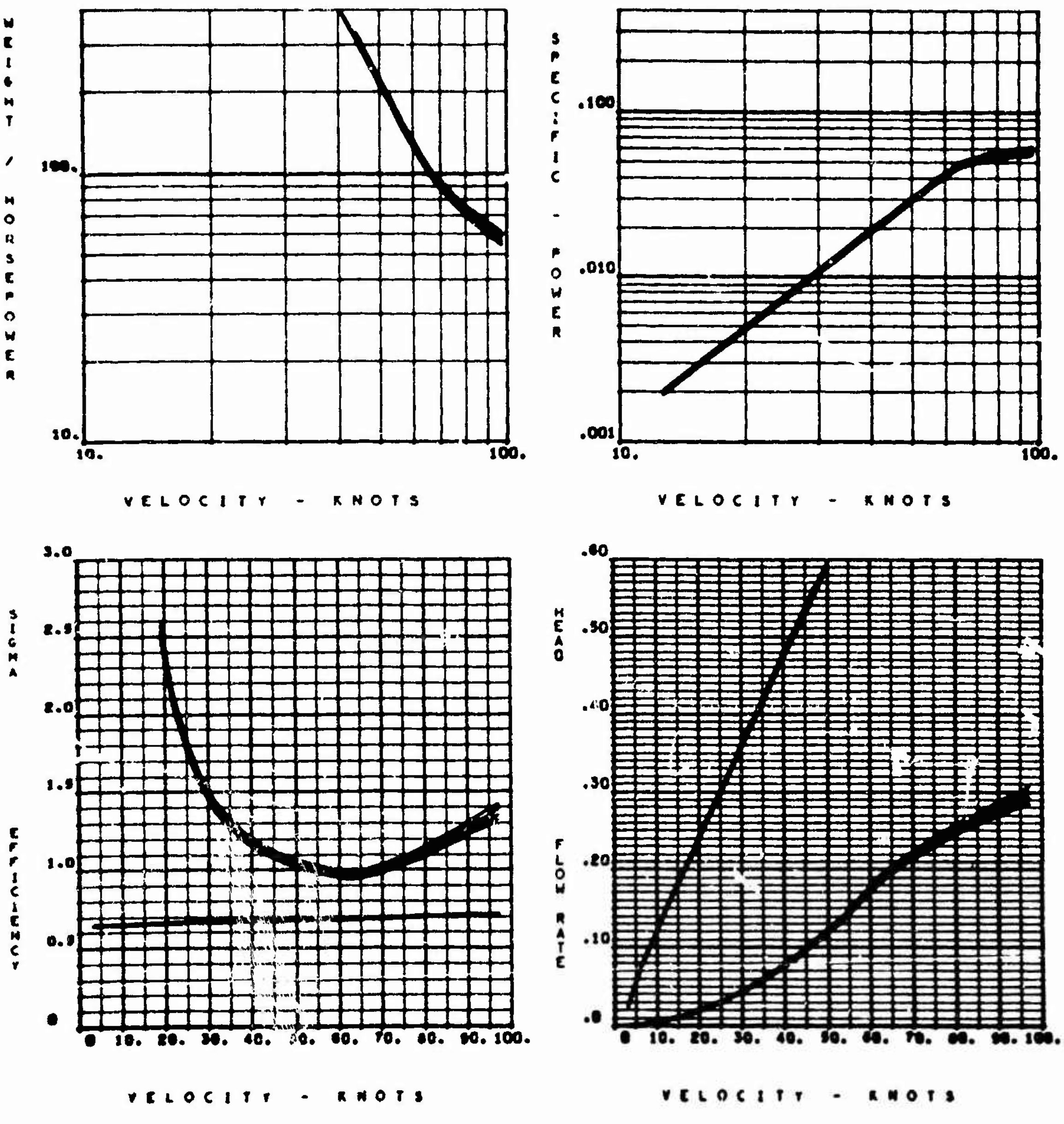

Figure 16 (Continued)

(b) Concluded

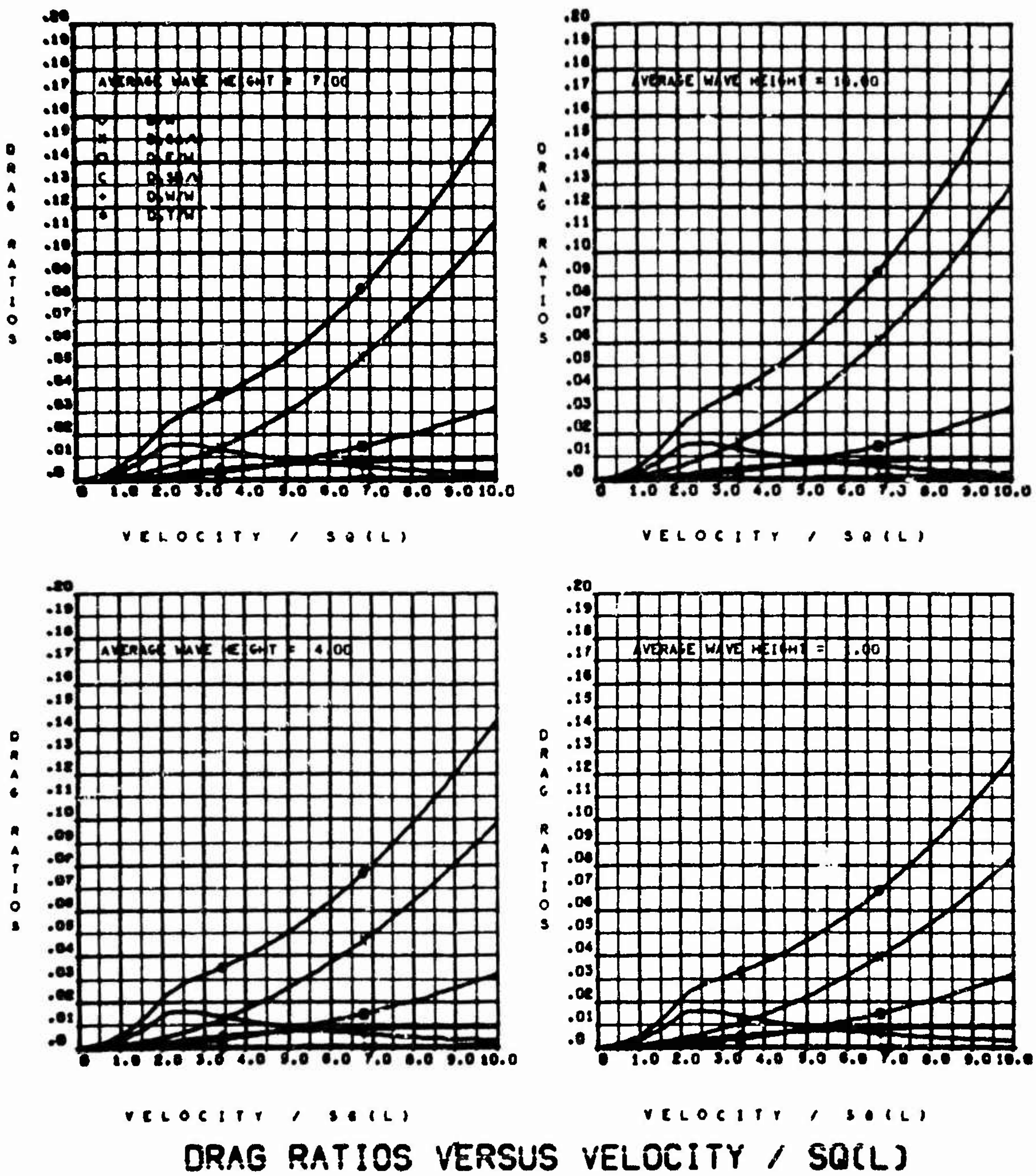

Figure 16 (Continued)

(c) $K_{D_D} = 0.08$, $K_{D_s} = 0.16$, $w/\sqrt{S} = 1.1$

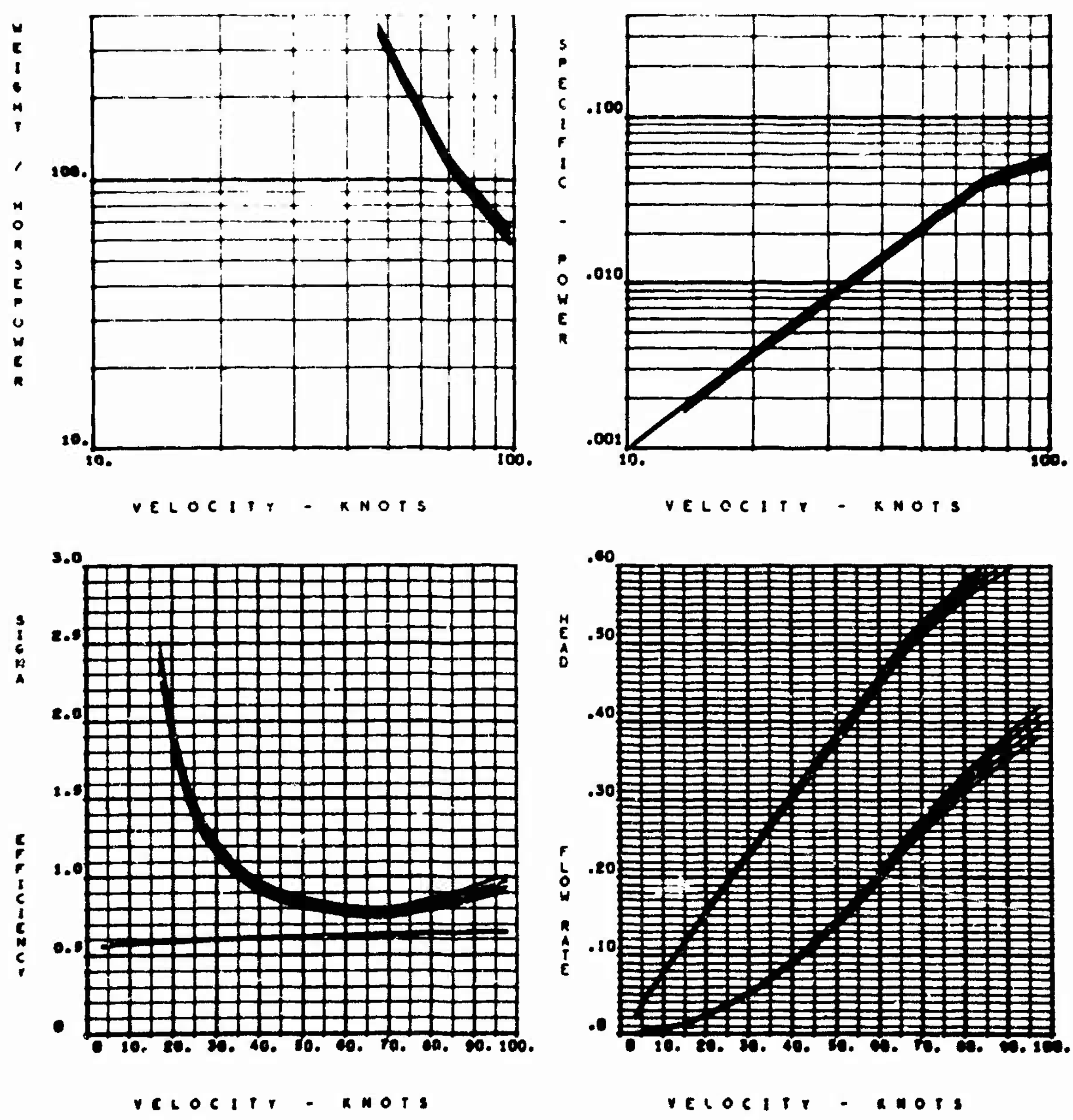

Figure 16 (Continued)

(c) Concluded

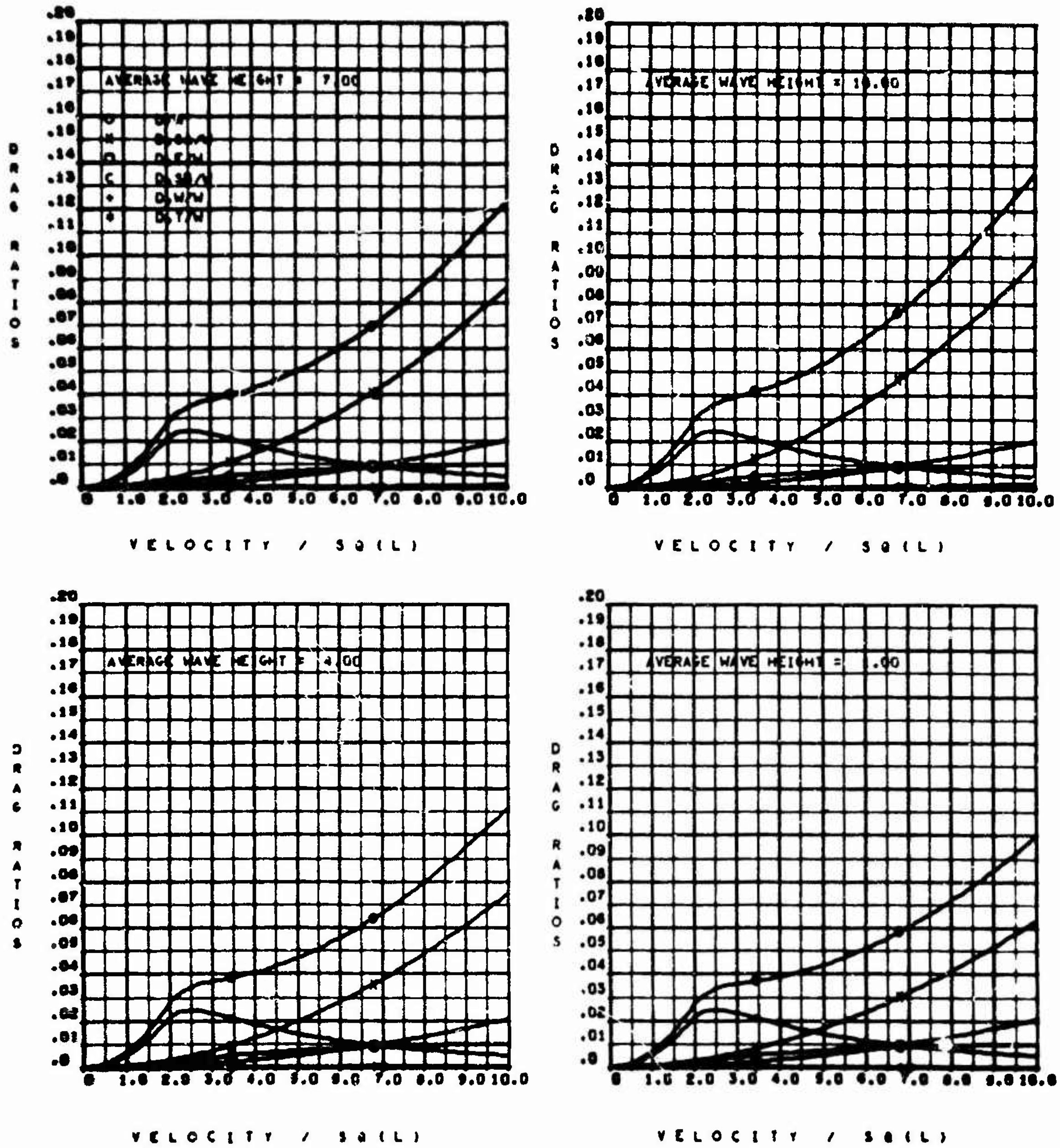

DRAG RATIOS VERSUS VELOCITY / SQ(L)

Figure 16 (Continued)

(d) $K_{D_D} = 0.08$, $K_{D_s} = 0.16$, $w/\sqrt{S} = 1.7$

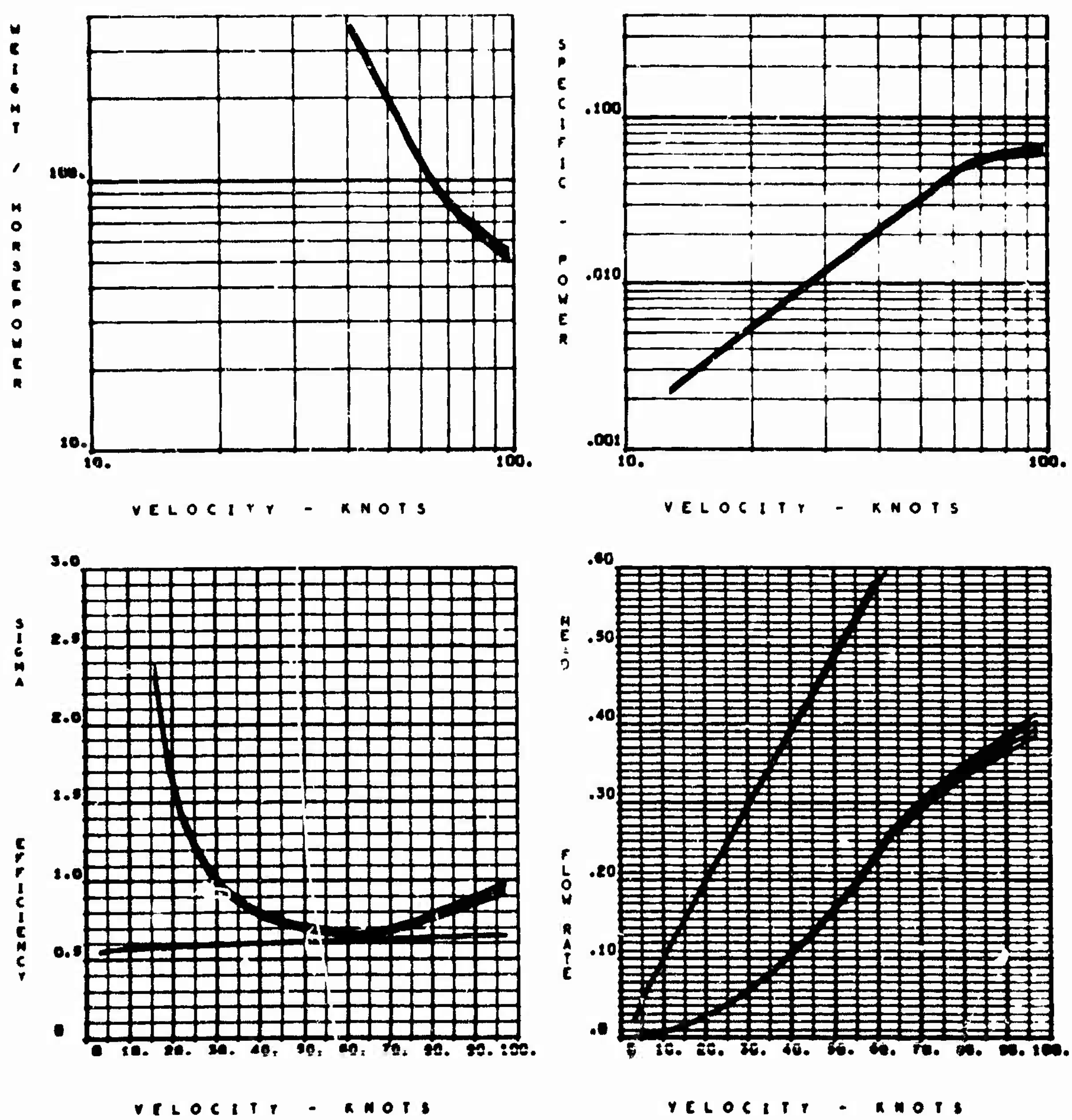

Figure 16 (Concluded)

(d) Concluded

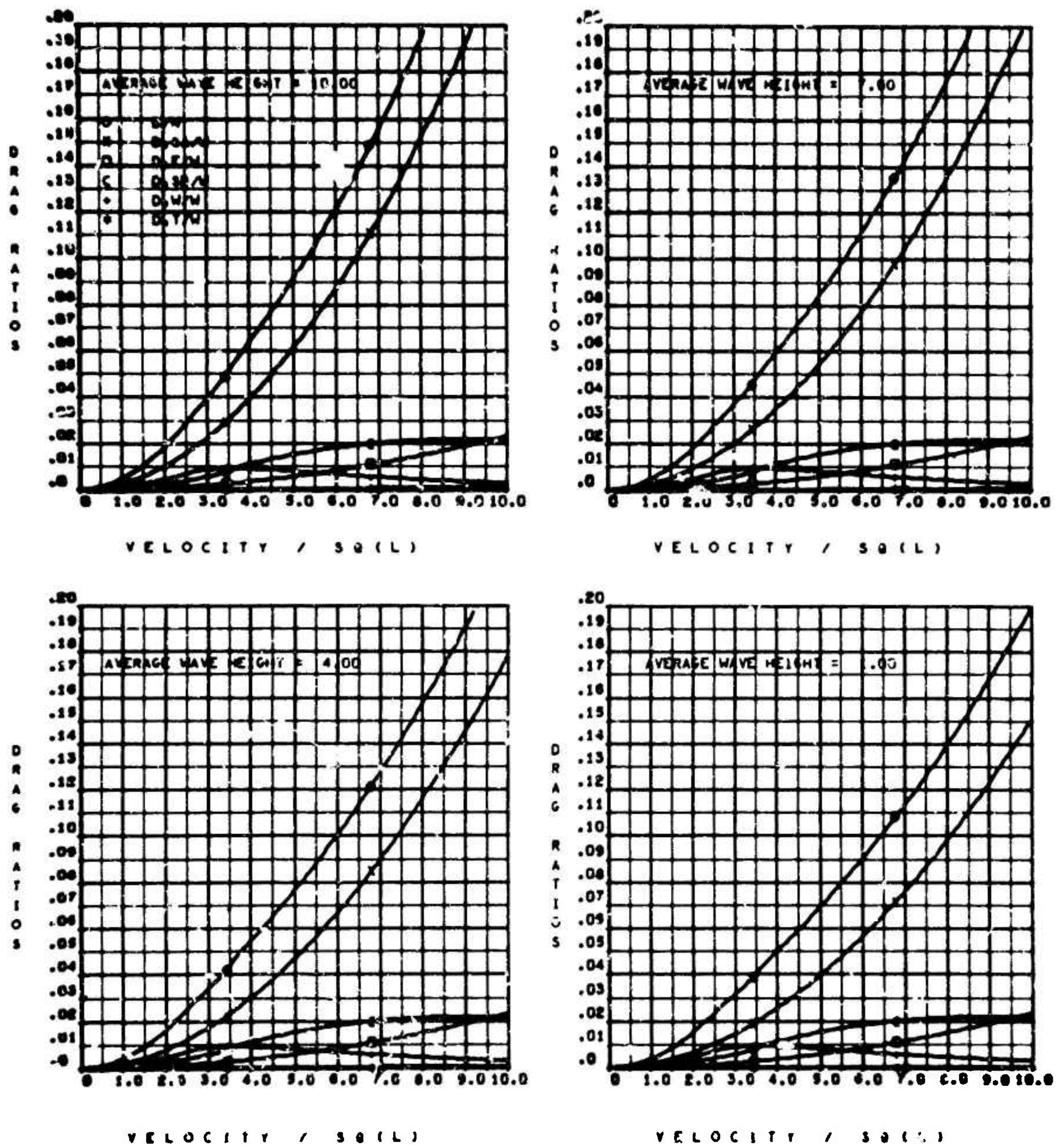

DRAG RATIOS VERSUS VELOCITY / SQ(L)

Figure 17 - General Performance Parameters of 100,000 Ton CAB With $\ell/b = 7.0$

(a) $K_{D_D} = 0.04$, $K_{D_s} = 0.08$, $w/\sqrt{S} = 1.1$

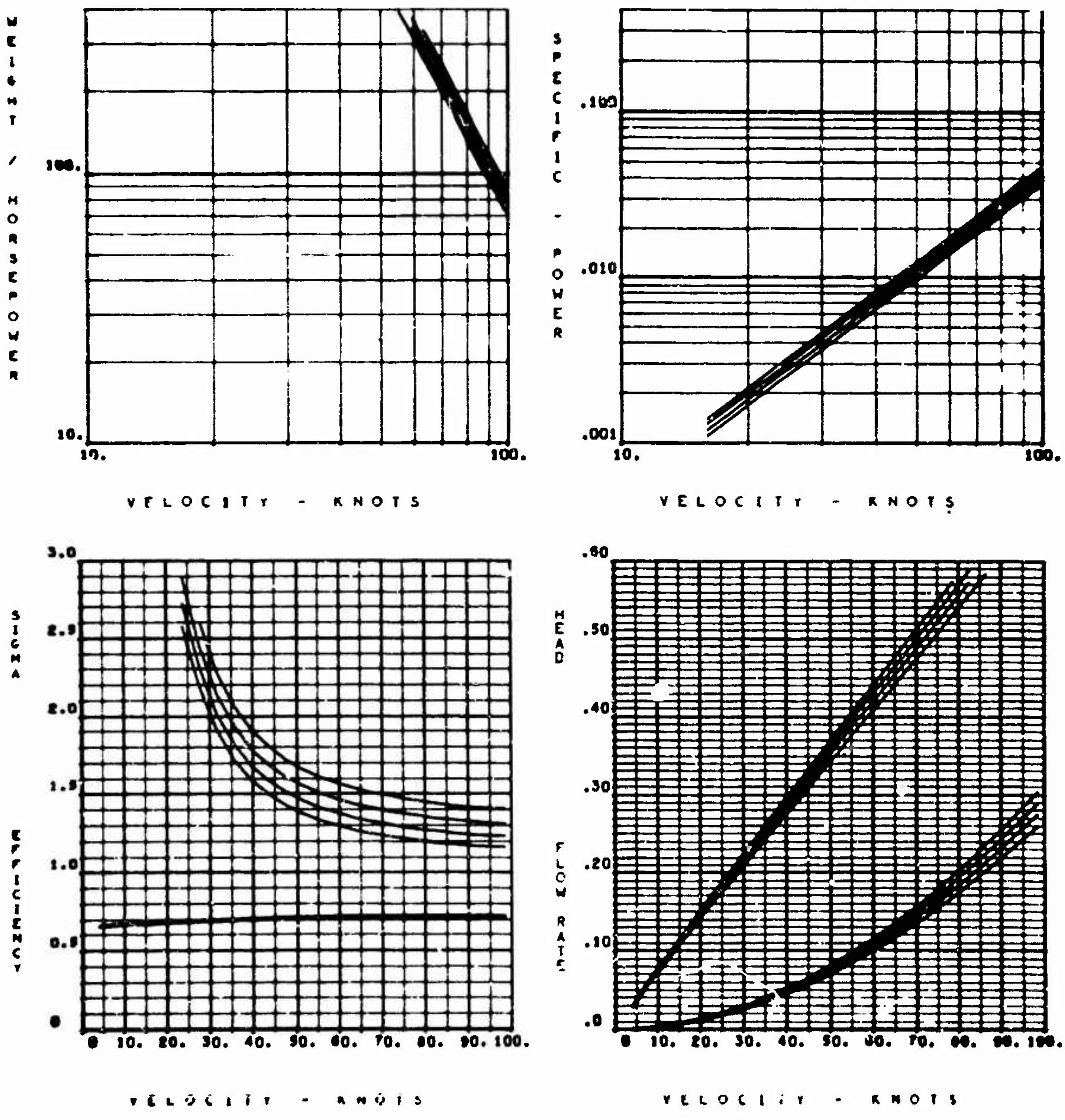

Figure 17 (Continued)
(a) Concluded

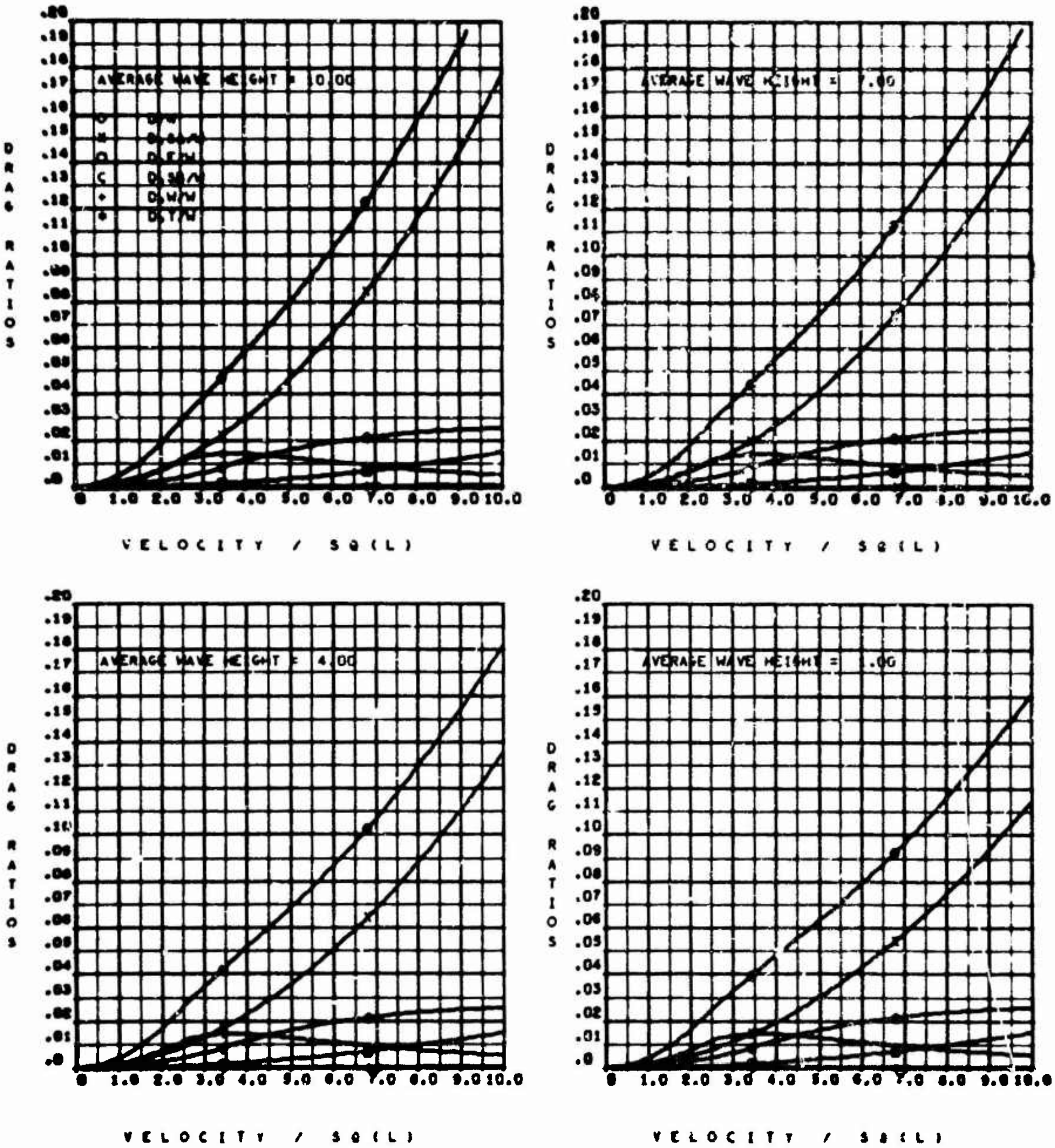

DRAG RATIOS VERSUS VELOCITY / SQ(L)

Figure 17 (Continued)

(b) $K_{D_D} = 0.04$, $K_{D_S} = 0.08$, $w/\sqrt{S} = 1.7$

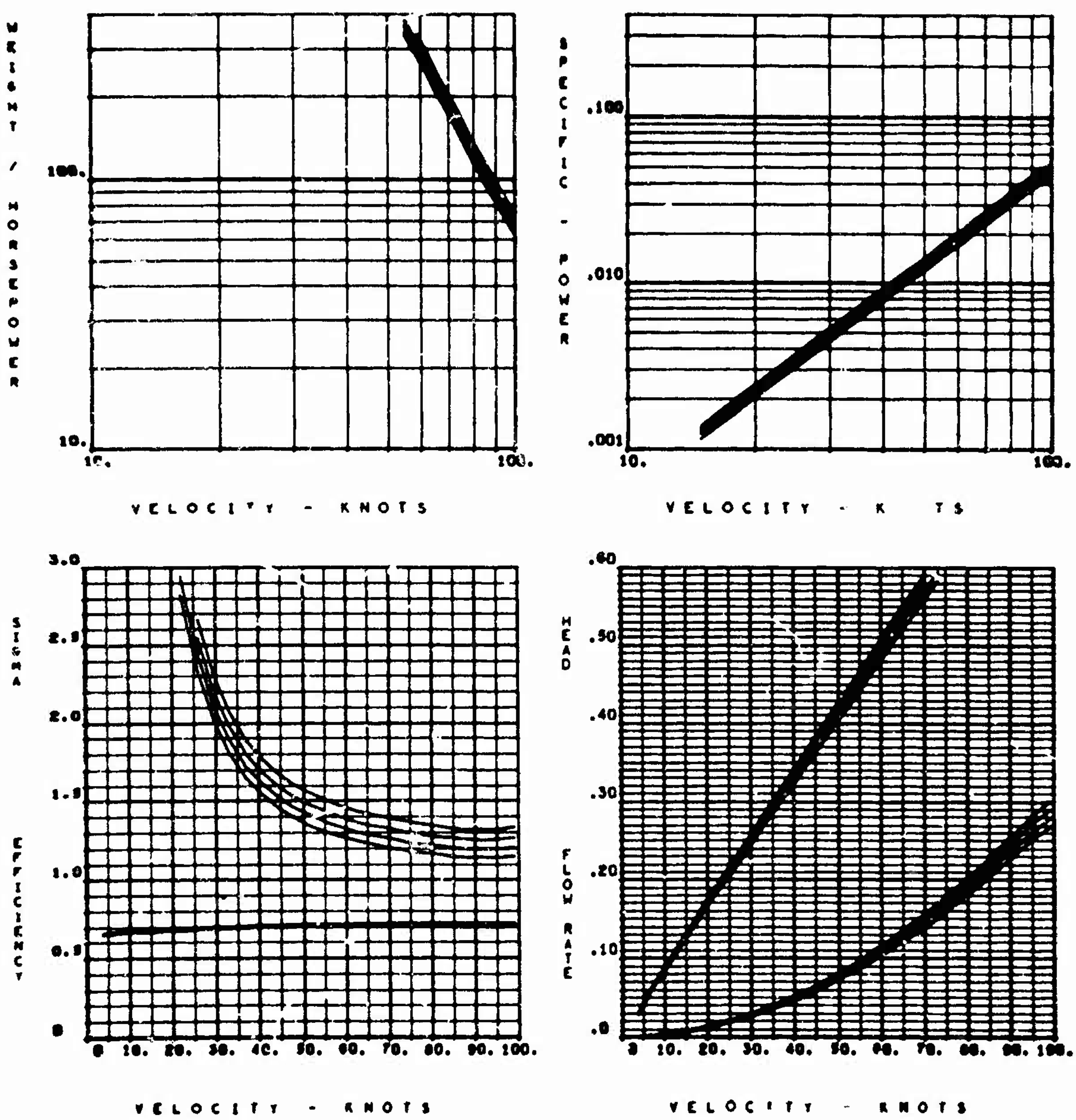

Figure 17 (Continued)

(b) Concluded

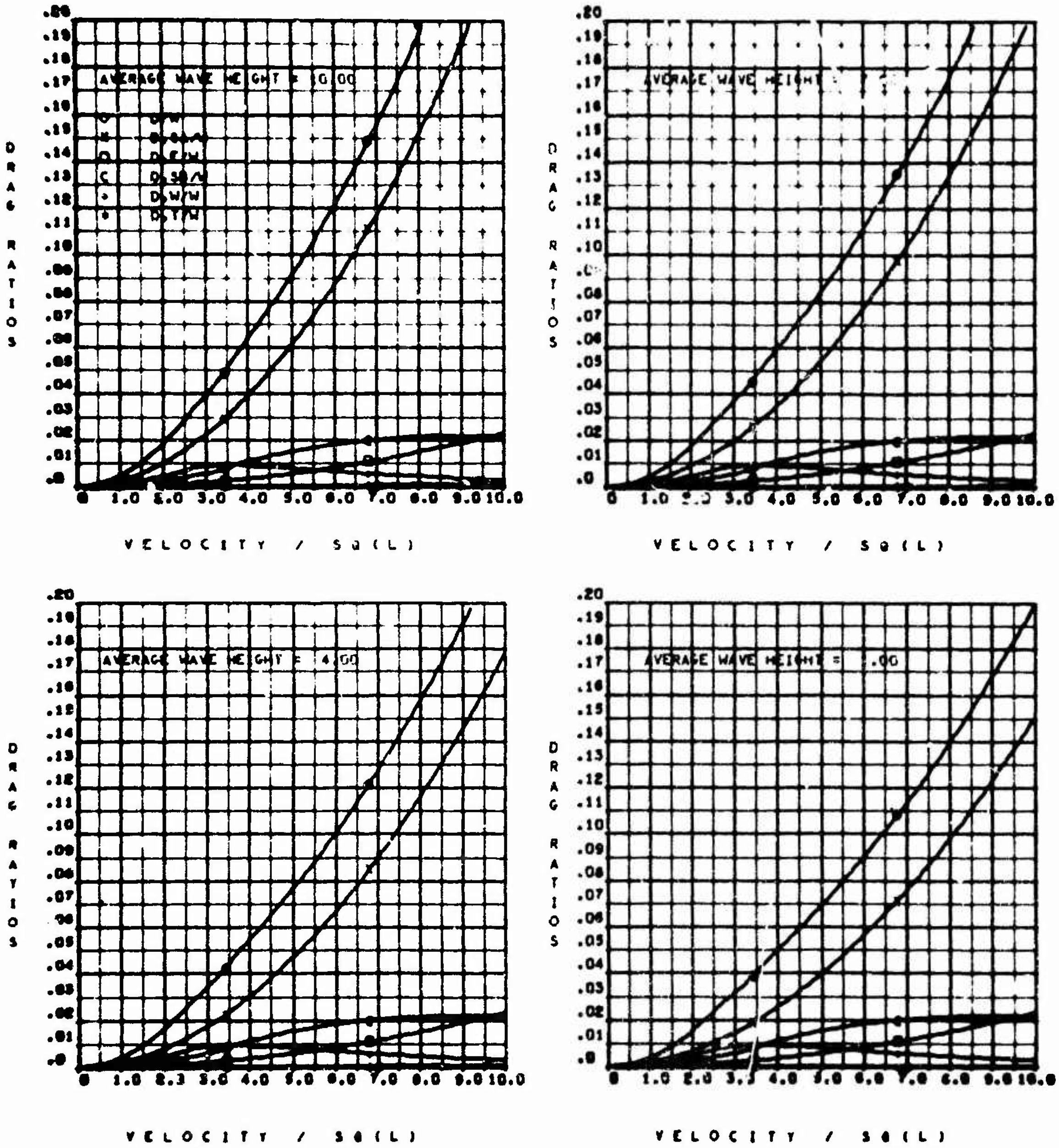

DRAG RATIOS VERSUS VELOCITY / SQ(L)

Figure 17 (Continued)

(c) $K_{D_D} = 0.08$, $K_{D_s} = 0.16$, $w/\sqrt{S} = 1.1$

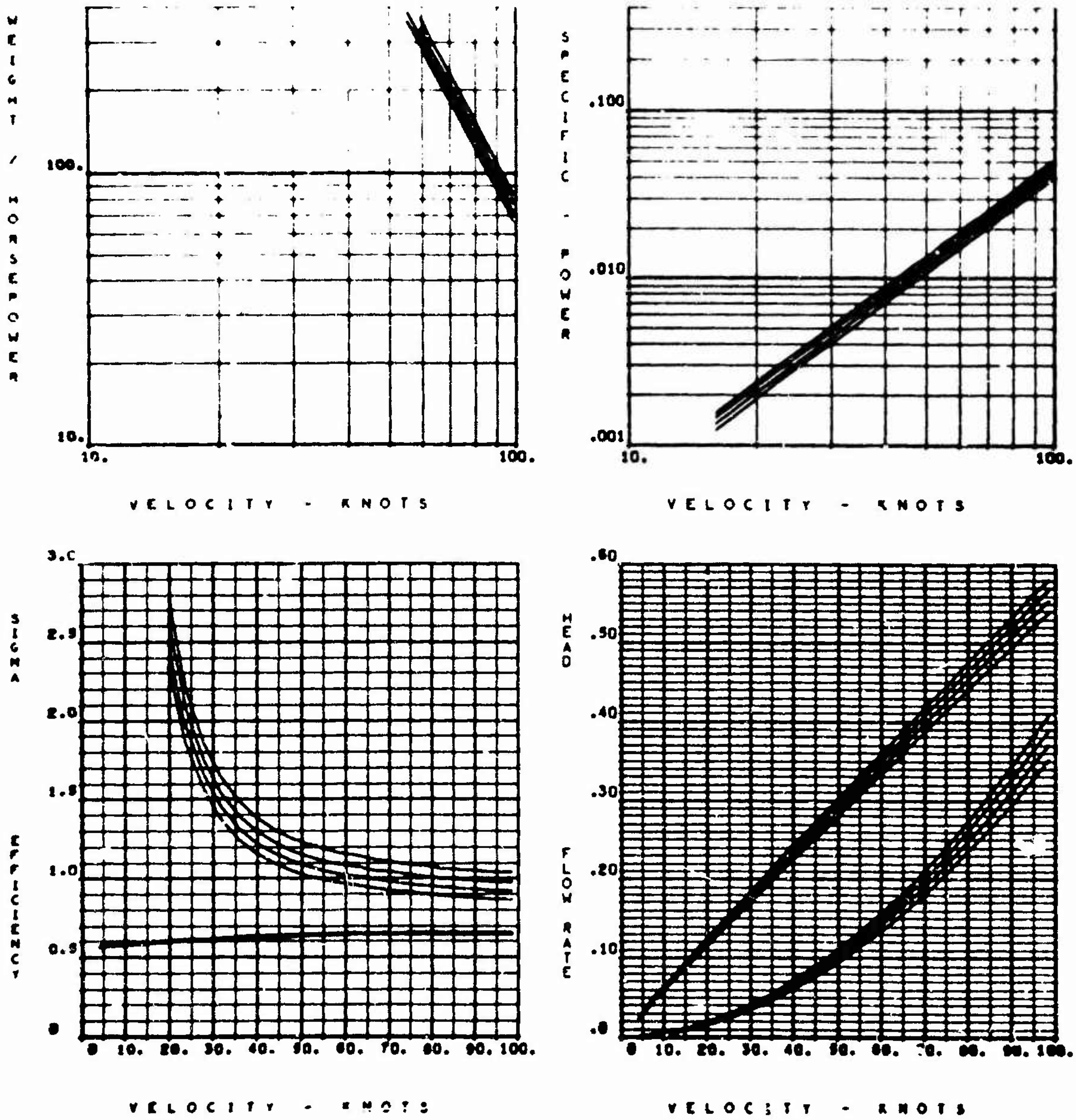

Figure 17 (Continued)
(c) Concluded

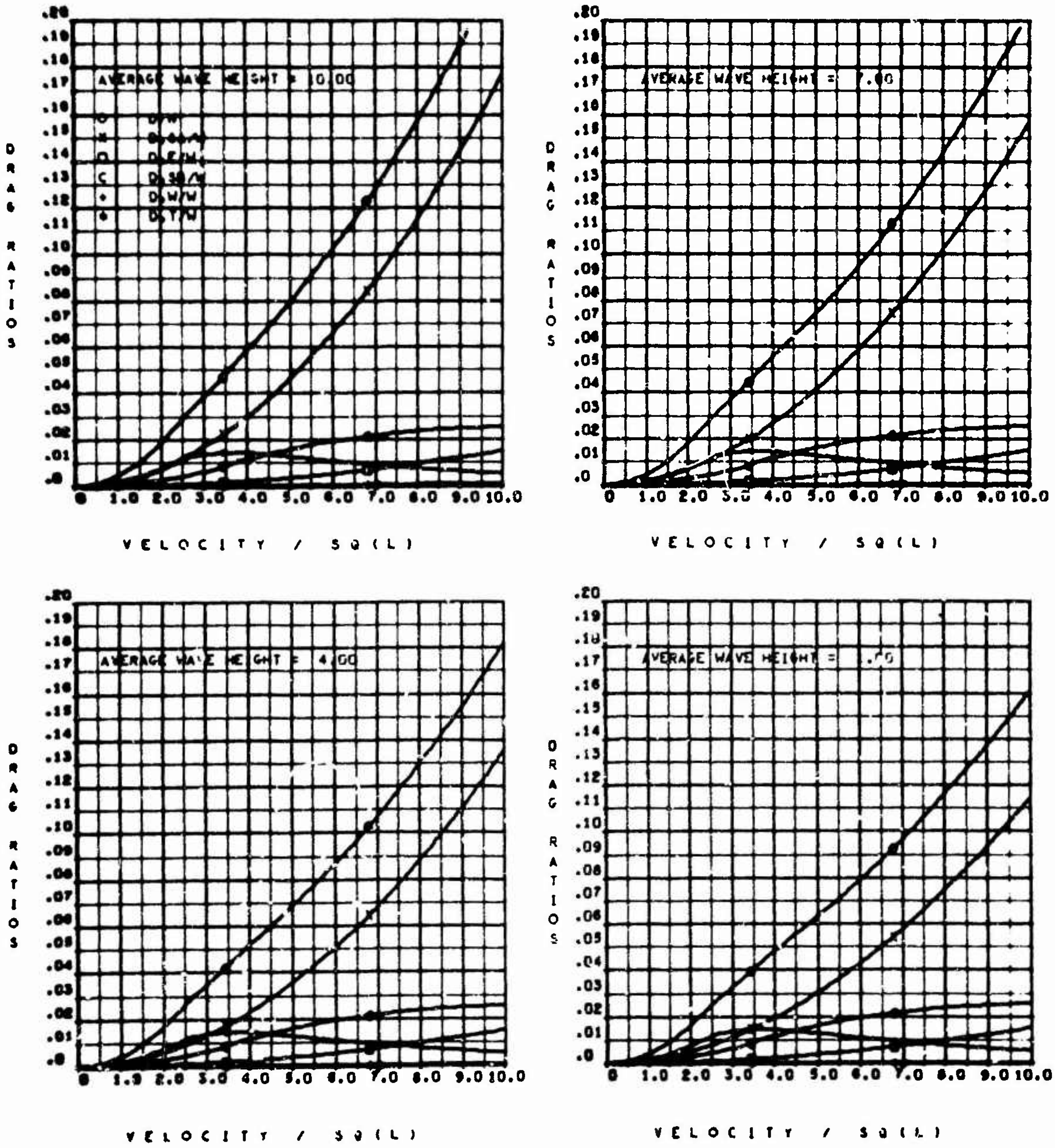

DRAG RATIOS VERSUS VELOCITY / SQ(L)

Figure 17 (Continued)

(d) $K_{D_D} = 0.08$, $K_{D_S} = 0.16$, $w/\sqrt{S} = 1.7$

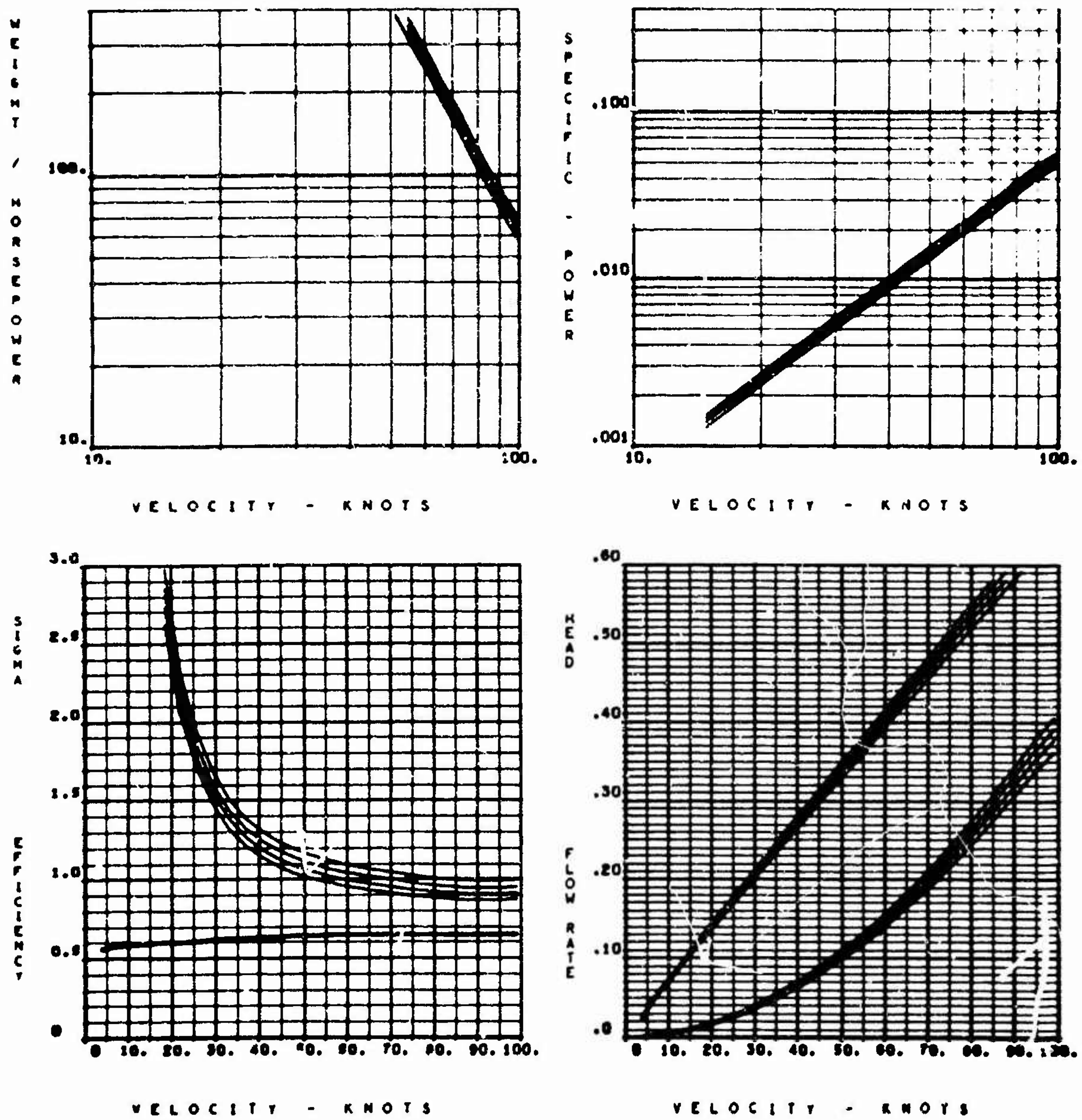

Figure 17 (Concluded)

(d) Concluded

Unclassified

Security Classification

DOCUMENT CONTROL DATA - R&D

(Security classification of title, body of abstract and indexing annotation must be entered when the overall report is classified)

1 ORIGINATING ACTIVITY (Corporate author) Aerodynamics Laboratory David Taylor Model Basin Washington, D. C. 20007	2a REPORT SECURITY CLASSIFICATION Unclassified 2b GROUP

3 REPORT TITLE

PERFORMANCE ESTIMATES OF CAPTURED AIR BUBBLE VEHICLES WITH WATER JET PROPULSION

4 DESCRIPTIVE NOTES (Type of report and inclusive dates)

5 AUTHOR(S) (Last name, first name, initial)

Williams, Robert M.

6 REPORT DATE February 1967	7a TOTAL NO OF PAGES 117[7]	7b NO OF REFS 3
8a CONTRACT OR GRANT NO b. PROJECT NO 061-008 c d	9a ORIGINATOR'S REPORT NUMBER(S) Report 2334 9b OTHER REPORT NO(S) (Any other numbers that may be assigned this report) Aero Report 1119	

10 AVAILABILITY/LIMITATION NOTICES

The distribution of this document is unlimited.

11 SUPPLEMENTARY NOTES	12 SPONSORING MILITARY ACTIVITY Naval Ship Systems Command Department of the Navy Washington, D. C. 20360

13 ABSTRACT

Performance predictions of Captured Air Bubble (CAB) vehicles utilizing water jet propulsion are presented. The analysis was made for various combinations of gross weight, specific loading, length-to-beam ratio, and wave height. In addition, the effect of varying the ducting loss coefficient has also been investigated.

It was found that the total drag "hump" of low length-to-beam ratios (ℓ/b) was eliminated at higher ℓ/b values. This effect is due to the complex behavior of the wavemaking drag component. It was further found that for a particular length-to-beam ratio (ℓ/b) a value of specific cushion loading existed which optimized the performance (as measured by the ratio of weight to horsepower required). The lighter specific cushion loadings offered definite performance advantages at the lower length-to-beam ratios.

DD FORM 1 JAN 64 1473

Unclassified

Security Classification

Unclassified

Security Classification

14 KEY WORDS	LINK A		LINK B		LINK C	
	ROLE	WT	ROLE	WT	ROLE	WT
CAB Vehicle						
Surface Effect Ship						
Drag/Weight						
Water Jet Propulsion						
Efficiency						
Computer Simulation						
Design Parameters						

Unclassified

Security Classification